Dissertation zur Erlangung des Doktorgrades

der Fakultät für Chemie und Pharmazie

der Ludwig-Maximilians-Universität München

Stage Specific Proteome Signatures in Bovine Oocyte Maturation and Early Embryogenesis

Daniela R. Deutsch

aus München

2014

Erklärung

Diese Dissertation wurde im Sinne von § 7 der Promotionsordnung vom 28. November 2011 von Herrn Prof. Dr. Eckhard Wolf betreut und von Herrn Prof. Dr. Ernst Wagner von der Fakultät für Chemie und Pharmazie vertreten.

Eidesstattliche Versicherung

Diese Dissertation wurde eigenständig und ohne unerlaubte Hilfe erarbeitet.

München, den …….

…….

Daniela Deutsch

Dissertation eingereicht am: 12.09.2014

1. Gutachterin / 1. Gutachter: Prof. Dr. Ernst Wagner

2. Gutachterin / 2. Gutachter: Prof. Dr. Eckhard Wolf

Mündliche Prüfung am: 09.07.2015

Dedicated to my family

Table of contents

1. Introduction

1.1 Early mammalian development

Early mammalian development is a well-orchestrated process involving dynamic molecular and structural changes. Oocytes start to develop in the ovary at prenatal age and pause maturation in late fetal life. Reaching puberty, in the first menstrual cycle (humans and primates) or estrous cycle (non-primate vertebrates), fully grown oocytes resume maturation in response to gonadotropins. As soon as the hormones induce meiosis, the germinal vesicles (GV) breaks down, the cytoskeleton rearranges, and the spindle assembles. Matured oocytes finally arrest in metaphase II (MII). At this stage, the first polar body is extruded, by which the extra haploid set of chromosomes resulting from meiosis is discarded (Figure 1) [1].

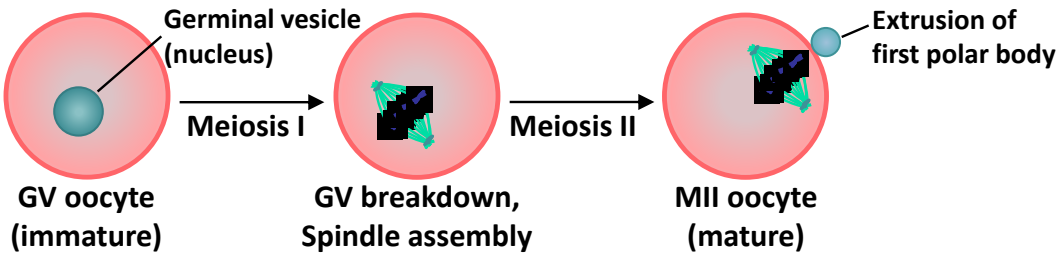

Figure 1. Maturation of mammalian oocytes. Maturation of immature germinal vesicle (GV) oocytes is induced by gonadotropins. In the maturation process, the germinal vesicle (GV) breaks down, followed by meiosis I spindle assembly and chromosome migration. The first polar body is extruded and the meiosis II spindle forms subcortically. Mature metaphase II (MII) oocytes arrest and are released into the oviduct (adapted from Li *et al.* [1]).

In monovulatory species such as humans and cows, usually one arrested MII oocyte enclosed by cumulus cells is released from the dominant follicle into the oviduct, a tube connecting ovary and uterus, in a process referred to as ovulation. Ovulation is initiated by a surge of luteinizing hormone (LH) at about day 14 of the menstrual cycle in humans [2] and at about day 0, at estrus, in cows [3]. Estrus is a phase of the estrous cycle of non-primate vertebrates characterized by receptivity to males and to mating, often referred to as "heat". LH acts synergistically with follicle stimulating hormone (FSH) which reaches its peak level at the same time as well [4, 5]. The release of FSH and LH from the pituitary is caused by hypothalamic secretion of gonadotropin-releasing hormone (GnRH), whose release is in turn caused by rising levels of estrogen. Following ovulation, in the luteal phase of the menstrual cycle, progesterone is produced by the remains of the dominant follicle, referred to as corpus luteum. This stimulates the growth of the uterine lining (endometrium) to prepare for a potential implantation of an embryo. If no pregnancy is established, the uterine lining is sloughed off during menstruation. The human menstrual cycle is illustrated in Figure 2 [6]. In animals with estrous cycles, the endometrium is restructured if no conception occurs [7].

Arrested MII oocytes are fertilizable for about 24 hours in the oviduct. Fertilization triggers resumption of meiosis in the oocyte and the extrusion of the second polar body. Subsequently, the membranes of the male and female haploid pronuclei dissolve, the chromosomes combine and become part of a single diploid nucleus. At this stage, the fertilized oocyte is called zygote [1]. Shortly afterwards, embryonic mitotic cleavage divisions begin and form the blastomeres of subsequent embryonic stages. During these initial cleavages, the embryo does not increase in size, i.e. the total volume of the early embryo remains unchanged from that of the zygote stage [8].

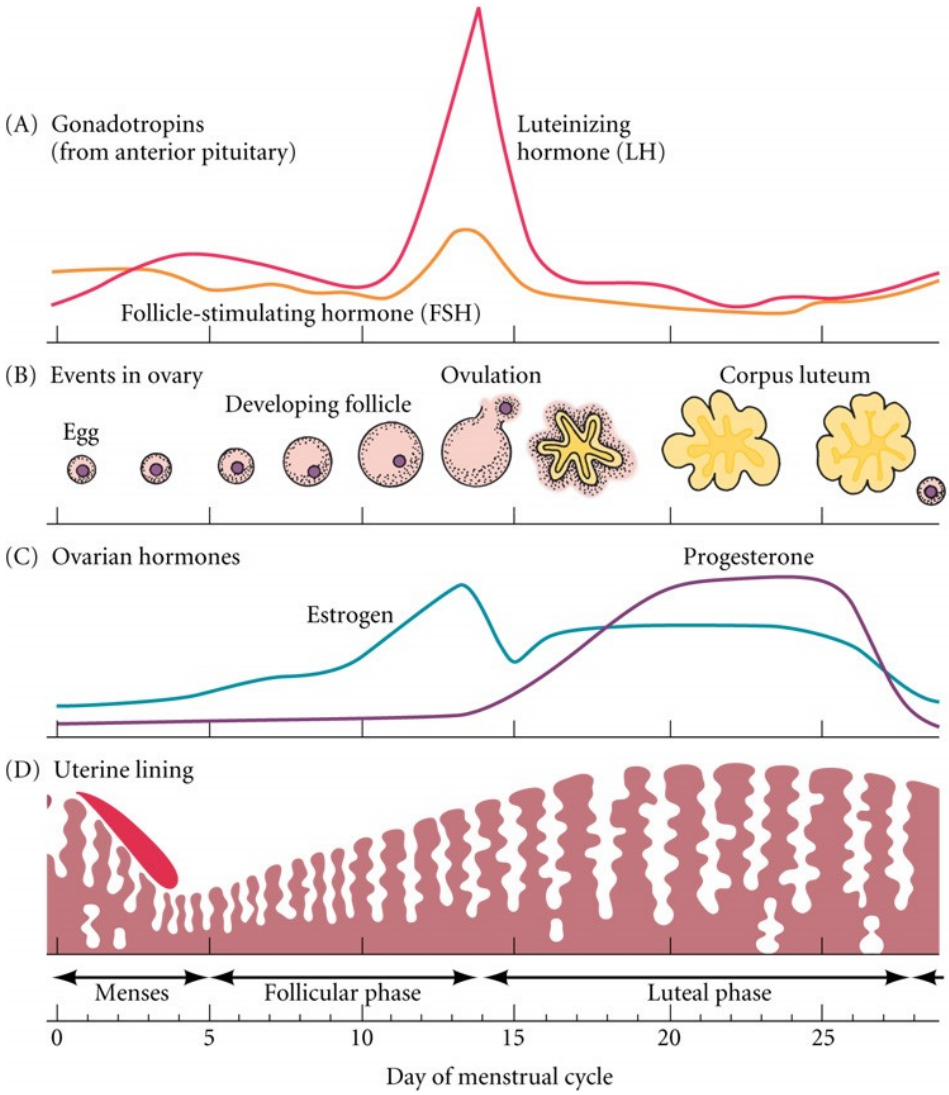

Figure 2. The human menstrual cycle. Gonadotropins **(A)** and ovarian hormones **(C)** control the ovarian **(B)** and the uterine **(D)** cycle. During the follicular phase of the uterine cycle, the oocyte matures within the follicle of the ovary and the uterine lining prepares for implantation of a blastocyst. Ovulation occurs around day 14 by which a mature oocyte is released into the oviduct. If no blastocyst implants in the uterus, the uterine wall begins to break down, leading to menstruation. Source: Developmental Biology, 10th edition, Chapter 17, Scott F. Gilbert, 2013, ISBN 9781605351735 [6].

Completion of oocyte meiosis and the first embryonic cleavage cycles are under the control of maternal gene products, requiring adequate translation of maternal RNAs as well as activation, inactivation and relocation of proteins [9]. Maternal transcripts and proteins are accumulated and stored during oogenesis and gradually depleted while the embryonic genome activation (EGA) occurs and the embryo starts to produce its own transcripts and

proteins [10-12]. The shift from maternal to embryonic control, also referred to as maternal-to-embryonic transition (MET), is characterized by major changes in the pattern of gene expression and protein synthesis. Major EGA occurs at the two-cell stage in mice [13], at the four- to eight-cell stage in humans [14] and pigs [13], and at the eight- to 16-cell stage in sheep [10]. In early bovine development, a gradual switch from maternal to embryonic control occurs with a minor EGA occurring between the one- to four-cell stage [15] followed by the major EGA at the eight- to 16-cell stage [16].

While the early embryo travels along the oviduct towards the uterus, compaction occurs, by which the outer blastomeres of the embryo acquire an apical-basal polarity and gain a tighter contact to each other by an increase of intercellular adhesions [17, 18]. Ongoing embryonic cleavage and compaction lead to formation of a solid mass of cells, at which stage the embryo is referred to as morula due to its shape resembling a mulberry (Latin, morus: mulberry). This is accompanied by a loss of pluripotency and resembles the first lineage decision, leading to the formation of trophectoderm (TE). The TE is a fluid-transporting epithelium responsible for formation of the blastocoel, a fluid-filled cavity, during blastocyst development [19] and resembles the progenitor cells of the embryonic part of the placenta. The inner blastomeres of the compacted morula form the inner cell mass (ICM), i.e. the pluripotent progenitor cells of the embryo proper. The embryo reaches the blastocyst stage at embryonic day 3 in mice, day 5 to 6 in humans and day 7 in cows [20-22]. Shortly afterwards, the blastocyst hatches out of the zona pellucida, which is the outer shell and functions as a protective envelope. On day 4 in mice [23], around day 9 in humans [23,24] and around day 19 to 20 postfertilization in cows [25-27], implantation occurs by which a physical and physiological contact between the blastocyst and the uterus is established. The embryo receives oxygen and nutrients by this direct contact, and later on by the placenta, to support growth [23]. The early embryo development of humans is depicted in Figure 3.

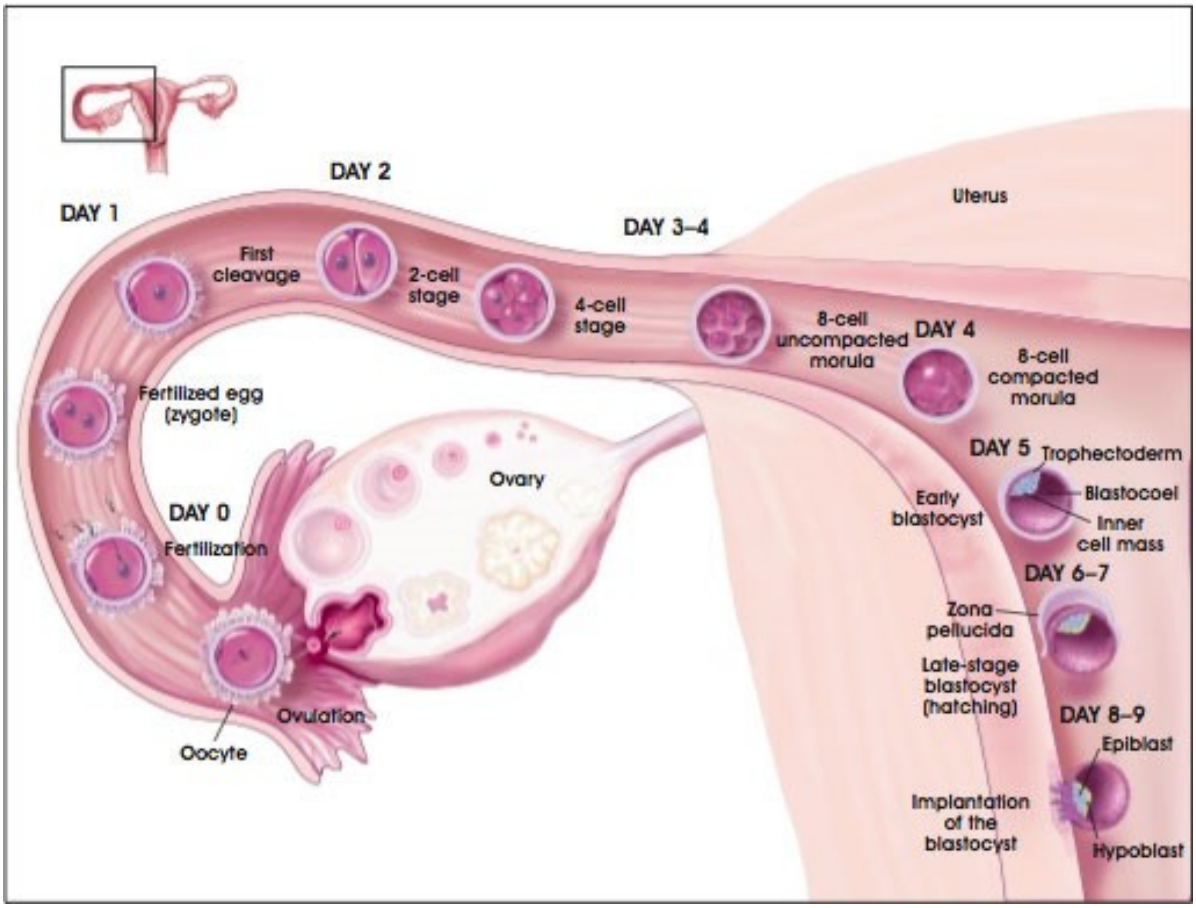

Figure 3. Early embryo development in humans. During ovulation, usually one arrested MII oocyte enclosed by cumulus cells is released from the ovary into the oviduct. Fertilization by sperm occurs in the oviduct at day 0. The male and female haploid pronuclei combine and a diploid zygote is formed. Embryonic cleavage begins shortly afterward and continues while the embryo travels along the oviduct towards the uterus. Soon after the embryo has reached the blastocyst stage, it hatches out of the zona pellucida and implants in the uterus at about day 9. Source: Early Development. In *Stem Cell Information* [World Wide Web site]. Bethesda, MD: National Institutes of Health, U.S. Department of Health and Human Services, 2009 [cited, June 25, 2014] (© 2001 Terese Winslow). Available at: http://stemcells.nih.gov/info/scireport/pages/appendixa.aspx

1.2 Considerations for the study of early mammalian development

1.2.1 The cow – an ideal model system for human reproduction

Ethical and practical reasons like the “German embryo protection law” prohibit direct analyses of human embryos, thus limiting mammalian embryo research to animals. The most widely used model organism for studying mammalian preimplantation embryo development is the mouse, but growing evidence suggests the bovine model to better reflect the human system [28]. Both cattle and humans are monovulatory, non-seasonal polycyclic and the duration of estrous and menstrual cycle are significantly longer compared to the mouse (21 and 28 days, respectively). Bovine and human reproductive biology also share important similarities regarding structure and function of the ovaries [29] and the role of the sperm centrosome for the first mitosis and the formation of a diploid genome [30, 31]. Furthermore, biochemical pathways and metabolism as well as size of oocytes and early embryos are comparable [28, 32-34].

Most molecular studies so far were performed in mice, and results can only be extrapolated to both non-rodent mammals and humans to a very limited extent because of the fundamental differences in their reproductive physiology and morphology. Therefore, besides addressing problems in ruminant reproduction and development, bovine oocytes and embryos can in a number of aspects serve as animal models for human reproduction and corresponding disorders and/or therapies [35], making research in this area especially valuable.

1.2.2 Generation of sample material

Mature bovine oocytes in large numbers can be generated *in vivo*, however, cows usually need to be subjected to hormonal superstimulation before oocytes can be aspirated about every five weeks, which is very costly, labor-intensive and time-consuming. In contrast, the *in vitro* maturation of bovine oocytes and generation of embryos can be performed with a significantly higher throughput by using ovaries easily accessible from abattoirs. The ovaries

are transferred to the laboratory where the oocytes are aspirated out of the follicles, which are the functional units of the ovary. These aspirated bovine oocytes are a heterogeneous group of immature GV oocytes surrounded by several layers of cumulus cells and are therefore referred to as cumulus-oocyte complexes (COCs). To obtain a mostly homogenous group of mature MII oocytes, the GV oocytes need to be matured *in vitro*, by which they develop into haploid gametes and become fertilizable. There is a variety of different protocols available, by which maturation can be induced. Frequently, the oocyte *in vitro* maturation (IVM) media is supplemented with estrous cow serum (ECS) and hormones. ECS is taken about 12 hours after ovulation, at estrus, when the female cow is sexually receptive. Just as common is the supplementation of IVM media with the hypophyseal gonadotropins FSH and LH, which has been shown to enhance maturation of immature oocytes, expansion of cumulus cells, fertilization and embryo development [32, 36, 37]. Further recurrently used supplementations are estrogens (estradiol) and androgens. Androgens may affect folliculogenesis directly via androgen receptors or indirectly through aromatization to estrogen [38]. Growth factors are deployed as well, e.g. the epidermal growth factor (EGF) [39] and the growth hormone somatotrophin (GH). GH has been shown to accelerate nuclear maturation and to enhance the yield of blastocysts after fertilization and embryo culture [40-42].

After 22 to 24 hours of maturation, mature MII oocytes, recognizable by the presence of an extruded polar body, are ready for fertilization with bull sperm by co-incubation for about 19 hours. Subsequently, the cumulus cells are removed by vortexing and the presumptive zygotes are cultured at a low oxygen level of 5 % until the desired stage, at which they are frozen. The process of *in vitro* embryo production is illustrated in Figure 4.

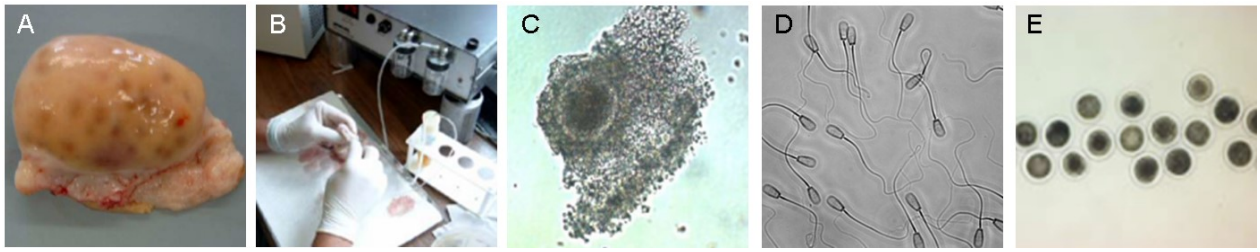

Figure 4. *In vitro* production of bovine oocytes and embryos. A: Bovine ovary collected from a local abattoir. **B:** Aspiration of cumulus-oocyte complexes (COCs) out of the ovarian follicles by vacuum pressure. **C:** Selection of COCs which are completely surrounded by cumulus cells using transmission light microscopy followed by hormone induced maturation for 22-to 24 h. **D:** Fertilization with bull sperm by co-incubation for 19 h. **E:** Removal of cumulus cells followed by embryo culture. Images were kindly provided by Dr. Myriam Demant.

1.2.3 The study of early mammalian development on a molecular level

The timing and morphology of pre-implantation development have been well studied [43, 44], but the underlying molecular mechanisms are only partially understood. Several peculiarities of oocytes make the understanding of crucial molecular processes during early embryogenesis challenging. For instance, unlike somatic cells, oocytes contain mRNAs which are extremely stable with an average half-life of around 12 days [45] and which are stored for longer periods of time. Similarily, many proteins are also already synthesized during oocyte growth and are stored for later use [46]. Furthermore, transcriptional activity is almost completely silenced starting several days before ovulation and ending with the major EGA at species-specific time points after fertilization [47, 48].

Only few studies so far have used proteomic approaches to analyze this highly critical period of mammalian development. Up to now, proteomic approaches require an expensive set of instruments and sophisticated know-how with respect to protein biochemistry, chromatography, mass spectrometry and bioinformatics. In contrast to RNAs, individual proteins differ enormously in their chemical and physicochemical properties (e.g. solubility) and the dynamic range of protein abundance in mammalian tissues or cells is in the order of 10^8. Initial attempts to use antibody arrays for highly parallel protein quantification [49], similar

to the RNA microarray strategies, suffered from the very limited number of suitable antibodies available and the narrow dynamic range of this approach. Until now, this technique is not powerful enough for holistic proteome analyses which usually are expected to cover several thousand proteins. In addition, an amplification procedure like PCR does not exist for proteins. Therefore, proteomic experiments have to include *de novo* identification by mass spectrometry. Probably as a consequence of the complex technology and experience required for proteomic analyses, many researchers have focused on the analysis of the transcriptome, which currently is much faster, cheaper and more comprehensive.

1.3 Molecular approaches applied to study early mammalian development

1.3.1 Transcriptomic studies

Several transcriptomic studies have targeted bovine embryogenesis so far [50-52], e.g., Vigneault and coworkers [50] studied genes associated with the MET by characterizing cDNA libraries enriched in embryonic transcripts expressed at this crucial step in embryogenesis. They demonstrated a high proportion of genes to be involved in gene transcription or RNA processing which is consistent with the presumably high transcriptional activity of late eight-cell embryos. In another study performed by Kues *et al.* [51], MII oocytes and preimplantation embryos were analyzed by Affymetrix GeneChip Bovine Genome Arrays. The authors detected approximately 350 genes which were transcribed in a stage-specific pattern before the major EGA at the eight-cell stage. Further, they described groups of transiently active genes and suggested dynamic changes in the embryo transcriptome. For example, they found a group of 48 genes which were up-regulated in the two-cell stage, down regulated in the four-cell stage, and then up-regulated again, and remaining highly transcribed until the blastocyst stage. Among them were IL18 and tumor protein, translationally-controlled 1 (TPT1). Graf and co-workers [52] established a comprehensive catalogue of transcripts from several bovine embryonic stages by RNA-Seq and detected genes activated between four-cell and blastocyst embryos. Genes activated at the four-cell stage were related to RNA processing, translation and transport, which was interpreted as preparatory event for major EGA. The largest proportion of gene activation was detected at the eight-cell stage, the time of major EGA.

It should be kept in mind, however, that analysis on the level of coding RNAs addresses the question whether or not the corresponding gene is more or less actively transcribed in a given sample. However, it does not give unambiguous evidence whether, and to what extent, the corresponding protein is either present in the sample or is going to be synthesized. This is a consequence of the numerous regulation steps in eukaryotic organisms between the appearance of the transcript or polyA+ RNA and the translation at the ribosome, e.g. splicing, 5’ capping and 3’ end proccessing [53]. Making matters even worse, protein processing by

proteolytic events, protein activation and signaling cascade activation by (de)phosphorylation is not accessible from either the genome or transcriptome [54, 55]. Therefore, analysis of the transcriptome is not a suitable surrogate for proteome analysis, and information about protein expression levels, abundance changes, or activation status can in general only be gained at the protein level.

1.3.2 Proteomic studies

1.3.2.1 Overview of proteomic techniques

The most popular analytical method for early proteomic experiments for a long period has been two-dimensional gel electrophoresis (2D-PAGE), which was described for the first time in 1975 [56, 57]. Since about ten years, a powerful alternative to 2D gel-based approaches has been developed and is referred to as nano liquid chromatography–tandem mass spectrometry or nano-LC-MS/MS (reviewed in [58]). In this approach, protein lysates of the original samples are digested with protease, separated by nano-chromatography and subsequently analysed by a tandem mass spectrometer. Tandem mass spectrometers can capture individual peptide ions in millisecond intervals and create peptide fragments by collision with gas molecules inside the instrument, a process referred to as collision-induced dissociation (CID) [59, 60]. Fortunately, fragmentation occurs predominantly at the peptide bond, yielding to a predictable fragmentation pattern. The peptide fragment masses are determined by the instrument and lead to so-called MS/MS spectra characteristic for each individual peptide. By correlation of all MS/MS spectra generated from a sample with theoretical MS/MS spectra calculated from a sequence database of the corresponding organism, proteins can be identified using dedicated software. The completeness of identification depends on the number of proteins present in the original lysate, their individual concentration, the effort taken to pre-fractionate proteins or peptides prior to RP chromatography, and the performance of both RP chromatography and mass spectrometer.

For relative quantification of individual proteins in LC-MS/MS approaches, several methods are available, based on either a direct quantification of MS or MS/MS signals or on a pre-labeling of proteins or peptides with chemical tags containing different compositions of stable isotopes prior to mass spectrometry. These tags introduce a characteristic mass shift between corresponding peptides obtained from different samples, facilitating co-analysis in the LC-MS/MS instrument [61]. The label free methods use either the signal intensity of the peptide in the MS spectrum (e.g., MAXQUANT [62]) or compare the number of MS/MS spectra obtained in different samples for each peptide by “spectral counting” [63]. Isotope labeling based quantification is generally regarded as more precise compared to label free methods, but requires additional efforts with respect to experimental procedures and costs. Non-radioactive stable isotope labels (SIL) are introduced either metabolically during cell culture, e.g., SILAC [64], or chemically at the level of proteins, e.g., ICAT [65] or of peptides, e.g., iTRAQ (isobaric tags for relative and absolute quantification) [66]. A benefit of the iTRAQ method is that it enables a multiplexed differential quantification between two to eight samples at the level of peptides. Samples are pooled prior to LC-MS/MS analysis, which increases the overall protein identification and quantification when working with low sample amounts, by far exceeding the results obtained by gel-based methods. Therefore, it is an ideal method when sample material is limited. The iTRAQ™ reagents enabling a 4-plex approach were developed by Darryl Pappin and coworkers in 2004 [66] and are depicted in Figure 5. They consist of four independent tags of the same mass which can be used for covalent labeling of the N-terminus and side chain amines of tryptic peptides from protein digests. Up to four samples are labeled individually with one of the iTRAQ reagents followed by combination of all samples and LC-MS/MS analysis. After fragmentation in MS/MS, four unique reporter ions (mass-to-charge ratio (*m/z)* = 114 - 117) are released from the tag which are used for quantification of the parent proteins [67]. An example of protein quantification using the iTRAQ method is given in Figure 6.

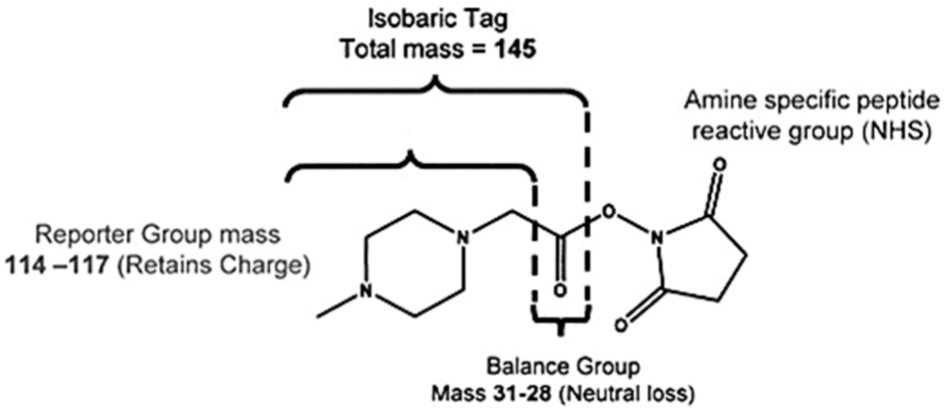

Figure 5. Chemical structure of the iTRAQ 4-plex reagents. The iTRAQ labels 114- to 117 are isobaric tags which consist of a charged reporter group, a neutral balance group to maintain an overall mass of 145, and an amine specific peptide reactive group [67].

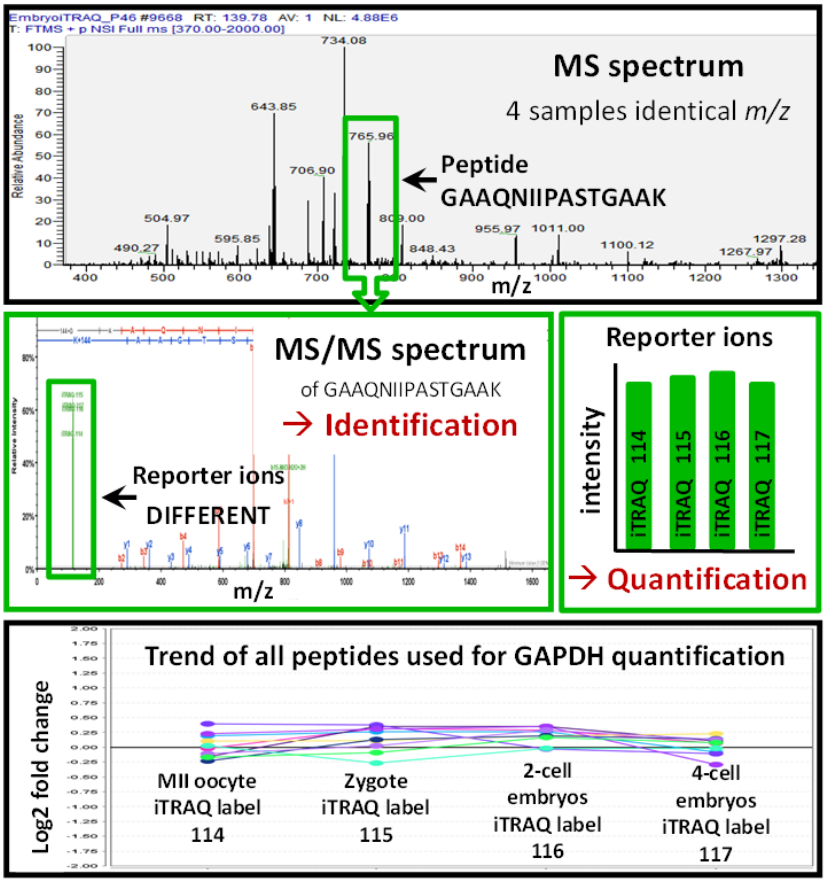

Figure 6. Example for quantification of the protein GAPDH using 4-plex iTRAQ. In the MS spectrum, all four labeled samples have identical *m/z* values and cannot be distinguished. After fragmentation in MS/MS, the reporter ions of the iTRAQ labels are released and can be used for quantification of individual peptides. Here, the quantification of the peptide GAAQNIIPASTGAAK is illustrated. This process is repeated many times and the mean of all quantified peptides is used for quantification of the corresponding protein.

A targeted proteomic method called selected reaction monitoring (SRM), also known as multiple reaction monitoring (MRM), is becoming increasingly popular for the quantification of pre-selected proteins in complex sample materials. It is based on stable isotope dilution and particularly eases protein quantification of samples from non-human species, because SRM requires no specific antibodies, only sequence information of the targeted protein. Additionally, it offers the option to study post-translational modifications and splice variants of proteins. SRM is also significantly more sensitive and specific than holistic proteomic approaches, enabling monitoring of unique ions amidst complex matrixes. For example, 100 amol of analyte can be quantified in only 1 µg total protein, making SRM the perfect method for quantification and verification of selected proteins in limited sample amounts. This is facilitated by two filtering steps: The first and third quadrupole of a triple quadrupole mass spectrometer serve as mass filters to isolate precursor ions and corresponding fragment ions, respectively. In the second quadrupole, the precursor ion is fragmented and the signal of the fragment ion is then monitored over the chromatographic elution time as illustrated in Figure 7 [68-70].

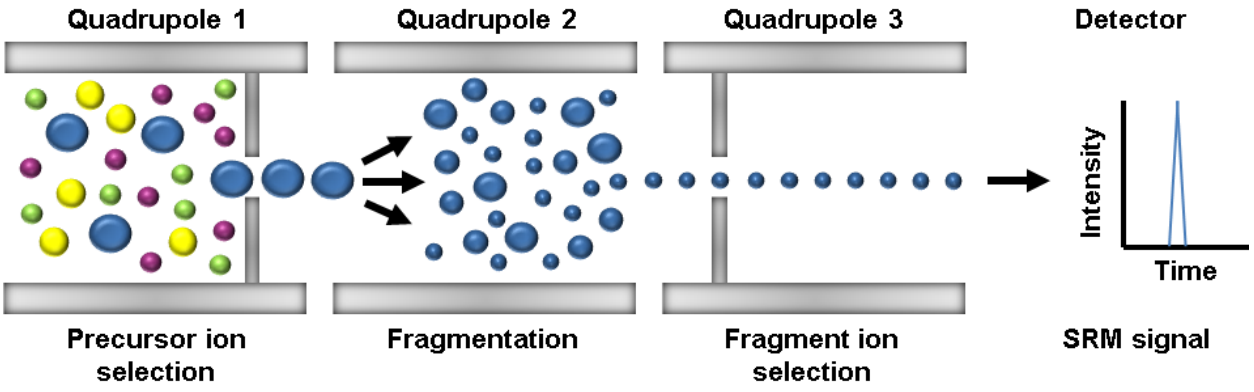

Figure 7. Principle of Selected Reaction Monitoring (SRM). SRM assays are usually performed on a triple quadrupole mass spectrometer. In the first quadrupole, a distinct precursor (peptide) ion is selected and fragmented in the second quadrupole. A corresponding fragment ion is selected in the third quadrupole and the SRM signal is monitored over the chromatographic elution time. (Adapted from: A. Schimdt, P. Picotti and R. Aebersold Proteomeanalyse und Systembiologie BIOspektrum, 1/2008, S. 44)

The establishment of an SRM assay starts with the selection of appropriate peptides, which are unique to the protein of interest (proteotypic), and show high mass spectrometry signal intensities. The next step is the selection of the most abundant peptide fragments. The specific precursor and corresponding fragment ion pairs represented by their *m/z* values are referred to as "transitions". Whenever possible, the most intense transition is used for quantification of the corresponding peptide and therefore referred to as “quantifier”. For additional improvement of the assay, usually one or two further transitions are monitored and referred to as “qualifiers”. Internal standards consisting of stable isotope-labeled (SI) peptides, also referred to as “heavy” peptides, enable relative and absolute quantification of proteins by calculation of the ratio endogenous (light) peptide to SI (heavy) peptide (Figure 8). SI peptides are chemically identical to the endogenous peptides, but their masses differ and their intensities can be co-detected [68, 71].

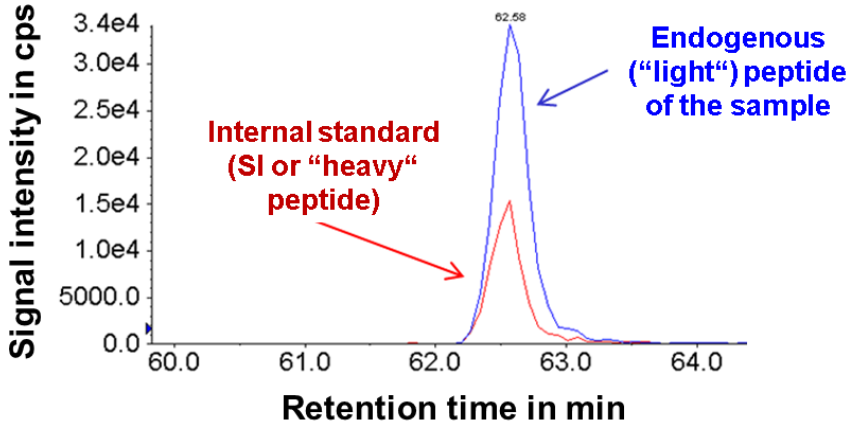

Figure 8. Protein quantification by SRM. The “light” peptide represents the endogenous peptide of the protein digest and the “heavy” peptide added stable isotope-labeled (SI) peptide. For quantification, the ratio between the signal intensities is calculated. Cps = counts per second.

1.3.2.2 Proteomic studies targeting bovine oocyte maturation and early embryogenesis

Proteomic data of oocyte maturation, and especially of early embryogenesis in large mammals like cattle, is scarce. One of the few studies in this research area used a 2D gel-based approach to study meiotic maturation of oocytes and identified differentially expressed proteins [72]. Bovine GV, MI, or MII oocytes were treated either with or without the cyclin dependent kinases (CDK) inhibitor butyrolactone I (BL I), and subjected to 2D-PAGE. There is increasing evidence that meiotic resumption is under the control of CDK1 kinase, which forms the maturation promoting factor MPF together with cyclin B, and mitogen-activated protein kinases MAPK [73, 74]. BL I is supposed to impair resumption of meiosis due to its CDK-inhibiting quality. In a preceding study [75], the group had already demonstrated that BL I inhibits phosphorylation of essential components of the translation initiation complex and therefore modulates translation. Nevertheless, BL I treatment seemed to have no apparent effect on the overall expression of proteins during IVM in the follow-up study [72] and the authors concluded that alterations in the proteome are mainly caused by protein degradation and not by changes in the turnover of proteins. Forty proteins could be identified in the study and four of them were differentially abundant, from which cyclin E2 and peroxiredoxin-2 were suggested to serve as molecular markers for meiotic maturation [72].

In another 2D gel-based approach targeting oocyte maturation [76], more than 3,000 protein spots were detected by fluorescence scanning, and 38 significant differences in protein abundance between GV and MII oocytes were found. Of these 38 spots, the intensities of 21 increased during maturation, while the intensities of 17 decreased. Among the proteins with decreased in abundances during maturation were clusterin (CLU), translationally controlled tumour protein (TCTP), peroxiredoxin-3 (PRDX3), and 14-3-3 protein epsilon (YWHAE). The latter has been suggested to mediate Cdc25 phosphatase inhibition [77], which is a phosphatase required for MPF activation [78]. Furthermore, changes in the abundance of different isoforms of “similar to glutathione-s-transferase Mu 5” (GSTM5) were shown.

A recently published study [79] used a nano-LC-MS/MS approach in combination with iTRAQ labeling to analyze the effect of the proteasomal inhibitor MG132 during bovine oocyte maturation. MG132 has already been shown to improve developmental competence of parthenogenetically activated oocytes in the pig [80]. The proteasome is a multisubunit proteolytic complex [81] and early in maturation, completion of meiosis I requires an inactivation of MPF through proteasomal cleavage of ubiquitinated cyclin B1 [82]. A total of 669 proteins were identified in MII oocytes, and 653 proteins could be quantified. Exposure to MG132 increased the abundance of six proteins, e.g. glyceraldehyde-3-phosphate dehydrogenase (GAPDH), an enzyme involved in glycolysis and related to developmental competence [83] and tubulin alpha-1C chain (TUBA1C), important for organellar movement [84]. The study demonstrated that treatment with MGF132 late in maturation improves oocyte competence in cattle.

One of the earliest studies addressing quantitative changes in the proteome of bovine embryos used a 1D gel-based approach. The amount of *de novo* protein synthesis during early embryogenesis was found to decrease between the zygote and the eight-cell stage and then to increase until the blastocyst stage [85]. These results supported the determination of the timing at the MET [86]. A more recent 2D gel-based study of bovine embryos [87] aimed to identify maternal housekeeping proteins (MHKP) translated during bovine oocyte maturation and early embryo development. It was demonstrated, that 92 proteins were synthesized *de novo* in oocyte maturation and 123 proteins in embryogenesis. A total of 46 proteins were contained in both periods which were therefore considered as possible MHKPs. Ten of these potential MHKPs were identified, including heat shock 70 kDa protein (HSP70) and ubiquitin carboxyl-terminal hydrolase isozyme L1 (UCH-L1).

An overview of proteomic studies concerning oocyte maturation and early embryogenesis using a bovine model system is presented in Table 1.

Table 1. Overview of proteomic studies concerning bovine oocyte maturation and early embryogenesis.

Study subject / Approach	Major findings	Conclusions	Reference
Oocyte maturation / radiolabeling + 2D-PAGE	Identification of cyclin B	Cyclin B may have an initiator role for meiotic resumption	Levesque & Sirard 1996
Oocyte maturation / radiolabeling + 2D-PAGE	Characteristic patterns of protein synthesis detected	Protein synthesis affects different proteins during the transition of GV to MII stage; 3 patterns of protein synthesis detected	Coenen *et al.* 2004
Oocyte maturation / 2D-PAGE	40 proteins identified; 4 were differentially expressed: tubulin-chain (TBB), cyclin E2 (CCNE2) and truncated CCNE2, protein disulfide isomerase (PDIA3), and peroxiredoxin 2 (PDX2)	CCNE2 and PDX2 as molecular markers for meiotic maturation suggested	Bhojwani *et al.* 2006
Oocyte maturation / 2D-DIGE saturation labeling	38 significant differences in protein abundance between GV and MII oocytes; 10 identified: clusterin (CLU), translationally controlled tumour protein (TCTP), E2, 6-phosphogluconolactonase (6PGL), peroxiredoxin-3 (PRDX3), Eukaryotic translation (EF-1ɣ), and 14-3-3 protein epsilon (YWHAE) and 3 different isoforms of glutathione-s-transferase Mu 5 (GSTM5)	Varying abundance changes between different isoforms of GSTM5 revealed; Decrease of YWHAE fits MPF activation to promote mitosis; Protein candidates for *in vitro* maturation suggested	Berendt *et al.* 2009
Oocyte maturation / iTRAQ labeling + LC-MS/MS	669 proteins identified and 653 quantified; relative abundance of 7 and 24 proteins increased and decreased in response to the proteasomal inhibitor MG132, respectively	Inhibition of proteasomes during the late phase of oocyte maturation can improve the developmental competence of oocytes	You *et al.* 2012b
Embryogenesis / radiolabeling + 1D-PAGE	Protein synthesis decreased between the zygote and the eight-cell stage and then increased until the blastocyst staged	The maternal-to-embryonic transition occurs at the eight- to 16-cell stage	Frei *et al.* 1989
Oocyte maturation + embryogenesis / radiolabeling + 2D-PAGE	46 proteins present during oocyte maturation as well as early embryogenesis; 10 identified: HSC71, HSP70, CypA, UCH-L1, GSTM5, Cct5, E-FABP, 2,3-BPGM, E2D3 and ß-actin/ɣ-actin	Translation affects different proteins during oocyte maturation and embryogenesis; Housekeeping proteins suggested	Massicotte *et al.* 2006

1.4 Aim of the thesis

Early embryogenesis is a highly critical period of mammalian development. The timing and morphology of pre-implantation development have been well studied, but molecular processes, particularly at the level of proteins, are still poorly understood. It is known that the rate of translation before embryonic genome activation is very low. This thesis will address the question if any significant differences in the proteome of oocytes and early embryos can be quantified which may be due to *de novo* translation, activation or degradation of proteins. Furthermore, a variety of rearrangement processes occur during maturation and embryonic cleavage which will be studied on a molecular level to identify relevant proteins. To achieve these objectives, modern LC-MS/MS-based proteomic techniques, such as iTRAQ and SRM, will be used to study the qualitative and quantitative proteome profiles during oocyte maturation and early embryogenesis. Due to crucial similarities to human reproduction, all analyses are performed with a bovine model system.

The first aim is to investigate the proteome profile of oocyte maturation by comparison of immature GV oocytes and mature MII oocytes. Additionally, the influence of hormones, such as LH/FSH and LH/FSH/GH, on the proteome during maturation is assessed. The first steps of mammalian embryogenesis are also studied, i.e., zygotes, two-cell embryos and four-cell embryos using MII oocytes as a reference group. For both analyses, the holistic iTRAQ method is applied which enables the simultaneous differential analysis of four sample groups. Data derived from these discovery proteomic approaches are used for the establishment of highly sensitive targeted SRM assays which will be used for verification of results in pools of only ten oocytes or embryos. Another objective to be achieved by SRM is the simultaneous relative quantification of at least ten selected proteins in a broader set of embryonic stages from the GV oocyte until the blastocyst stage. Absolute protein contents will also be determined for a subset of proteins. Compared to relative values, these protein concentrations have the additional benefit that they can be used as independent reference values for other laboratories, as read out for functional assays, and for characterization of biological systems.

This thesis presents a comprehensive proteomic analysis of early bovine development and demonstrates that oocyte maturation and passage through the first embryonic cleavage cycles is associated with distinct quantitative and qualitative changes of protein profiles.

2. Materials and Methods

2.1 Materials

2.1.1 Media and hormones for *in vitro* embryo production

TCM 199	Minitüb (Tiefenbach, Germany)
TL media for fertilization	Minitüb (Tiefenbach, Germany)
TL media for sperm cell capacitation	Minitüb (Tiefenbach, Germany)
SOF	Minitüb (Tiefenbach, Germany)
ECS	Produced by the group of Prof. Wolf
b-LH	Sioux Biochemical (SiouxCenter, IA, USA)
b-FSH	Sioux Biochemical (SiouxCenter, IA, USA)
rbGH	Biomol (Hamburg, Germany)

2.1.2 Plastic ware

Four-well plates	Nunc, Thermo Scientific (Rockford, IL, USA)
Sterile centrifuge tubes, 11 mL, PS, for IVF	Nunc, Thermo Scientific (Rockford, IL, USA)
40 mm tissue culture dish	Nunc, Thermo Scientific (Rockford, IL, USA)
94 mm petri dishes	Roth (Karlsruhe, Germany)

2.1.3 Instruments

Distal coated Silica Tips	New Objectiv (Woburn, MA, USA)

Eksigent Ultra nano-LC	Eksigent (Dublin, CA, USA)
Ettan MDLC	Amersham Biosciences (Freiburg, Germany)
Electronic aspiration pump, modell 3014	Labotect (Göttingen, Germany)
Heraeus Sepatech Megafuge	Hareus (Hanau, Germany)
LSM 510 Meta	Zeiss (Jena, Germany)
LTQ Orbitrap XL	Thermo Scientific (Rockford, IL, USA)
nanoACQUITY UPLC system	Waters (Milford MA, USA)
Sonorex RK 100	Bandelin (Berlin, Germany)
Thermomixer 5436	Eppendorf (Köln, Germany)
Transferpettor	Brand (Wertheim, Germany)
QTRAP 5500	AB SCIEX (Framingham, MA, USA)
Vacuum concentrator	Bachhofer (Reutlingen, Germany)
Vortex Genie 2	Bachhofer (Reutlingen, Germany)

2.1.4 Columns

SCX column	Biobasic/Thermo Scientific (Rockford, IL, USA)
C18 spin column	Pierce/Thermo Scientific (Rockford, IL, USA)
Trap column, C18 PepMap 100, 5 µm, 300 µm x 5 mm	LC Packings/Dionex (Idstein, Germany)
Separation column, 15 cm, ReproSil-Pur 120 C18 AQ, 2.4 µm bead size, 75 µm i.d.	Dr. Maisch (Ammerbuch-Entringen, Germany)

2.1.5 Antibodies

Rabbit polyclonal to WEE2, ab121943, IF: 1/80	Abcam (Cambridge, UK)
Rabbit polyclonal to Vimentin, ab45939, IF: 1/500	Abcam (Cambridge, UK)
Monoclonal mouse-anti-Vimentin, V6630, IF: 1/800	Sigma-Aldrich (Steinheim, Germany)
Monoclonal mouse-anti-α-Tubulin, clone DM1A, T6199, IF: 1/500	Sigma-Aldrich (Steinheim, Germany)
Goat-anti-mouse-FITC, Cat. No. 115-095-003, IF: 1/500	Dianova (Hamburg, Germany)
Goat-anti-rabbit-FITC, Cat.-No. 111-095-003, IF: 1/250	Dianova (Hamburg, Germany)
Goat-anti-mouse-Cy5, Cat.-No. 115-175-003, IF: 1/500	Dianova (Hamburg, Germany)
Goat-anti-rabbit-Cy5, Cat. No. 111-175-003, IF: 1/500	Dianova (Hamburg, Germany)
Phalloidin-TRITC, P1951, IF: 1/250	Sigma-Aldrich (Steinheim, Germany)

2.1.6 Solvents and water

Acetonitrile, LC-MS grade, LiChrosolv®	Merck Millipore (Darmstadt, Germany)
Deuterium oxide, 99.9 %	Merck Millipore (Darmstadt, Germany)
Ethanol, LC-MS grade	Merck Millipore (Darmstadt, Germany)
Methanol, LC-MS grade, LiChrosolv®	Merck Millipore (Darmstadt, Germany)
Water, LC-MS grade, LiChrosolv®	Merck Millipore (Darmstadt, Germany)

2.1.7 Chemicals, kits and stable isotope-labeled peptides

Aprotinin from bovine lung	Sigma-Aldrich (Steinheim, Germany)

Bovine serum albumin (BSA)	Sigma-Aldrich (Steinheim, Germany)
DAPI	Sigma-Aldrich (Steinheim, Germany)
Dithiothreitol (DTT)	Roth (Karlsruhe, Germany)
EGTA	Sigma-Aldrich (Steinheim, Germany)
Formic acid (FA)	Sigma-Aldrich (Steinheim, Germany)
HeavyPeptide AQUA™ Ultimate peptides	Thermo Fisher (Rockford, IL, USA)
Heparin sodium salt	Sigma-Aldrich (Steinheim, Germany)
iTRAQ® Reagent 4plex	AB SCIEX (Framingham, MA, USA)
Iodacetamide (IAA)	Sigma-Aldrich (Steinheim, Germany)
Mineral oil for embryo culture	Sigma-Aldrich (Steinheim, Germany)
Paraformaldehyde	Sigma-Aldrich (Steinheim, Germany)
PEPotec™ SRM peptides	Thermo Fisher (Rockford, IL, USA)
Pipes	Sigma-Aldrich (Steinheim, Germany)
Polyvinylpyrrolidon (PVP)	Sigma-Aldrich (Steinheim, Germany)
Potassium chloride (KCl)	Merck Millipore (Darmstadt, Germany)
Seq grade modified trypsin	Promega (Madison, WI, USA)
Sodium chloride (NaCl)	Merck Millipore (Darmstadt, Germany)
Sodium pyruvate	Sigma-Aldrich (Steinheim, Germany)
Taxol	Sigma-Aldrich (Steinheim, Germany)
Triton X-100	Sigma-Aldrich (Steinheim, Germany)
Tris	Roth (Karlsruhe, Germany)
Urea	Roth (Karlsruhe, Germany)
Vectashield® mounting medium (Anti fading, with DAPI)	LINARIS (Dossenheim, Germany)

2.2 Methods

2.2.1 Generation of oocytes and embryo production

2.2.1.1 Generation of GV oocytes

For post-mortem collection of cumulus-oocyte complexes (COCs), bovine ovaries were obtained from a local abattoir and transferred to the laboratory in phosphate-buffered saline (PBS) at 20-25 °C. COCs were aspirated from 2-8 mm follicles with a 20-gauge needle and a vacuum pressure of approximately 50 mm Hg and selected as previously described [88]. Oocytes with a compact layer of cumulus cells and a homogeneous ooplasm were selected and denuded mechanically by vortexing for four minutes in PBS. The denuded oocytes were washed three times in PBS containing 1 mg/mL PVP, frozen buffer-free on dry ice and stored at -80 °C until analysis.

2.2.1.2 In vitro oocyte maturation

COCs were prepared as described above and washed three times in maturation media consisting of tissue culture medium 199 (TCM 199, Minitüb, Tiefenbach, Germany) supplemented with 5 % ECS, 0.025 IU/mL b-FSH and 0.0125 IU/mL b-LH (Sioux Biochemical, IA USA). If required, the medium was supplemented with 100 ng/mL GH. The COCs were transferred to four-well plates (Nunc, Thermo Scientific, Rockford, IL, USA) and matured in 400 µL of maturation media for 23 h at 39 °C in a humidified atmosphere with 5 % CO_2 in air.

2.2.1.3 In vitro embryo production

COCs were collected and matured as described above. They were washed three times in fertilization medium consisting of TL fertilization media (Minitüb) enriched with 6 mg/mL bovine serum albumin (BSA), 22 µg/mL sodium pyruvate and 10 µg/mL heparin sodium salt followed by fertilization in 400 µL droplets of media. Frozen-thawed spermatozoa were subjected to the swim-up procedure described by Parrish *et al*. [89] for 60 min and were subsequently co-incubated with COCs for 19 h at 39 °C in a humidified atmosphere with 5 % CO_2 in air. Presumptive zygotes were mechanically denuded by vortexing and washed three times in culture medium consisting of synthetic oviduct fluid (SOF, Minitüb) supplemented with 5 % ECS, 1 % MEM non-essential amino acids solution, 4 % BME amino acids solution and 0.36 mg/mL sodium pyruvate. For embryo culture at 39 °C in a humidified atmosphere with 5 % CO_2, 5 % O_2, and 90 % N_2, they were placed in 400 µL droplets of culture medium under mineral oil in four-well dishes.

2.2.2 Sample preparation for iTRAQ and SRM analysis

For iTRAQ and SRM analysis, batches of ten and 50 GV oocytes, MII oocytes, zygotes, two-cell embryos, four-cell embryos, eight- to 16-cell embryos, morulae and blastocysts each were prepared. MII oocytes were collected after 23 h of maturation and mechanically denuded by vortexing in PBS. Zygotes, two-cell embryos, four-cell embryos and eight- to 16-cell embryos were collected at 19, 35, 43 and 70 hours post insemination (hpi), respectively. Morulae were collected at day 5 post insemination and blastocysts were collected at day 7 post insemination. Hatched blastocysts were collected at day 8 post insemination. Oocytes and embryos were evaluated microscopically, washed three times in PBS containing 1 mg/mL PVP, frozen on dry-ice and stored at -80 °C until analysis.

2.2.3 Preparation of stable-isotope dilution for SRM analysis

For SRM analyses, SI peptides corresponding to all targeted peptides were purchased which served as internal standards. For relative and absolute quantification, crude PEPotec™ SRM peptides and HeavyPeptide AQUA™ Ultimate peptides (Thermo Fisher,Rockford, IL, USA) were purchased, respectively. All SI peptides were modified with a heavy K [Lysine (13C6; 15N2)] or R [Arginine (13C6;15N4)] at the C-terminus. Stock solutions of both PEPotec and AQUA peptides were prepared. Disclosed amounts of PEPotec™ SRM peptides were provided by the manufacturer suspended in 0.1 % trifluoroacetic acid (TFA) in 50 % (v/v) acetonitrile (ACN)/water. Depending on the provided amount of peptide, the peptides were pre-diluted with 50 % ACN to 1000x the desired concentration in the final sample (listed in Supplementary Table 10), and combined in one stock solution which was stored in 10 µL aliquots at -20 °C. Prior to use, this stock solution was diluted 1/100 with 5 % ACN. The HeavyPeptide AQUA™ Ultimate peptides were provided by the manufacturer in a concentration of 5 pmol/µl suspended in 5 % (v/v) ACN/water. The peptides were pre-diluted with 5 % ACN to 10x the desired concentration in the final sample (listed in Supplementary Table 10), and combined in one stock solution which was stored in 100 µL aliquots at -20 °C.

2.2.4 Trypsin digestion

Samples were lysed in 0.5 µL denaturation buffer (8 M urea, 50 mM Tris-HCl, pH 8.0) per oocyte or embryo and homogenized by ice-cooled sonification for 10 min (Sonorex RK100, Bandelin, Berlin, Germany) and freezing on dry-ice. For trypsin digestion of SRM samples, the two stock solutions containing either PEPotec or AQUA SI peptides were combined 1/1. Denaturation buffer containing 10 M urea, 50 mM Tris-HCl, pH 8.0 was diluted with an aliquot of the combined SI peptide solution to give a final concentration of 8 M urea, which was used for sample lysis. The lysates were prepared for trypsin digestion by reduction of cysteine residues during 30 min incubation in 4.5 mM dithiothreitol (DTT) at 65 °C followed by alkylation in 10 mM iodoacetamide (IAA) for 15 min at room temperature in darkness. For

trypsin digestion, samples were diluted with water to reach a final concentration of 1 M urea and 5 ng porcine trypsin (Seq Grade Modified Trypsin, Promega, Madison, WI, USA) per oocyte or embryo was added. Incubation was performed overnight at 37 °C and the peptide solution was subsequently dried using a vacuum concentrator (Bachofer, Reutlingen, Germany) and stored at -80 °C.

2.2.5 iTRAQ labeling and pre-fractionation by strong cation exchange chromatography (SCX)

Preceding iTRAQ labeling, all sample batches belonging to one sample were combined and desalted using C18 spin columns (Pierce, Thermo Scientific, Rockford, IL, USA) according to the manufacturer's protocol with an additional wash step (0.5 % TFA, 5 % ACN) prior to elution and subsequent drying in a vacuum concentrator (Bachofer, Reutlingen, Germany). Each sample was dissolved in 15 µL iTRAQ dissolution buffer (AB SCIEX, Framingham, MA, USA) and half of each corresponding iTRAQ reagent was added (iTRAQ aliquots with undisclosed concentrations suitable to label 5 to 100 µg of protein, iTRAQ-4plex kit, AB SCIEX, Framingham, MA, USA). After labeling for 1 h at room temperature, the peptides of all four pools belonging to one biological replicate were combined. The sample complexity was reduced by a pre-fractionation step using SCX. Peptides were eluted from the SCX column (Biobasic, Thermo Scientific, Rockford, IL, USA) stepwise using different molarities of potassium chloride (KCl) and subsequently desalted using C18 spin columns (Pierce, Thermo Scientific). SCX fractions were evaporated to dryness under vacuum (vacuum concentrator, Bachofer) and stored at -80 °C until LC-MS/MS analysis.

2.2.6 LC-MS/MS analysis of iTRAQ samples

The SCX fractionated and desalted peptides belonging to the analysis of oocyte maturation were subjected to LC-MS/MS analysis using an Ettan MDLC (Amersham Biosciences, Freiburg, Germany) connected to an Orbitrap XL instrument (Thermo Scientific, Rockford, IL, USA). The SCX fractionated and desalted peptides belonging to the analysis of early embryogenesis were subjected to LC-MS/MS analysis using an Eksigent Ultra nano-LC device (Eksigent, Dublin, CA, USA) connected to the Orbitrap XL instrument. Peptide solutions were injected and trapped at 10 µL/min on a guard column packed with C18 PepMap 100, 5 µm, 300 µm x 5 mm (LC Packings/Dionex, Idstein, Germany) and separated at a constant flow rate of 280 nL/min with a 15 cm separation column (ReproSil-Pur 120 C18 AQ, 2.4 µm bead size, 75 µm i.d., Dr. Maisch, Ammerbuch-Entringen, Germany). Long 5 h chromatographic gradients for separation were used with a linear ramp from 8-40 % B (0.1 % formic acid, 84 % ACN) over 265 min. The chromatographic system was coupled online to the Orbitrap XL instrument via a distal coated SilicaTip (FS-360-20-10-D-20, New Objective, Woburn, MA, USA) and the electrospray ionization was operated at a needle voltage of 1.6 kV. For data acquisition, collision induced dissociation (CID) spectra for protein identification in the linear ion trap and higher energy collision-induced dissociation (HCD) spectra for protein quantification via the lower mass iTRAQ reporter ions in the Orbitrap mass analyzer were acquired. Acquisition cycles consisted of one MS scan (mass range m/z 300–2000) followed by three data dependent CID and HCD MS/MS scans each. The mass spectrometer was run in positive ion mode, dynamic exclusion was implemented and a collision energy of 35 % was applied. For analysis of oocyte maturation, each SCX fraction was measured trice consecutively with additional mass exclusion lists applied based on the peptide identifications of the first run, or based on the first and second run combined. For analysis of early embryogenesis, each SCX fraction was measured twice consecutively and in the second run, an additional mass exclusion list based on the peptide identifications of the first run was applied. Mass exclusion lists were generated with Proteome Discoverer 1.3 (Thermo Scientific, Rockford, IL, USA).

2.2.7 iTRAQ data processing and assessment

MS RAW data was transformed into a mascot generic format (mgf) file and low mass range iTRAQ reporter ion peaks from HCD scans were merged into CID scans via the MassSpecUtils tool (The University of Washington's Proteomic Resource Facility). Merged mgf files were searched with MASCOT Daemon [90] and MASCOT Server version 2.4 (Matrix Science, Boston, USA) against the bovine Uniprot database (release 05/2012, 31468 entries) including an automatic "Decoy Database". Search parameters comprised trypsin as enzyme with maximal one missed cleavage allowed, carbamidomethylation at cysteine and iTRAQ labeling at lysine and N-terminal residues as fixed modifications. As variable modification, oxidation at methionine was set. Further parameters were: peptide charge: 2+ and 3+; peptide tol. ±: 2 Da and MS/MS tol. ±: 0.8 Da. MASCOT files were then further evaluated with the Scaffold software 4.0.5 (Proteome Software, Portland, OR, USA) to obtain a list of protein identifications. At least two individual peptides per protein were required and the probability threshold for the identified proteins was set to ≥ 99 % controlling for a false-discovery rate (FDR) below 1 % and a mass accuracy of precursors <10 ppm. Quantification of iTRAQ signals was accomplished with the Q+ module of the Scaffold software and results were exported to Microsoft Excel (2010) for statistical evaluation.

2.2.8 Subcellular localization and functional annotation clustering

Subcellular location of identified proteins was determined by the DAVID Bioinformatics Resources 6.7 [91, 92], available at http://david.abcc.ncifcrf.gov/home.jsp according to the category GOTERM_CC_FAT. Self-organizing tree algorithm (SOTA) [93] clustering was accomplished by the R (R Development Core Team, 2011) plug ins clValid and LSD and four clusters were created. Functional and network analysis of proteins was performed with the Cytoscape 3.1.0 plug-ins ClueGO v2.0.8 [94] and CluePedia v1.0.9 [95]. GO tree levels 5 to 6 were displayed with a minimum number of 2 genes per cluster. For statistics, the right-sided hypergeometric test was applied to calculate enrichment for terms and groups according to the GO biological process. Functional grouping was based on κ-score (> 0.3) and GO term fusion was activated for redundancy reduction in large clusters.

2.2.9 Establishment of a multiplexed SRM assay

For each targeted protein, two high-confidence proteotypic peptides and three fragment ions per peptide were selected based on discovery LC-MS/MS data of iTRAQ experiments and *in silico* digests of the proteins generated with the MRMPilot™ 2.0 software (AB SCIEX, Framingham, MA, USA). SI peptides corresponding to each analyzed peptide were used as internal standard and were applied in test runs for transition selection and optimization of collision energies. Whenever possible, the most intense transition was used for quantification ("quantifier"), and two more transitions were selected for "qualifiers". All selected precursor ions had a charge state of + 2 or + 3 and the majority were y-ions. The amount of internal standard added to each sample was adjusted to closely reflect the protein amount of the corresponding endogenous peptides. Details of the multiplexed SRM assay are listed in Supplementary Table 10.

2.2.10 LC-MS/MS analysis of SRM samples and data analysis

Samples for SRM analysis were desalted using C18 spin columns (Pierce, Thermo Scientific) according to the manufacturer's protocol and subsequently dried in a vacuum concentrator (Bachofer). SRM analyses were performed with a combination of a nano-HPLC system (nanoACQUITY UPLC system, Waters, Milford MA, USA) and a triple quadrupole linear ion trap mass spectrometer (QTRAP 5500, AB SCIEX). Injected peptide solutions were loaded at a flow-rate of 10 µL/min on a reversed phase trap column with C18 PepMap 100, 5 µm, 300 µm x 5 mm (LC Packings/Dionex, Idstein, Germany) and separated at a constant flow rate of 280 nL/min with a 15 cm separation column (ReproSil-Pur 120 C18 AQ, 2.4 µm bead size, 75 µm i.d., Dr. Maisch, Ammerbuch-Entringen, Germany) with a gradient from 1-60 % B (0.1 % formic acid in ACN) in 30 min followed by a second ramp to 80 % B in 15 min. The chromatographic system was coupled online to the triple quadrupole instrument via a distal coated SilicaTip (FS-360-20-10-N-20, New Objective, Woburn, MA, USA) and for electrospray ionization, and a needle voltage of 2.5 kV was applied to ionize peptides in "positive ionization mode". A MRM detection window of 240 s and a target scan time of 3 s (1280 cycles) were used. SRM data was exported to Multiquant 2.1.1 (AB SCIEX, Framingham, MA, USA) and manually evaluated. Quantification was performed by calculating the ratios of the quantifier signal intensities of endogenous peptides and corresponding SI peptides. A signal to noise ratio ≥ 10 was used for valid signals. Relative quantification values were expressed as log2 fold change and absolute quantification values as amol or fmol per oocyte or embryo.

2.2.11 Statistical analysis

Protein abundance in pair wise comparisons of groups in iTRAQ studies was considered significantly altered with a log2 fold change ≥ |0.6| and a t-test significance level of $p \leq 0.05$. iTRAQ intensity data of all groups was compared using analysis of variance (ANOVA, $p < 0.05$, fold change > 1.5). T-tests, ANOVA and principle component analysis (PCA) analysis were performed using R (R Development Core Team, 2011). Analyses with R were

performed in collaboration with Kathrin Otte. GraphPad Prism 6.04 (GraphPad Software, La Jolla, CA, USA) was used for graphical illustration of SRM and iTRAQ data and for statistical analysis of SRM data (multiple T-tests). Differences were regarded as significant in case of $p < 0.05$ and log2 fold change ≥ |0.6|.

2.2.12 Immunoflourescence and confocal microscopy of oocytes and embryos

Cumulus cells were removed by gentle pipetting and oocytes or embryos were fixed in 400 µL of Albertini fixation solution (0.1 M Pipes, pH 6.9, 5 mM $MgCl_2$, 2.5 mM EGTA, 50 % deuterium oxide, 2 % paraformaldehyde, 0.5 % triton X-100, 0.01 % aprotinin, 1 µM taxol) for 20 min at 37 °C and subsequently washed with PBS containing 1 mg/mL PVP. For intracellular staining, samples were permeabilized in 0.5 % Triton X-100 in PBS containing 1 mg/mL PVP for 1 h at room temperature followed by washing with PBS containing 1 mg/mL PVP. Incubation with indicated primary antibodies and subsequently with respective secondary antibodies was performed for 30 min at 37 °C followed by washing with PBS containing 1 mg/mL PVP each time. After staining, the oocytes were mounted in Vectashield® mounting medium (Linaris, Dossenheim, Germany) between two coverslips, thereby maintaining the 3-D structure of the oocytes and embryos. Images were captured using a confocal laser scanning microscope (LSM 510 Meta, Zeiss, Germany) with a 40x PlanApochromat (numerical aperture 1.3) oil immersion objective in collaboration with Dr. Felix Habermann.

3. Results

3.1 Generation of oocytes and embryos

For the generation of oocytes and embryos, ovaries were obtained from a local abattoir and transported to the laboratory. Cumulus oocyte complexes (COCs) were aspirated out of the ovaries, which delivered on average seven COCs per ovary. COCs were washed, and either denuded for preparation of GV oocytes or subjected to *in vitro* oocyte maturation and fertilization, followed by *in vitro* embryo culture until the desired stage. All oocytes and embryos were evaluated microscopically before washing with PBS containing 1 % PVP. Further, the oocytes and embryos were frozen buffer-free on dry ice and stored at -80 °C until analysis.

The success of *in vitro* embryo production (IVP) was controlled regularly (about two times per month) by determination of the two-cell embryo and blastocyst rate compared to presumptive zygotes subjected to embryo culture. On average, about 70 % of the zygotes cleaved into two-cell embryos. About 30 % of the zygotes reached the blastocyst stage at day 7 post insemination, and this rate increased to about 40 % at day 8 post insemination (Figure 9).

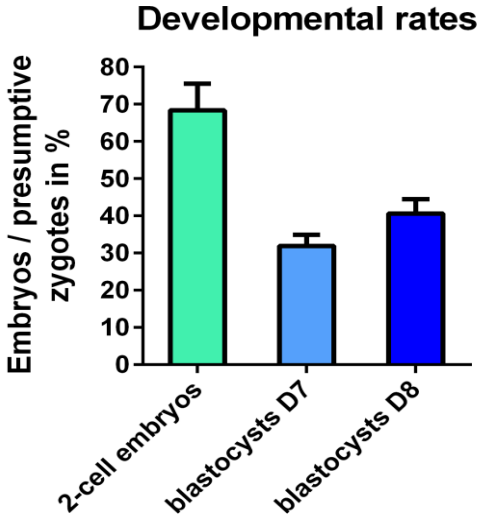

Figure 9. Developmental rates of *in vitro* embryo production. Developmental rates were determined by subjecting 50 to 150 presumptive zygotes to embryo culture until the blastocyst stage. The ratios between presumptive zygotes and two-cell embryos (n=10), blastocysts D7 (n=10) and blastocysts D8 (n=3) ± SD were calculated. D7 = day 7 post insemination; D8 = day 8 post insemination.

3.2 Proteome signatures of bovine oocyte maturation

3.2.1 General remarks and experimental strategy

The aim of this study was to investigate the effects of IVM on the proteome of oocytes and to assess the influence of different hormone supplementations to maturation media. Three maturation protocols were chosen and an iTRAQ 4-plex based approach was applied. COCs were matured for 23 hours in TCM-199 containing ECS with no hormone, LH/FSH (standard protocol) or LH/FSH/GH supplementation, respectively. The cumulus cells were removed and the oocytes were evaluated by transmission light microscopy for extrusion of the first polar body (Figure 10A and B). An LSM analysis of mature and immature oocytes is depicted in Figure 10C and D, which was performed by Dr. Felix Habermann.

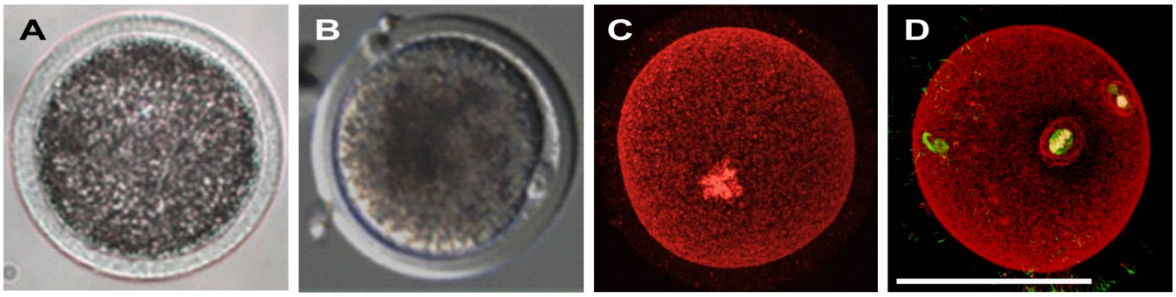

Figure 10. Microscopic analysis of mature and immature bovine oocytes. A and B: Transmission light images of an immature GV oocyte (A) and a mature MII oocyte with the first polar body (B). Images were kindly provided by Dr. Myriam Demant. **C and D:** Confocal laser scanning microscopic analyses of an immature GV oocyte (C) and a mature MII oocyte with the first polar body (D). DNA staining with DAPI is shown in white, f-actin filaments (phalloidin-TRITC) in red and alpha-tubulin in green. The scale bar in (D) represents 100 µm. Image capturing and interpretation was performed in collaboration with Dr. Felix Habermann.

The developmental rates did not differ between the three maturation protocols used (Figure 11). However, it was observed that the cumulus cells surrounding the oocytes appeared the most expanded after maturation under GH supplementation while they appeared the least expanded after maturation without additional hormone supplementation (ECS only) by light microscopic evaluation.

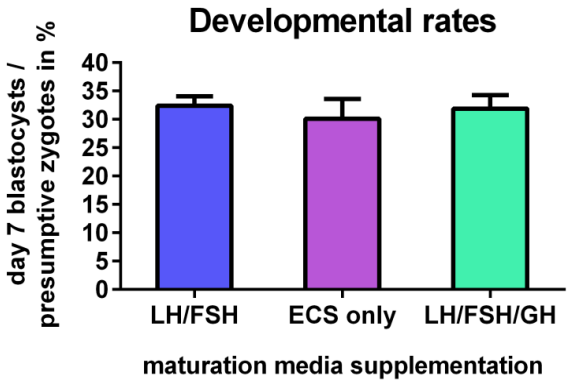

Figure 11. Developmental rates after maturation according to three different protocols. COCs were matured in maturation media containing ECS with no hormone supplementation (ECS only), LH/FSH (standard protocol) or LH/FSH/GH supplementation, respectively. The ratios between presumptive zygotes and day 7 blastocysts ± SD were determined (n=3).

Six biological replicates containing 150 oocytes each were prepared for each sample type, i.e. GV oocytes and three groups of differently matured MII oocytes. In total, each biological replicate contained 600 oocytes corresponding to about 54 µg total protein content. The average protein content of one bovine oocyte was determined to be 90 ng (Dr. Myriam Demant, personal communication). For identification and quantification of individual proteins, samples were lysed, reduced with dithiothreitol (DTT), alkylated with iodoacetamide (IAA) and digested over night with trypsin. Samples were chemically labeled with the iTRAQ reagent and pre-fractionated by SCX chromatography using six salt steps (0, 25, 50, 75, 125 and 350 mM KCl), leading to 36 fractions in total. Each SCX fraction was split into three aliquots which were subjected to nano-LC-MS/MS analysis. Aliquots were measured consecutively, with application of an additional mass exclusion list applied to aliquots two and three, derived from peptide identifications of the previous runs. The experimental strategy is illustrated in Figure 12.

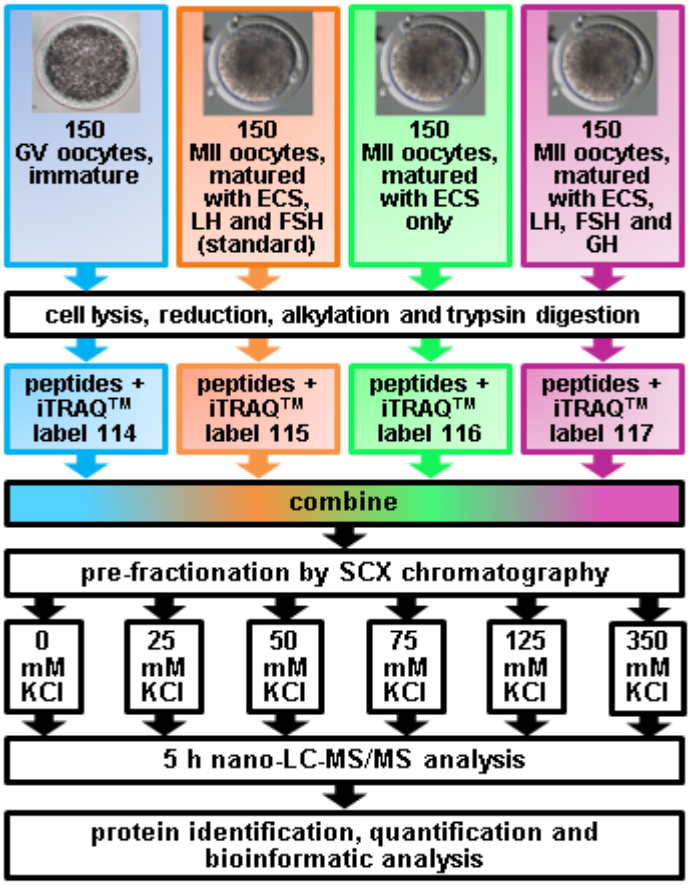

Figure 12. Workflow for iTRAQ-based proteome analysis of oocyte maturation. The workflow for one biological replicate is depicted. In the iTRAQ-based approach, six biological replicates of immature GV and mature MII oocytes were analyzed. Additionally, the influence of different hormone supplementations was investigated.

3.2.2 Comparative proteomic analysis of oocyte *in vitro* maturation using iTRAQ

In six biological replicates, a total of 3,600 oocytes were analyzed and 1,115 proteins were identified (FDR < 1 %) by at least two individual peptides. Of those, 565 ± 69 proteins were identified in each biological replicate by LC-MS/MS analysis of the first aliquot of each SCX fraction. The combination with the second aliquot increased the number of identified proteins by 28 % to about 720 ± 98. The number of identified proteins could be further augmented to 784 ± 98 by combination with the third aliquot, which corresponds to 11 % additional protein identifications. A total of 1,092 proteins were quantified with the Q+ module of Scaffold. For the quantitative pair-wise comparisons, a log2 fold change ≥ |0.6| and $p \leq 0.05$ with the Student's t-test was considered as significant. Calculation of *P* values was performed with R

in collaboration with Kathrin Otte. According to these criteria, a total of 53 proteins were detected which were significantly altered in protein abundance in at least one of the six pair-wise comparisons. In Table 2, the 42 significant differences in protein abundance between GV oocyte (reference group) and differently matured MII oocytes are listed. In Table 3, significant differences in protein abundance between MII oocytes matured according to different maturation protocols are listed. The numbers of Table 3 refer to the numbers used in Table 2 and 11 additional differences in protein abundances are listed in Table 3. In the pair-wise comparison between GV oocytes and MII oocytes matured according to standard protocol with LH and FSH supplementation, a total of 26 proteins were found to be significantly altered in abundance which is illustrated in the Volcano plot in Figure 13.

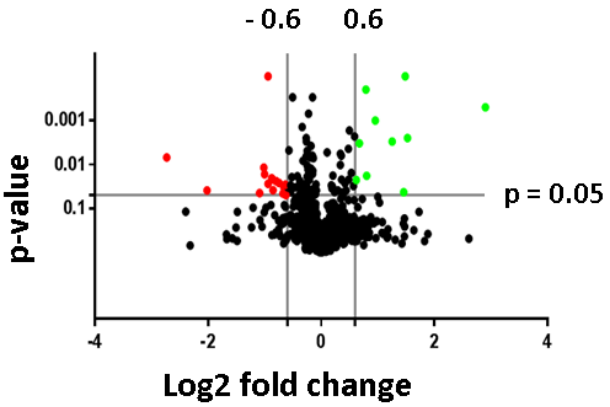

Figure 13. Volcano plot of the pair-wise comparison between GV oocytes and MII oocytes matured according to the standard protocol with LH and FSH supplementation. A total of 15 proteins are decreased in abundance in MII oocytes (red dots), 11 proteins are increased in abundance (green dots), whereas the not significantly altered proteins are reflected by black dots.

Table 2. Significant differences in protein abundance between GV oocytes (reference group) and MII oocytes matured according to different protocols.

				GV vs. MII (LH + FSH)*		GV vs. MII (no hormones)*		GV vs. MII (LH + FSH + GH)*	
#	Protein name	Gene Symbol	Accession Number	log2 FC	P value	log2 FC	P value	log2 FC	P value
1	Microtubule-associated protein RP/EB family member 1	MAPRE1	F1MHV5_BOVIN	-6.27	NA	-6.29	NA	-6.46	0.02
2	Stathmin	STMN1	STMN1_BOVIN	-2.73	0.01	-2.97	0.00	-2.95	0.01
3	CD81 antigen	CD81	CD81_BOVIN	-2.02	0.04	-2.34	0.03	-2.25	0.27
4	IGL@ protein	IGL@	Q3T101_BOVIN	-1.21	0.10	-1.86	0.05	-1.92	0.01
5	Zygote arrest protein 1	ZAR1	Q1PSA0_BOVIN	-1.09	0.04	-1.28	0.04	-0.96	0.03
6	Apolipoprotein A-I	APOA1	APOA1_BOVIN	-1.02	0.01	-0.89	0.01	-0.33	0.40
7	Eukaryotic translation initiation factor 4E transporter	EIF4ENIF1	E1BG99_BOVIN	-1.00	0.02	-1.26	0.03	-0.66	0.12
8	Tropomyosin 4-like	LOC540799	F1MV90_BOVIN	-0.94	0.00	-0.77	0.00	-0.83	0.00
9	Mitochondrial import receptor subunit TOM34	TOMM34	E1BGD1_BOVIN	-0.94	0.03	-0.49	0.03	-0.24	0.22
10	ES cell-associated transcript 1 protein	KHDC3L	E1BPE9_BOVIN	-0.88	0.02	-1.18	0.02	-1.41	0.01
11	Beta-1,4-galactosyltransferase 4	B4GALT4	Q32LF7_BOVIN	-0.85	0.04	-1.40	0.29	-1.86	0.13
12	Retinol-binding protein 4	RBP4	G1K122_BOVIN	-0.80	0.02	-0.70	0.05	-0.73	0.08
13	ZAR1-like protein	ZAR1L	ZAR1L_BOVIN	-0.75	0.03	-0.80	0.08	-0.47	0.14
14	Synaptophysin-like protein 1	SYPL1	A8PVV5_BOVIN	-0.68	0.05	-0.01	0.98	-0.10	0.78
15	Gametocyte-specific factor 1	GTSF1	GTSF1_BOVIN	-0.66	0.03	-0.92	0.08	-0.82	0.04
16	Tubulin-specific chaperone E	TBCE	TBCE_BOVIN	-0.64	0.03	-0.53	0.04	-0.07	0.70
17	Isoleucine-tRNA ligase, mitochondrial	IARS2	G3MWG4_BOVIN	-0.63	0.05	-0.37	0.14	-0.12	0.18
18	Apolipoprotein E	APOE	A7YWR0_BOVIN	-0.54	0.04	-0.62	0.02	-0.91	0.01
19	Y-box-binding protein 2	YBX2	A5D7M4_BOVIN	-0.45	0.06	-0.53	0.05	-0.71	0.04
20	40S ribosomal protein S	RPS4Y1	A2VE06_BOVIN	-0.14	0.38	-0.71	0.06	-1.07	0.01
21	Calcium-binding mitochondrial carrier protein Aralar2	SLC25A13	F1MX88_BOVIN	-0.09	0.87	-1.93	0.01	-0.68	0.62
22	Vimentin	VIM	VIME_BOVIN	-0.08	0.85	0.24	0.51	1.12	0.05
23	Isocitrate dehydrogenase [NAD] subunit beta, mitochondrial	IDH3B	IDH3B_BOVIN	0.28	0.62	0.62	0.19	0.94	0.04
24	putative MAGE domain-containing protein MAGEA13P-like	LOC101112889	G3MYS0_BOVIN	0.34	0.06	0.54	0.01	0.63	0.02
25	ATP-dependent RNA helicase DDX3X	DDX3X	G5E631_BOVIN	0.37	0.05	0.47	0.06	0.64	0.05
26	Endoplasmic reticulum resident protein 44	ERP44	ERP44_BOVIN	0.41	0.34	0.74	0.08	0.90	0.05
27	ADP-ribosylation factor 4	ARF4	ARF4_BOVIN	0.54	0.25	0.62	0.09	0.72	0.04
28	Proteasome subunit alpha type-5	PSMA5	PSA5_BOVIN	0.58	0.06	0.62	0.07	0.81	0.04
29	Caspase-6	CASP6	CASP6_BOVIN	0.62	0.02	0.40	0.04	0.70	0.01
30	Activator of 90 kDa heat shock protein ATPase homolog 1	AHSA1	Q3T0G3_BOVIN	0.68	0.00	0.59	0.08	0.43	0.20
31	Aurora kinase A	AURKA	AURKA_BOVIN	0.79	0.00	0.72	0.00	0.67	0.00
32	Cyclin-dependent kinase 1	CDK1	CDK1_BOVIN	0.80	0.02	1.07	0.02	0.10	0.75
33	Fructose-2,6-bisphosphatase TIGAR	TIGAR	TIGAR_BOVIN	0.83	0.18	0.91	0.03	0.82	0.19
34	Plasminogen activator inhibitor 1	SERPINE1	PAI1_BOVIN	0.93	0.21	3.03	0.01	1.02	0.12
35	Importin subunit alpha-8	KPNA7	IMA8_BOVIN	0.96	0.00	1.00	0.00	1.03	0.01
36	Bcl-2-like protein 10	BCL2L10	E1B9B3_BOVIN	1.00	0.05	1.42	0.00	1.34	0.00
37	Transforming acidic coiled-coil-containing protein 3	TACC3	A6QL93_BOVIN	1.25	0.00	1.17	0.00	1.33	0.00
38	Sequestosome 1	SQSTM1	A7E3V0_BOVIN	1.27	NA	1.52	0.03	1.79	0.03
39	smg-5 homolog, nonsense mediated mRNA decay factor	LOC521950	F1MLM3_BOVIN	1.46	0.04	1.17	0.07	0.72	0.34
40	Probable inactive 1-aminocyclopropane-1-carboxylate synthase-like protein 2	ACCSL	F1MBE7_BOVIN	1.49	0.00	1.45	0.00	1.53	0.00
41	E3 ubiquitin-protein ligase UHRF1	UHRF1	UHRF1_BOVIN	1.53	0.00	1.64	0.00	1.58	0.00
42	Wee1-like protein kinase 2	WEE2	F1MZD1_BOVIN	2.90	0.00	3.09	0.00	3.07	0.00

Log2 fold change ≤ -0.6 and t-test with a significance level of $p \leq 0.05$

Log2 fold change ≥ 0.6 and t-test with a significance level of $p \leq 0.05$

*In each pair-wise comparison, positive or negative values represent an increase or decrease of protein abundance, respectively, in the indicated group. GV = GV oocyte; MII = MII oocyte. FC = Fold change.

Table 3. Significant differences in protein abundance between MII oocytes matured according to different protocols.

				MII (no hormones) vs. MII (LH + FSH)*		MII (no hormones) vs. MII (LH + FSH + GH)*		MII (LH + FSH) vs. MII (LH + FSH + GH)*	
#	Protein name	Gene Symbol	Accession Number	log2 FC	P value	log2 FC	P value	log2 FC	P value
4	IGL@ protein	IGL@	Q3T101_BOVIN	0.65	0.04	-0.07	0.64	-0.71	0.12
18	Apolipoprotein E	APOE	A7YWR0_BOVIN	0.38	0.12	-0.35	0.25	-0.73	0.03
22	Vimentin	VIM	VIME_BOVIN	-0.40	0.09	0.77	0.09	1.32	0.05
23	Isocitrate dehydrogenase [NAD] subunit beta, mitochondrial	IDH3B	IDH3B_BOVIN	-1.52	0.13	-0.58	0.04	1.53	0.16
26	Endoplasmic reticulum resident protein 44	ERP44	ERP44_BOVIN	-0.06	0.82	0.59	0.02	0.39	0.09
32	Cyclin-dependent kinase 1	CDK1	CDK1_BOVIN	-0.34	0.24	-0.81	0.01	-0.74	0.01
34	Plasminogen activator inhibitor 1	SERPINE1	PAI1_BOVIN	-2.16	0.00	-2.12	0.00	0.06	0.71
43	Growth differentiation factor 9	GDF9	D0EZ62_BOVIN	-0.77	0.01	-0.16	0.56	0.44	0.13
44	Heat shock 70 kDa protein 1B	HSPA1B	HS71B_BOVIN	-0.25	0.25	0.29	0.25	0.61	0.00
45	Regakine-1	LOC504773	REG1_BOVIN	0.96	0.02	0.80	0.40	-0.68	0.45
46	Tropomyosin alpha-1 chain	TPM1	TPM1_BOVIN	-0.62	0.04	-0.54	0.14	0.05	0.90
47	Alpha-2-HS-glycoprotein	AHSG	B0JYN6_BOVIN	1.37	0.01	0.91	0.38	0.44	0.33
48	Catenin alpha-1	CTNNA1	CTNA1_BOVIN	-0.51	0.26	0.22	0.41	0.76	0.04
49	Serine/threonine-protein phosphatase 2A activator	PPP2R4	PTPA_BOVIN	-0.24	0.39	0.23	0.06	0.81	0.03
50	HSPA (Heat shock 70kDa) binding protein, cytoplasmic cochaperone 1	HSPBP1	Q2KJ77_BOVIN	0.82	0.01	0.44	0.23	0.09	0.85
51	Vesicle-associated membrane protein 3	VAMP3	VAMP3_BOVIN	0.88	0.03	0.81	0.08	-0.12	0.63
52	Nucleosome assembly protein 1-like 4	NAP1L4	F1N7X3_BOVIN	0.70	0.00	-0.60	0.22	-0.93	0.04
53	ATP synthase subunit alpha, mitochondrial	ATP5A1	ATPA_BOVIN	2.31	NA	0.17	NA	2.57	0.04

Log2 fold change ≤ -0.6 and t-test with a significance level of $p \leq 0.05$

Log2 fold change ≥ 0.6 and t-test with a significance level of $p \leq 0.05$

*In each pair-wise comparison, positive or negative values represent an increase or decrease of protein abundance, respectively, in the indicated group. GV = GV oocyte; MII = MII oocyte. FC = Fold change. # refers to the # in Table 2.

To uncover functional categories related with the proteins of the pair-wise comparison, they were subjected to the Cytoscape [96] plugins ClueGO [94] and CluePedia [95] which grouped genes significantly enriched in the respective Gene Ontology (GO) terms involved in biological processes. For the comparison between GV oocytes and MII oocytes matured according to standard protocol with LH and FSH supplementation (Table 2 and Figure 14), this network analysis revealed among the proteins increasing in abundance in MII oocytes an enrichment of proteins related to the terms “positive regulation of ATPase activity”, “microtubule cytoskeleton organization”, “protein import” and “mitosis”. Among the proteins decreasing in abundance in MII oocytes, an enrichment of proteins related to the terms “regulation of protein secretion”, “regulation of protein phosphorylation” and “glycerophospholipid biosynthetic process” was found.

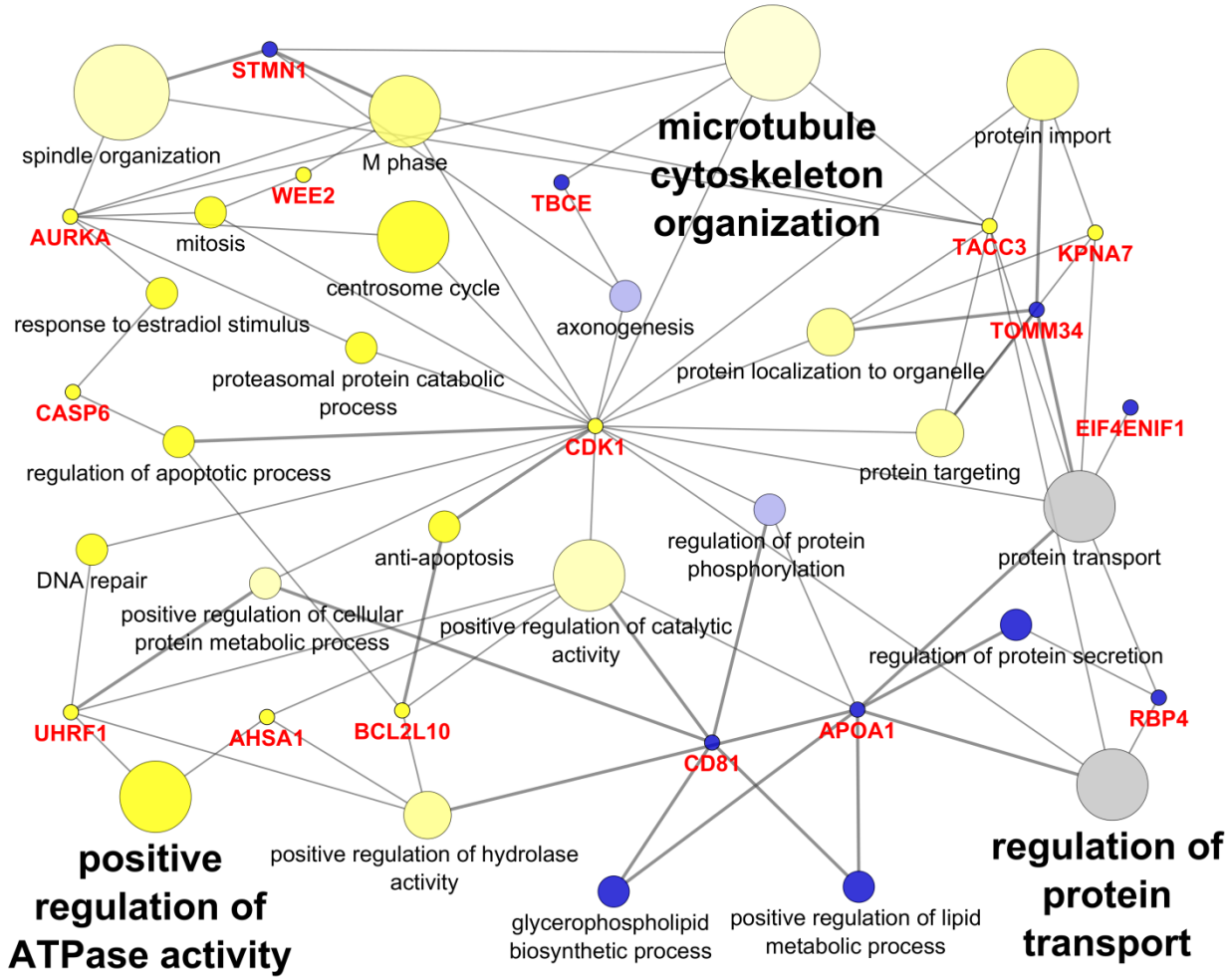

Figure 14. Cytoscape analysis of differently abundant proteins in the pair-wise comparisons between GV oocytes and MII oocytes matured according to standard protocol with LH and FSH supplementation. Analysis was performed according to the GO terms of “biological process”. Yellow colored nodes reflect significantly enriched GO-terms by proteins with increased abundance in MII oocytes. Blue colored nodes reflect significantly enriched GO-terms by proteins with decreased abundance in MII oocytes. Grey colored nodes: Protein abundance increase and decrease. In the functionally grouped network, terms and their associated genes (colored in red) are linked based on a κ score (≥ 0.3) and the edge thickness indicates the association strength. The node size corresponds to the statistical significance of each term.

The pair-wise comparisons of MII oocytes matured without hormone supplementation (ECS only) and MII oocytes matured according to standard protocol with LH and FSH supplementation revealed nine differences in protein abundance (Table 3 and Figure 15A). Three proteins showed a decreased abundance in MII oocytes matured according to standard

protocol and network analysis of these proteins demonstrated an enrichment of proteins related to the GO term “negative regulation of cell migration” (Figure 15B).

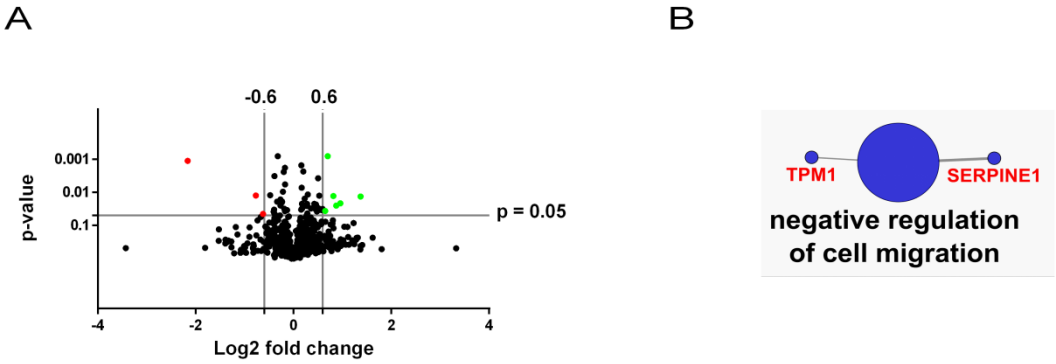

Figure 15. Volcano plot and Cytoscape analysis of differently abundant proteins between MII oocytes matured without hormone supplementation (ECS only) vs. MII oocytes matured according to standard protocol with LH and FSH supplementation. A: Volcano plot. Proteins decreased or increased in abundance in MII oocytes matured according to standard protocol are represented as red dots and green dots, respectively. Black dots: Proteins not significantly altered in abundance. **B:** Cytoscape analysis according to the GO term “biological process”. Blue colored nodes reflect significantly enriched GO-terms by proteins with decreased abundance in MII oocytes. In the functionally grouped network, terms and their associated genes (colored in red) are linked based on a κ score (≥ 0.3) and the edge thickness indicates the association strength. The node size corresponds to the statistical significance of each term.

Supplementation of the maturation medium with GH lead to an abundance change of eight proteins compared to MII oocytes matured according to standard protocol (Table 3 and Figure 16A). Network analysis of proteins decreased in abundance by GH addition revealed an enrichment of proteins related to “DNA packaging”, “regulation of protein kinase activity” and “positive regulation of cellular metabolic process”. For proteins increased in abundance by GH addition, the network analysis revealed an enrichment of proteins involved in “regulation of apoptotic process” and “ribonucleotide catabolic process” (Figure 16B).

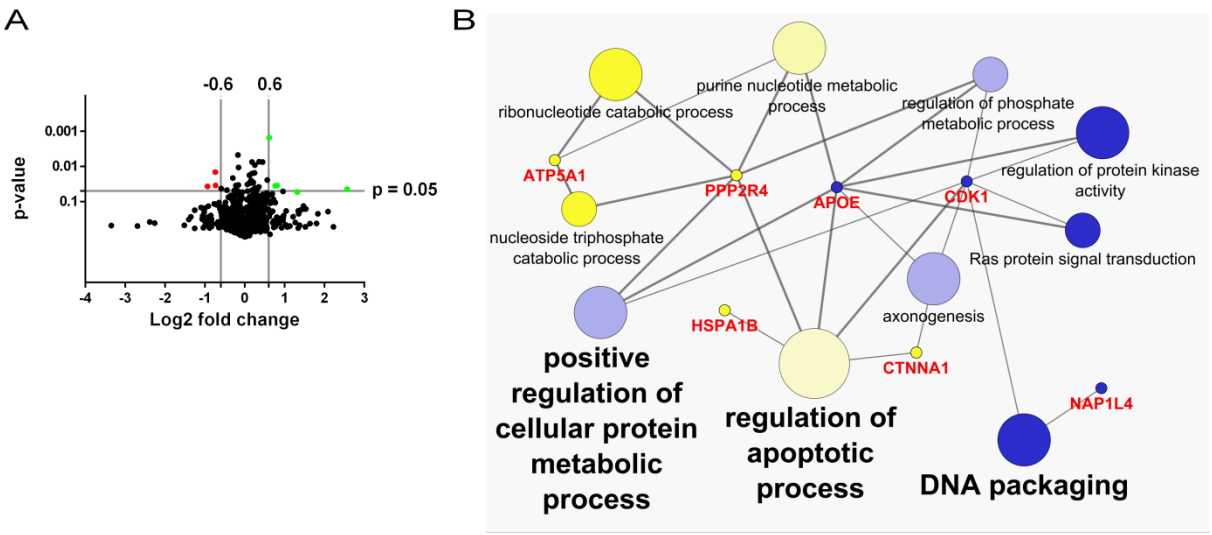

Figure 16. Volcano plot and Cytoscape analysis of differently abundant proteins between MII oocytes matured according to standard protocol with LH and FSH supplementation and MII oocytes matured with LH, FSH and GH supplementation. A: Volcano plot. Proteins increased or decreased in abundance in MII oocytes matured with LH, FSH and GH supplementation are represented as green dots or red dots, respectively. Black dots: Proteins not significantly altered in abundance. **B:** Cytoscape analysis according to the GO term "biological process". Yellow and blue colored nodes reflect significantly enriched GO-terms by proteins with increased or decreased abundance in MII oocytes matured with LH, FSH and GH supplementation, respectively. Grey colored nodes: Protein abundance increase and decrease. In the functionally grouped network, terms and their associated genes (colored in red) are linked based on κ score (≥ 0.3) and the edge thickness indicates the association strength. The node size corresponds to the statistical significance of each term.

3.2.3 Localization of vimentin in MII oocytes by confocal laser scanning microscopy

Vimentin (VIM) was found to strongly increase (log2 FC 1.3) between MII oocytes matured either according to standard protocol with LH and FSH or matured with LH, FSH and GH supplementation (Table 3). To determine if VIM is localized inside or on the surface of oocytes, immunofluorescence and confocal laser scanning microscopy (LSM) of MII oocytes with extruded first polar body (Figure 17) was performed. Image capturing and interpretation was performed in collaboration with Dr. Felix Habermann. Staining for VIM protein revealed small foci scattered over the surface of the MII oocyte matured according to standard protocol (Figure 17A). In accordance with the iTRAQ data, these focis were increased in abundance in MII oocytes matured with GH supplementation (Figure 17B). Notably, there was a considerable variability among the *in vitro* matured MII oocytes. For improved localization of VIM, a part of the zona pellucida was magnified which was sketched for clarification in Figure 18A. In the magnification, VIM staining revealed the VIM protein to be localized inside of the cytoplasmic extensions and to be accumulated at the gap junctions that connect the cumulus cells with the oocyte (Figure 18B).

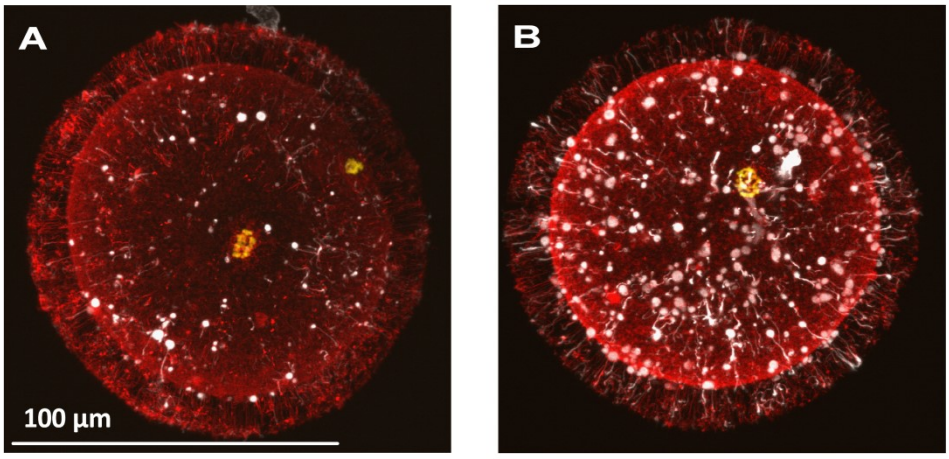

Figure 17. Confocal laser scanning microscopic analyses of vimentin (VIM) in mature MII oocytes. VIM staining is shown in white, DNA staining with DAPI is in yellow and f-actin filaments (phalloidin-TRITC) is shown in red. Scale bar represents 100 µm. Image capturing and interpretation was performed in collaboration with Dr. Felix Habermann. **A:** MII oocyte matured according to standard protocol with LH and FSH. **B:** MII oocyte matured with LH, FSH and GH supplementation.

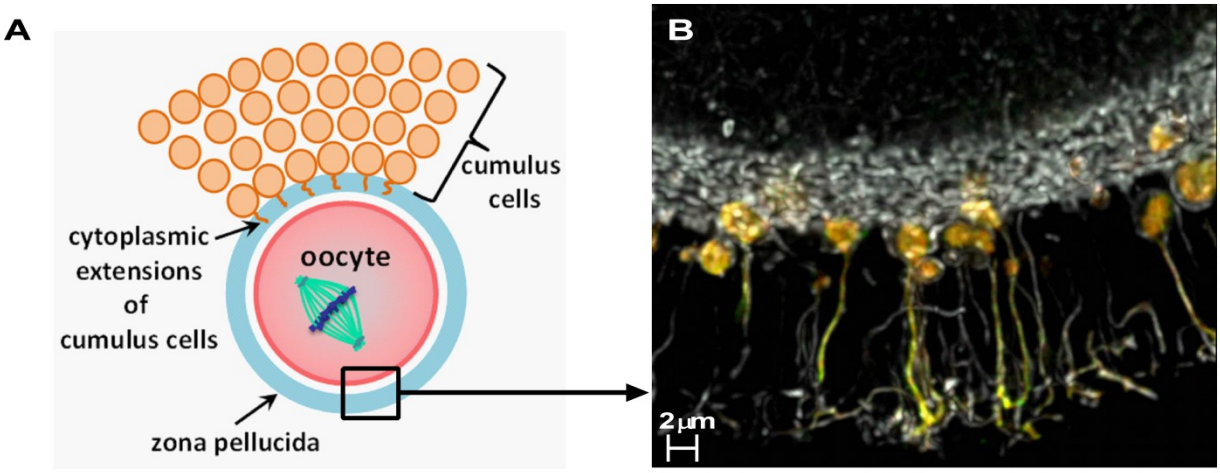

Figure 18. Vimentin analysis in oocytes. A: Sketch of an oocyte. The oocyte is surrounded by cumulus cells from which cytoplasmic extensions protrude into the zona pellucida of the oocyte. **B:** Confocal laser scanning microscopic analysis of vimentin in MII oocytes matured with LH, FSH and GH supplementation. A part of the zona pellucida is shown. Vimentin staining is shown in orange and green and f-actin filaments (phalloidin-TRITC) staining is shown in white. Scale bar represents 2 µm. Image capturing and interpretation was performed in collaboration with Dr. Felix Habermann.

3.3 Proteome signatures in early bovine embryo development

3.3.1 General remarks and experimental strategy

This study focuses on the quantitative and qualitative proteome changes during the first steps of mammalian embryogenesis, i.e., zygotes, two-cell embryos and four-cell embryos using MII oocytes as a reference. MII oocytes were collected after 23 hours of maturation and mechanically denuded by vortexing in PBS. Zygotes, two-cell embryos and four-cell embryos were collected at 19, 35 and 43 hours post insemination (hpi), respectively. All oocytes and embryos were evaluated microscopically before they were frozen on dry ice.

The experimental strategy comprised an iTRAQ-based discovery approach followed by SRM-based verification as illustrated in Figure 19. For the iTRAQ study, four biological replicates were prepared containing 400 oocytes or embryos corresponding to about 36 µg protein each. For the identification and quantification of individual proteins, samples were lysed, reduced with DTT, alkylated with IAA and digested over night with trypsin. Prior to nano-LC-MS/MS analysis, samples were chemically labeled with the iTRAQ reagent and pre-fractionated by SCX using eight salt steps (0, 45, 75, 90, 110, 135, 175 and 350 mM KCl), leading to 24 fractions in total. Each fraction was split into two aliquots which were measured consecutively with application of an additional mass exclusion list in the second run based on the peptide identifications of the first run. For verification of the protein profiles obtained by this holistic LC-MS/MS approach, a multiplexed SRM assay was established. A subset of five interesting proteins relevant for early embryogenesis was selected and proteins were quantified in pools of ten oocytes or embryos corresponding to about 0.9 µg protein each.

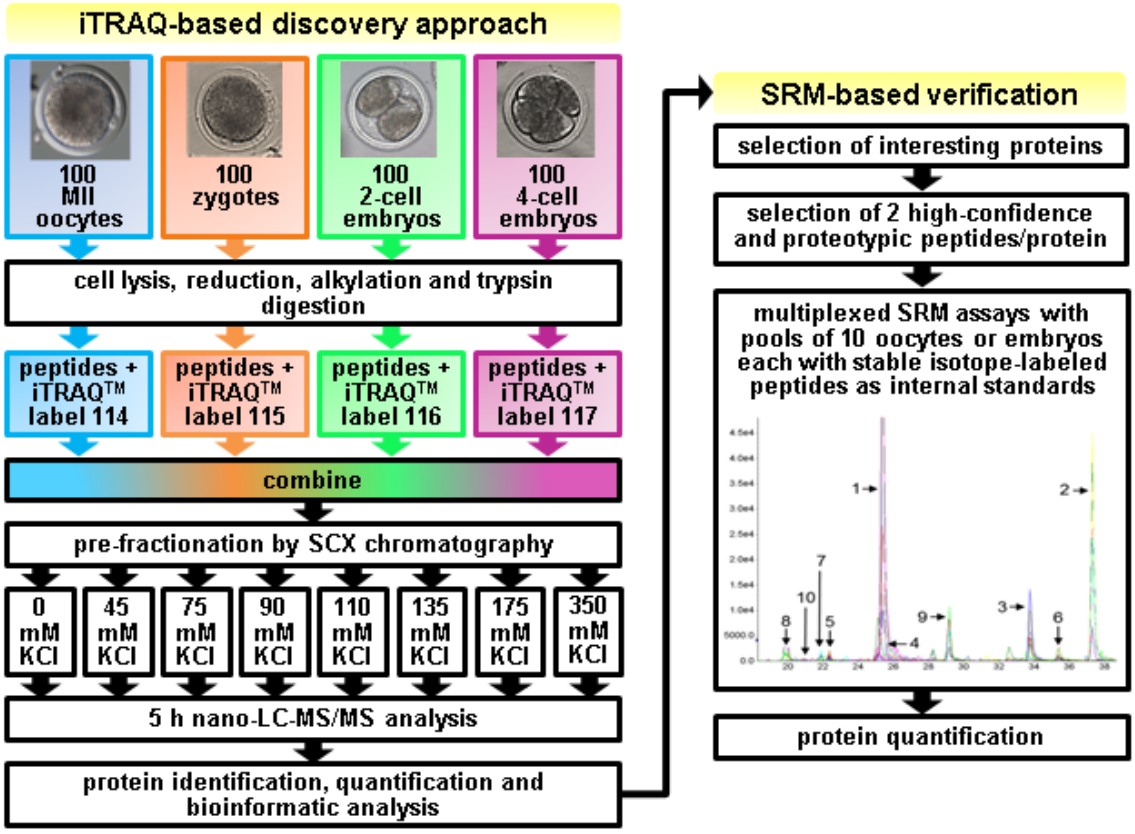

Figure 19. Workflow for the 4-plex iTRAQ-based proteome analysis and the SRM verification studies. The panel "iTRAQ-based discovery approach" illustrates the generation and analysis of one out of four biological replicates, each of which contains 100 oocytes, zygotes, two-cell and four-cell embryos. SRM assays were established for five proteins which were quantified in pools of 10 oocytes or embryos (n=4) in a multiplexed setup.

3.3.2 Comparative proteomic analysis of early embryonic stages using iTRAQ

In four biological replicates, a total of 1,600 oocytes or embryos were analyzed and 1,072 proteins in 1,020 protein clusters were identified (FDR < 1 %) by at least two individual peptides. Of those, 732 protein clusters were identified in the first run while combination with the second run increased the number of identified proteins by 39 % to 1,020 identified protein clusters in total (Figure 20A). A total of 579 (57 %) protein clusters were identified in all four analyzed biological replicates, while 624 (61 %), 689 (68 %) and 809 (79 %) protein clusters were identified in at least three, two and one biological replicate, respectively. In total, 187 (18 %) protein clusters were identified exclusively in one of the four replicates (Figure 20B). The identified 1,020 protein clusters were subjected to functional Gene Ontology (GO)

analysis with respect to cellular localization in “The Database for Annotation, Visualization and Integrated Discovery (DAVID)” [91, 92]. A total of 873 proteins could be assigned to GO terms (Figure 21). The GO analysis with DAVID revealed, among others, 158 proteins (18.1 %) to be grouped to mitochondrion, 114 (13.1 %) proteins to non-membrane-bounded organelle, 83 (9.5 %) proteins to organelle lumen, 73 (8.4 %) proteins to cytoskeleton and 70 (8.0 %) to cytosol. The DAVID analysis of oocyte and embryo proteomes also revealed three mitochondrion related annotation clusters (Table 4) with high enrichment scores of 25.5, 11.5 and 1.7. An enrichment score of 1.3 is equivalent to a *P* value of 0.05 and higher scores indicate that the gene members in the group are involved in more important (enriched) terms in a given study [91].

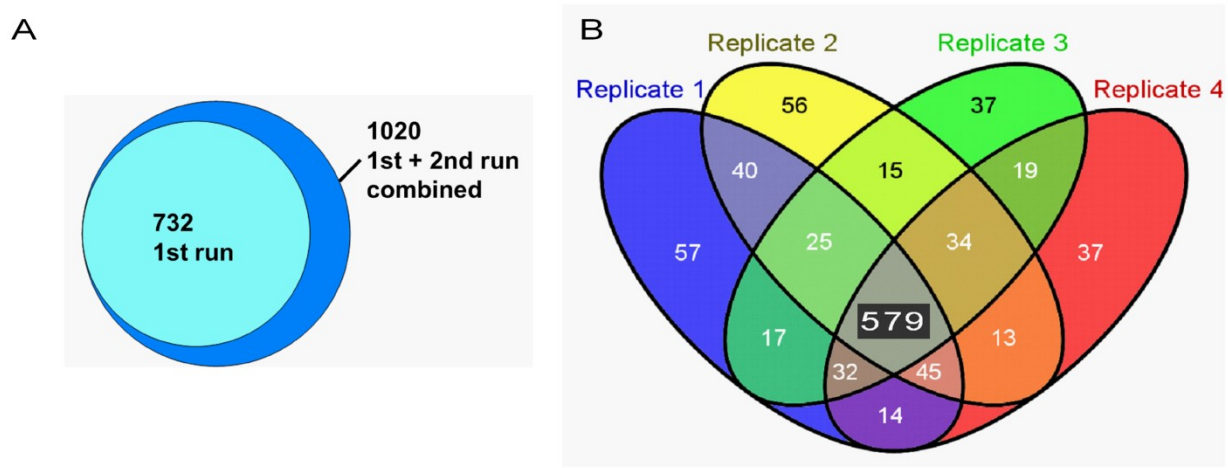

Figure 20. Venn diagrams of protein clusters identified from four biological replicates. A: A total of 732 protein clusters were identified in the first run and combination with the second run increased the number of identified protein clusters to 1,020. **B:** In total, 1,020 protein clusters were identified, 579 of them in four replicates.

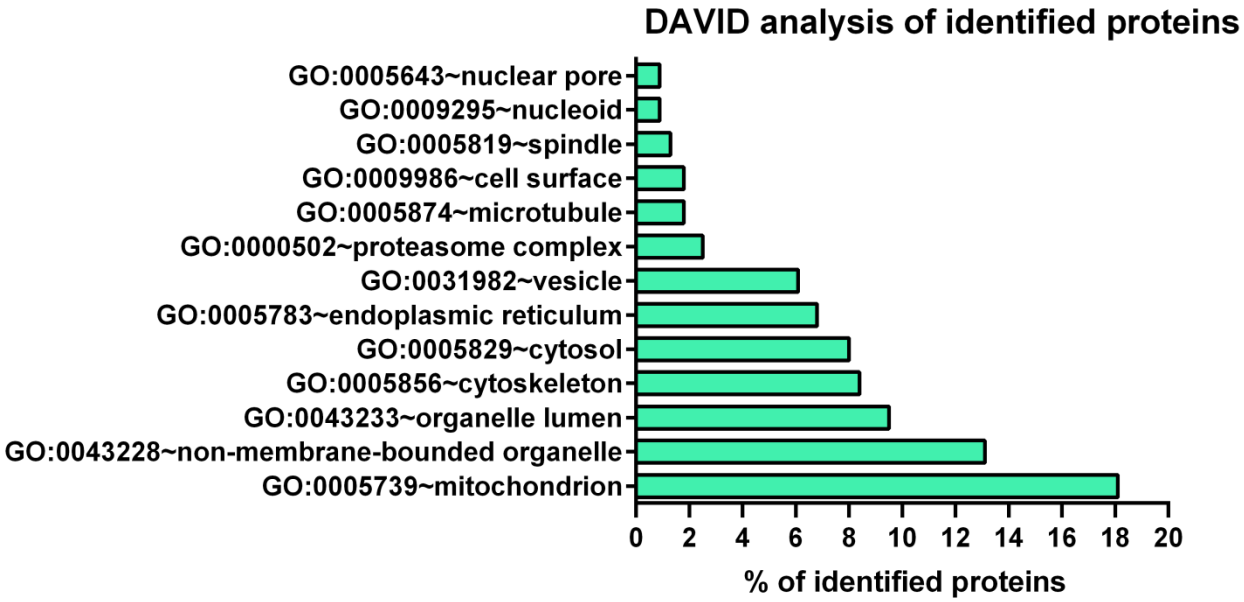

Figure 21. DAVID analysis of all proteins identified in MII oocytes, zygotes, two-cell and four-cell embryos according to the GO term "cellular localization". The percentage of enriched proteins associated with a GO term compared to the total number of identified proteins is indicated. An extract of the most significant terms is shown.

Table 4. DAVID annotation clustering of all proteins identified in MII oocytes, zygotes, two-cell and four-cell embryos according to the GO term "cellular localization". Clusters associated with the mitochondrion are shown.

Cluster 1, Enrichment Score: 25.6 **term**	**count**	**%**	**P value**	**fold enrichment**	**FDR**
GO:0005739~mitochondrion	158	18.1	8.89E-38	2.8	1.24E-34
GO:0044429~mitochondrial part	103	11.8	4.24E-32	3.5	5.92E-29
GO:0019866~organelle inner membrane	74	8.5	1.29E-26	4.0	1.80E-23
GO:0031967~organelle envelope	93	10.7	1.06E-25	3.2	1.49E-22
GO:0031975~envelope	93	10.7	1.31E-25	3.2	1.83E-22
GO:0005743~mitochondrial inner membrane	71	8.1	6.27E-25	3.9	8.75E-22
GO:0005740~mitochondrial envelope	76	8.7	1.04E-22	3.4	1.46E-19
GO:0031966~mitochondrial membrane	74	8.5	1.20E-22	3.5	1.68E-19
GO:0031090~organelle membrane	103	11.8	2.75E-19	2.5	3.84E-16
Cluster, 3 Enrichment Score: 11.5 **term**	**count**	**%**	**P value**	**fold enrichment**	**FDR**
GO:0005759~mitochondrial matrix	40	4.6	8.67E-17	4.6	1.55E-13
GO:0031980~mitochondrial lumen	40	4.6	8.67E-17	4.6	1.55E-13
GO:0031974~membrane-enclosed lumen	89	10.2	6.05E-10	1.9	8.44E-07
GO:0070013~intracellular organelle lumen	83	9.5	1.03E-08	1.9	1.44E-05
GO:0043233~organelle lumen	83	9.5	1.13E-08	1.9	1.58E-05
Cluster 11, Enrichment Score: 1.7 **term**	**count**	**%**	**P value**	**fold enrichment**	**FDR**
GO:0005758~mitochondrial intermembrane space	6	0.7	9.32E-03	4.4	1.23E+01
GO:0031970~organelle envelope lumen	7	0.8	1.17E-02	3.5	1.51E+01
GO:0042719~mitochondrial intermembrane space protein transporter complex	3	0.3	9.40E-02	5.6	7.48E+01

Within the four biological replicates, a total of 1,051 proteins could be quantified with the Q+ module of Scaffold. For the quantitative pair-wise comparisons, a log2 fold change ≥ |0.6| and a *P* value ≤ 0.05 with the Student's t-test was considered as significant. According to these criteria, a total of 87 proteins were quantified, which were significantly altered in abundance in at least one of the six pair-wise comparisons. A total of 55 proteins are significantly altered in abundance with MII oocytes as reference group (Table 5). In Table 6, the significant differences in protein abundance between the embryonic stages with either zygotes or two-cell embryos serving as reference group are listed. The numbers of Table 6 refer to the numbers used in Table 5 and 32 additional differences in protein abundance are listed in Table 6.

The 87 differences in protein abundance were clustered using the self-organizing tree algorithm (SOTA) analysis [93], leading to four clusters (Figure 22). The first cluster consists of 44 proteins which gradually decrease in abundance up to a maximum log2 fold change of about -2 (Figure 22A) while cluster 2 contains 32 proteins which increase from the MII oocyte stage up to a log2 fold change of about 1.3 at the four-cell stage (Figure 22B). The abundance of the 7 proteins of cluster 3 increased to the zygote stage, stayed fairly constant until the two-cell stage and increased upon development to the four-cell stage up to a Log2 fold change of about 2.5 (Figure 22C). The fourth cluster comprises 4 proteins, the abundance of which sharply increased to the zygote stage by a log2 fold change up to a maximum of about 5, followed by a gradual decrease until the four-cell stage to the initial value (Figure 22D). Calculation of *P* values and the SOTA analysis were performed with R in collaboration with Kathrin Otte.

To uncover functional categories related with the proteins of the four SOTA clusters, they were subjected to the Cytoscape [96] plugins ClueGO [94] and CluePedia [95] which grouped the most relevant biological processes in a network with GO terms and associated genes (Figure 23). For SOTA cluster 1, this network analysis revealed an enrichment of proteins related to the terms "protein folding", "mitotic spindle organization", "tricarboxylic acid cycle", "translation", "maturation of SSU-rRNA" and "high-density lipoprotein particle assembly"

(Figure 23A). For the proteins of SOTA cluster 2, which all increase in abundance during development, the biological terms “cellular macromolecular complex assembly”, “cellular amino acid metabolic process”, “purine ribonucleotide metabolic process”, “regulation of organelle organization” and “response to unfolded protein” were assigned (Figure 23B). In SOTA cluster 3 (Figure 23C), two proteins each were found to be connected to “M phase” and “protein transport” and in SOTA cluster 4 (Figure 23D), two proteins were involved in “protein polymerization”.

Table 5. Significant differences in protein abundance between the embryonic stages with MII oocytes serving as reference group.

#	Quantified Proteins	Gene Symbol	Accession Number	MII oocyte vs. zygote*		MII oocyte vs. two-cell embryo*		MII oocyte vs. four-cell embryo*	
				Log2 FC	P value	Log2 FC	P value	Log2 FC	P value
1	40S ribosomal protein S18	RPS18	Q861U5_BOVIN	-0.05	0.498	-0.73	0.013	-0.44	0.042
2	40S ribosomal protein S8	RPS8	RS8_BOVIN	-0.70	0.107	-1.07	0.164	-1.11	0.042
3	Apolipoprotein A-I	APOA1	APOA1_BOVIN	-0.71	0.040	-0.48	0.045	-0.71	0.010
4	Apolipoprotein E	APOE	A7YWR0_BOVIN	-0.42	0.469	-0.34	0.539	-0.93	0.009
5	Astacin-like metalloendopeptidase	ASTL	F1MP41_BOVIN	-0.75	0.000	-0.81	0.021	-1.09	0.000
6	Chromogranin-A	CHGA	CMGA_BOVIN	-1.10	0.002	-1.01	0.011	-1.07	0.082
7	Cochlin	COCH	COCH_BOVIN	-1.20	0.000	-1.57	0.001	-1.92	0.002
8	COP9 signalosome complex subunit 4	COPS4	CSN4_BOVIN	-0.42	0.249	-0.71	0.049	0.11	0.580
9	COP9 signalosome complex subunit 7b	COPS7B	CSN7B_BOVIN	1.15	0.016	-3.11	0.541	-3.15	0.533
10	E3 ubiquitin-protein ligase UHRF1	UHRF1	UHRF1_BOVIN	0.88	0.008	0.90	0.001	1.22	0.003
11	Endoplasmic reticulum resident protein 44	ERP44	ERP44_BOVIN	-0.23	0.635	-0.26	0.345	-0.65	0.013
12	Enoyl-CoA delta isomerase 2, mitochondrial	ECI2	F1MWY9_BOVIN	-0.71	0.032	-0.05	0.255	-0.22	0.434
13	Fructose-2,6-bisphosphatase TIGAR	TIGAR	TIGAR_BOVIN	0.54	0.120	0.79	0.022	-0.44	0.235
14	Glutamine--fructose-6-phosphate aminotransferase [isomerizing] 1	GFPT1	A8E645_BOVIN	0.42	0.082	0.57	0.003	0.79	0.018
15	Growth/differentiation factor 3	GDF3	F1MH37_BOVIN	-0.44	0.114	-0.36	0.223	-0.86	0.043
16	Heat shock 27kDa protein 1	HSPB1	E9RHW1_BOVIN	0.86	0.018	0.03	0.813	0.43	0.003
17	Heterogeneous nuclear ribonucleoprotein K	HNRNPK	HNRPK_BOVIN	0.77	0.132	0.46	0.507	0.83	0.025
18	Histone chaperone ASF1B	ASF1B	ASF1B_BOVIN	-0.07	0.720	-0.69	0.018	-1.56	0.043
19	Histone H2A	HIST3H2A	A4IFU5_BOVIN	0.47	0.015	0.08	0.842	1.01	0.013
20	Hyaluronan and proteoglycan link protein 3	HAPLN3	A5PK97_BOVIN	-1.48	0.003	-1.49	0.005	-1.32	0.006
21	Inhibin alpha chain	INHA	INHA_BOVIN	-1.15	0.388	-0.61	0.017	-0.71	0.659
22	Inorganic pyrophosphatase	PPA1	IPYR_BOVIN	-0.50	0.081	-0.64	0.017	-0.09	0.785
23	KHDC3-like protein	C6orf221	E1BPE9_BOVIN	-0.98	0.021	-0.71	0.011	-0.62	0.016
24	Lysosome membrane protein 2	SCARB2	A6QQP4_BOVIN	1.13	0.356	2.98	0.004	2.97	NA
25	NAD(P)H-hydrate epimerase	APOA1BP	NNRE_BOVIN	0.66	0.112	0.88	0.088	1.03	0.040
26	Nicastrin	NCSTN	Q3SZQ1_BOVIN	-0.01	0.954	-0.66	0.036	-0.73	0.242
27	Nuclear pore complex protein Nup93	NUP93	NUP93_BOVIN	-0.26	0.354	-0.24	0.138	-0.64	0.014
28	PABPC4 protein	PABPC4	A4IFC3_BOVIN	-0.52	0.121	-0.28	0.001	-0.82	0.034
29	Peptidyl-prolyl cis-trans isomerase D	PPID	PPID_BOVIN	-1.01	0.013	-0.64	0.153	-0.37	0.052
30	Peptidyl-prolyl cis-trans isomerase FKBP4	FKBP4	FKBP4_BOVIN	-0.79	0.064	-1.05	0.020	-0.78	0.097
31	Poly(A)-specific ribonuclease PARN-like domain-containing protein 1	PNLDC1	F1MX01_BOVIN	0.82	0.427	-1.27	0.048	-0.40	0.775
32	Polyadenylate-binding protein 4	ABCE1	A4IFE6_BOVIN	-0.83	0.102	-0.82	0.032	-0.52	0.272
33	Probable inactive 1-aminocyclopropane-1-carboxylate synthase-like protein 2	ACCSL	F1MBE7_BOVIN	0.72	0.001	0.99	0.003	1.11	0.001

34	Protein FAM49B	FAM49B	FA49B_BOVIN	1.56	0.001	1.52	0.002	-6.64	NA
35	protein LSM14 homolog B	LSM14B	E1BEY9_BOVIN	-0.27	0.184	-0.58	0.044	-1.06	0.000
36	Protein regulator of cytokinesis 1	PRC1	Q2T9P1_BOVIN	-0.50	0.018	-1.17	0.008	-1.08	0.002
37	protein transport protein Sec31A	SEC31A	E1BMP2_BOVIN	0.46	0.453	0.97	0.012	0.63	0.473
38	rab GTPase-activating protein 1	RABGAP1	F1N746_BOVIN	2.69	0.179	0.84	0.047	-0.04	0.954
39	Ras GTPase-activating-like protein IQGAP2	IQGAP2	F1MTR1_BOVIN	0.17	0.668	0.78	0.000	0.46	0.301
40	Ras-related protein Rab-10	RAB10	A6QLS9_BOVIN	0.61	0.047	0.29	0.437	0.91	0.028
41	Ras-related protein Rab-21	RAB21	RAB21_BOVIN	0.46	0.012	-0.03	0.954	0.73	0.001
42	Ribosomal protein S14	RPS14	Q3T076_BOVIN	-0.24	0.386	-0.89	0.023	-0.38	0.145
43	S-adenosylmethionine synthase	MAT2A	A7E3T7_BOVIN	-0.74	0.024	-0.65	0.015	-0.40	0.227
44	Sec1 family domain-containing protein 1	SCFD1	E1BG76_BOVIN	0.98	0.005	0.82	0.101	0.82	0.014
45	Sodium/potassium-transporting ATPase subunit alpha-1	ATP1A1	AT1A1_BOVIN	-0.57	0.089	-0.35	0.155	-0.79	0.013
46	Stathmin	STMN1	STMN1_BOVIN	2.09	0.001	2.44	0.001	2.38	0.000
47	Succinate dehydrogenase [ubiquinone] flavoprotein subunit, mitochondrial	SDHA	DHSA_BOVIN	-0.24	0.333	-0.68	0.038	-0.34	0.057
48	T-complex protein 1 subunit zeta	CCT6A	TCPZ_BOVIN	-0.46	0.048	-0.43	0.124	-0.75	0.021
49	TRAF-type zinc finger domain-containing protein 1	TRAFD1	TRAD1_BOVIN	0.67	0.112	0.65	0.015	0.39	0.094
50	Translocase of outer mitochondrial membrane 70	TOMM70A	Q08E34_BOVIN	-0.34	0.169	-0.82	0.019	-0.70	0.214
51	Transmembrane protein 160	TMEM160	TM160_BOVIN	0.44	0.184	0.35	0.281	0.69	0.034
52	Tudor and KH domain-containing protein	TDRKH	F1MUI1_BOVIN	-0.54	0.032	-1.43	0.040	-1.70	0.003
53	Uncharacterized protein (Fragment)	LOC522998	F1N091_BOVIN	0.45	0.255	0.71	0.235	1.28	0.033
54	Vimentin	VIM	VIME_BOVIN	-0.05	0.356	-2.32	0.003	-2.30	0.002
55	Wee1-like protein kinase 2	WEE2	F1MZD1_BOVIN	0.87	0.010	0.85	0.016	0.78	0.020

Log2 fold change ≤ -0.6 and t-test with a significance level of $p \leq 0.05$

Log2 fold change ≥ 0.6 and t-test with a significance level of $p \leq 0.05$

*In each pair-wise comparison, positive or negative values represent an increase or decrease of protein abundance, respectively, in the indicated group. FC = Fold change.

Table 6. Significant differences in protein abundance between the embryonic stages with either zygotes or two-cell embryos serving as reference group.

#	Quantified Proteins	Gene Symbol	Accession Number	zygote vs. two-cell embryo*		zygote vs. four-cell embryo*		two-cell embryo vs. four-cell embryo*	
				Log2 FC	P value	Log2 FC	P value	Log2 FC	P value
1	40S ribosomal protein S18	RPS18	Q861U5_BOVIN	-0.66	0.033	-0.38	0.100	0.28	0.288
7	Cochlin	COCH	COCH_BOVIN	-0.56	0.003	-0.95	0.002	-0.41	0.111
13	Fructose-2,6-bisphosphatase TIGAR	TIGAR	TIGAR_BOVIN	0.11	0.705	-0.26	0.384	-0.71	0.023
16	Heat shock 27kDa protein 1	HSPB1	E9RHW1_BOVIN	-0.95	0.001	-0.52	0.007	0.37	0.015
31	Poly(A)-specific ribonuclease PARN-like domain-containing protein 1	PNLDC1	F1MX01_BOVIN	-1.62	0.036	-1.32	0.036	0.21	0.790
35	protein LSM14 homolog B	LSM14B	E1BEY9_BOVIN	-0.19	0.661	-0.88	0.003	-0.69	0.024
36	Protein regulator of cytokinesis 1	PRC1	Q2T9P1_BOVIN	-0.68	0.007	-0.58	0.002	0.09	0.550
42	Ribosomal protein S14	RPS14	Q3T076_BOVIN	-0.72	0.035	-0.16	0.677	0.37	0.149
43	S-adenosylmethionine synthase	MAT2A	A7E3T7_BOVIN	0.12	0.738	0.93	0.001	0.27	0.064
52	Tudor and KH domain-containing protein	TDRKH	F1MUI1_BOVIN	-1.27	0.033	-0.97	0.005	-0.23	0.190
54	Vimentin	VIM	VIME_BOVIN	-2.21	0.001	-2.05	0.003	-0.40	0.113
56	4F2 cell-surface antigen heavy chain	SLC3A2	F1N2B5_BOVIN	0.66	0.091	-0.32	0.422	-0.92	0.000
57	60S ribosomal protein L19	RPL19	RL19_BOVIN	-0.56	0.107	-0.74	0.003	-0.18	0.442
58	6-phosphogluconolactonase	PGLS	F1MM83_BOVIN	0.18	0.420	-0.34	0.098	-0.65	0.003
59	Ankyrin repeat and FYVE domain-containing protein 1	ANKFY1	F1MD79_BOVIN	-1.10	0.217	-0.58	0.722	1.02	0.046
60	Citrate synthase, mitochondrial	CS	CISY_BOVIN	-0.93	0.044	-0.32	0.129	0.18	0.030
61	Cysteine and histidine-rich domain-containing protein 1	CHORDC1	CHRD1_BOVIN	0.42	0.277	0.84	0.105	0.65	0.026
62	Cysteine dioxygenase type 1	CDO1	CDO1_BOVIN	0.05	0.985	-1.26	0.001	1.71	0.109
63	Cytochrome b-c1 complex subunit 6, mitochondrial	UQCRH	QCR6_BOVIN	-0.10	0.906	-0.43	0.322	-0.97	0.037
64	cytoplasmic FMR1-interacting protein 1	CYFIP1	E1BN47_BOVIN	0.62	0.040	0.08	0.867	-0.04	0.915
65	Eukaryotic translation initiation factor 4E transporter	EIF4ENIF1	E1BG99_BOVIN	-0.80	0.048	-0.88	0.004	-0.20	0.469
66	Formin-like protein 2	FMNL2	E1BB06_BOVIN	1.38	0.011	1.27	0.001	-0.27	0.732
67	Glutathione S-transferase Mu 1	GSTM1	GSTM1_BOVIN	0.63	0.002	0.38	0.144	-0.12	0.713
68	Importin subunit alpha	KPNA2	Q3SYV6_BOVIN	4.34	0.200	-0.72	0.622	-5.45	0.045
69	Inner membrane protein, mitochondrial	IMMT	A7E3V3_BOVIN	-0.71	0.476	0.68	0.025	0.64	0.481
70	Mesencephalic astrocyte-derived neurotrophic factor	MANF	MANF_BOVIN	-0.56	0.359	-0.76	0.036	-0.38	0.351
71	NADH-ubiquinone oxidoreductase 75 kDa subunit, mitochondrial	NDUFS1	NDUS1_BOVIN	0.43	0.197	0.77	0.004	0.11	0.689
72	Nuclease EXOG, mitochondrial	EXOG	E1BAZ9_BOVIN	0.61	0.003	0.45	0.498	-0.16	0.785
73	Peptidyl-prolyl cis-trans isomerase FKBP1A	FKBP1A	FKB1A_BOVIN	0.16	0.715	0.82	0.087	0.73	0.044
74	Prolyl 4-hydroxylase subunit alpha-1	P4HA1	A6QL77_BOVIN	0.69	0.023	0.36	0.056	-0.34	0.006
75	Proteasome subunit alpha type-7	PSMA7	A7E3D5_BOVIN	-0.89	0.088	-0.09	0.158	1.02	0.040
76	Protein PAT1 homolog 2	PATL2	F1N6C5_BOVIN	-0.46	0.071	-0.78	0.043	-0.23	0.462
77	Putative zinc finger protein 840	ZNF840	G3MXP4_BOVIN	-1.65	0.162	-2.17	0.022	-0.99	0.120
78	Ras-related protein Rab-6A	RAB6A	F1MBF6_BOVIN	0.80	0.128	0.95	0.023	0.07	0.762
79	Sarcoplasmic/endoplasmic reticulum calcium ATPase 2	ATP2A2	F1MPR3_BOVIN	-0.86	0.040	0.89	0.677	1.42	0.459
80	Serine/threonine-protein phosphatase PP1-gamma catalytic subunit	PPP1CC	PP1G_BOVIN	-0.35	0.367	-2.60	0.006	-1.03	0.500
81	Similar to prefoldin subunit 2	PFDN2	Q862M6_BOVIN	0.38	0.285	-0.26	0.508	-0.70	0.029
82	Spectrin beta chain, non-erythrocytic 1	SPTBN1	F1MYC9_BOVIN	1.10	0.024	-1.95	0.494	-0.45	0.076
83	Stimulated by retinoic acid gene 6 protein homolog	STRA6	F1N4Q6_BOVIN	-0.61	0.002	-0.08	0.858	0.36	0.341
84	Synaptic vesicle membrane protein VAT-1 homolog	VAT1	F1MUP9_BOVIN	-1.42	0.461	1.37	0.000	0.11	0.743
85	tubulin alpha-1C chain-like	LOC100141266	F1MNF8_BOVIN	0.69	0.029	0.23	0.590	-0.33	0.341
86	Tubulin beta-5 chain	TUBB5	TBB5_BOVIN	2.08	0.007	-6.64	NA	-1.06	0.502
87	Twinfilin-1	TWF1	TWF1_BOVIN	0.06	0.858	0.96	0.042	0.26	0.245

Log2 fold change ≤ -0.6 and t-test with a significance level of p ≤ 0.05

Log2 fold change ≥ 0.6 and t-test with a significance level of p ≤ 0.05

*In each pair-wise comparison, positive or negative values represent an increase or decrease of protein abundance, respectively, in the indicated group. FC = Fold change. # refer to the # used in Table 5.

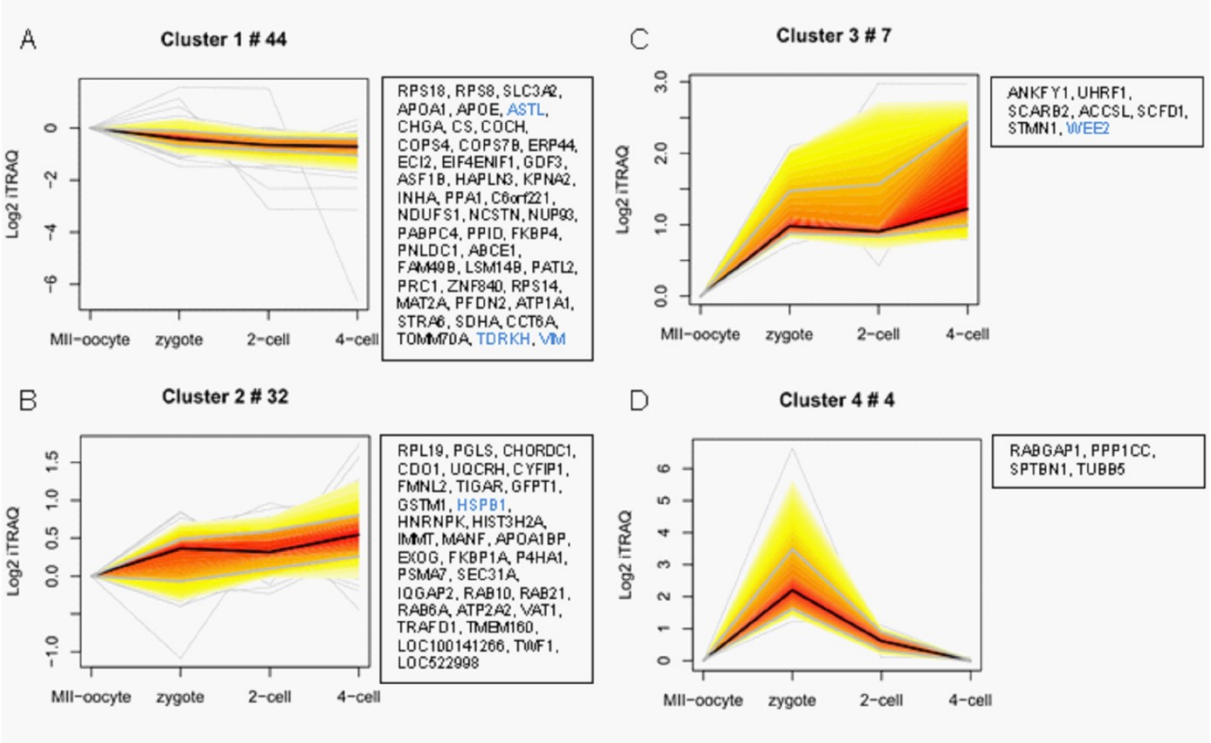

Figure 22. SOTA plot of the 87 proteins significantly different in abundance between MII oocytes, zygotes, two-cell and four-cell embryos. Relative protein abundance with MII oocytes as reference group is expressed as log2 fold change (y-axis) and developmental stages are outlined on the x-axis. Protein enrichment is encoded from low (yellow) to high (red). Proteins also quantified by SRM assay are highlighted in blue. The SOTA analysis was performed in collaboration with Kathrin Otte. **A:** Cluster 1 with 44 proteins, **B:** Cluster 2 with 32 proteins, **C:** Cluster 3 with 7 proteins and **D:** Cluster 4 with 4 proteins.

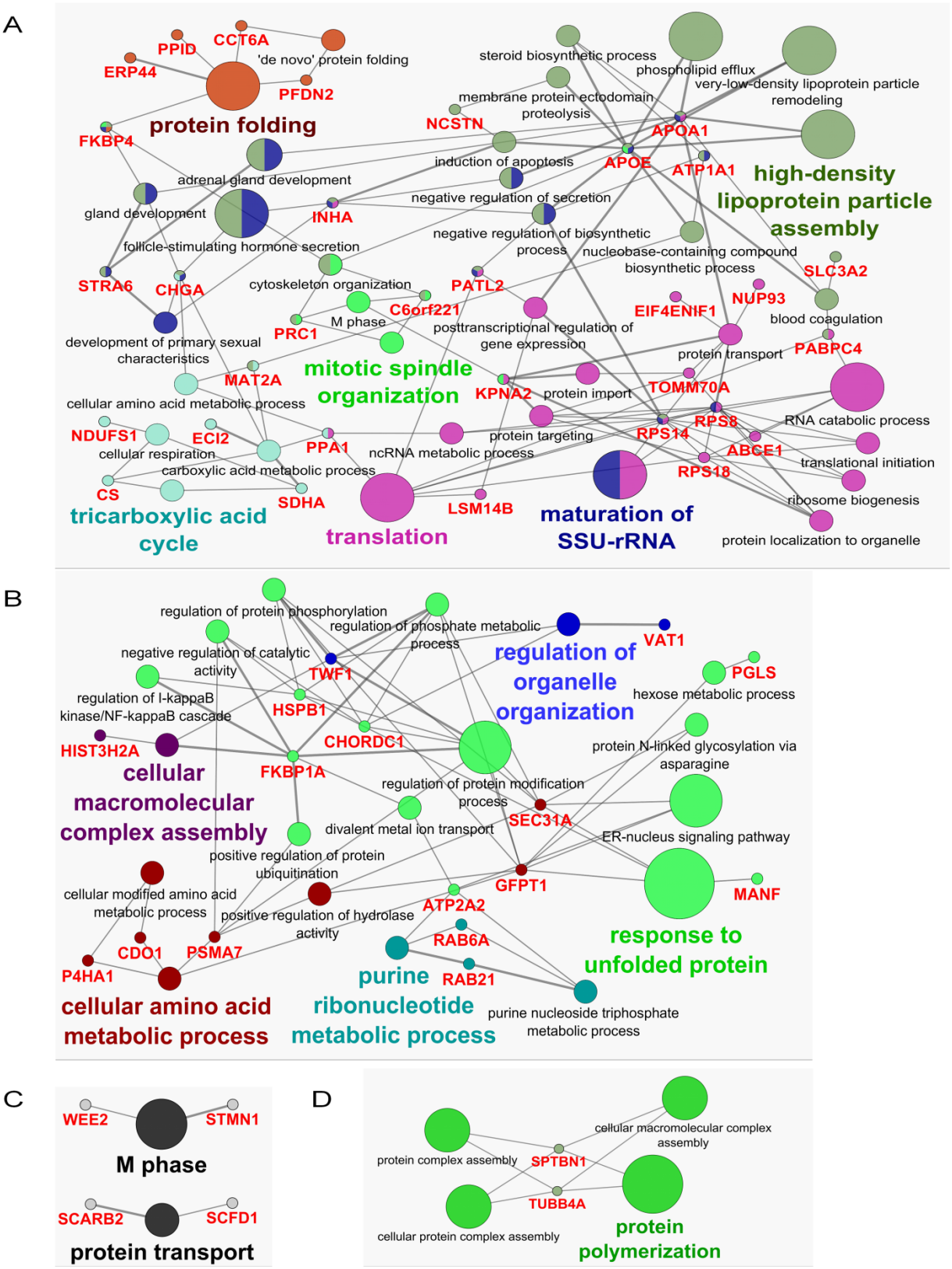

Figure 23. Cytoscape analyses of the four SOTA clusters according to the GO term "biological process". In the functionally grouped networks, terms and their associated genes (colored in red) are linked based on a κ score (≥ 0.3) and the edge thickness indicates the association strength. The node size corresponds to the statistical significance for each term. Cytoscape analyses were performed based on the proteins of **A:** SOTA cluster 1, **B:** SOTA cluster 2, **C:** SOTA cluster 3 and **D:** SOTA cluster 4.

The proteomes of two-cell and four-cell embryos differed most compared to the reference MII oocytes, with 32 and 31 significant differences in protein abundance, respectively. In contrast, the proteomes of two-cell and four-cell embryos were more similar to each other with only 11 detected abundance alterations (Figure 24A). Functionally grouped networks with terms and associated genes were generated by subjecting proteins increased and decreased in abundance to a comparative Cytoscape analyses according to the GO term “biological process”. These networks visualized functional categories significantly enriched during each step of early embryogenesis. First the proteomes of MII oocytes and zygotes were compared to study the effect of fertilization on the level of proteins. Between MII oocytes and zygotes, 9 proteins with increased and another 9 with decreased abundance in the zygote stage were detected. The affected proteins were related to the terms “cellular modified amino acid metabolic process” and “hormone metabolic process” (Figure 24B). During the first cleavage from the zygote stage to the two-cell stage, 11 proteins with increased and 21 proteins with decreased abundance in two-cell embryos were detected. Network analysis revealed proteins involved in “protein polymerization” to be increased and proteins related to the term “translational initiation” to be decreased in abundance from the zygote stage until the two-cell stage (Figure 24C). The second cleavage, leading to the four-cell stage, affected 11 proteins. Compared to two-cell embryos, proteins related to the GO term “regulation of protein ubiquitination” were found to be enriched in four-cell embryos according to the network analysis (Figure 24D).

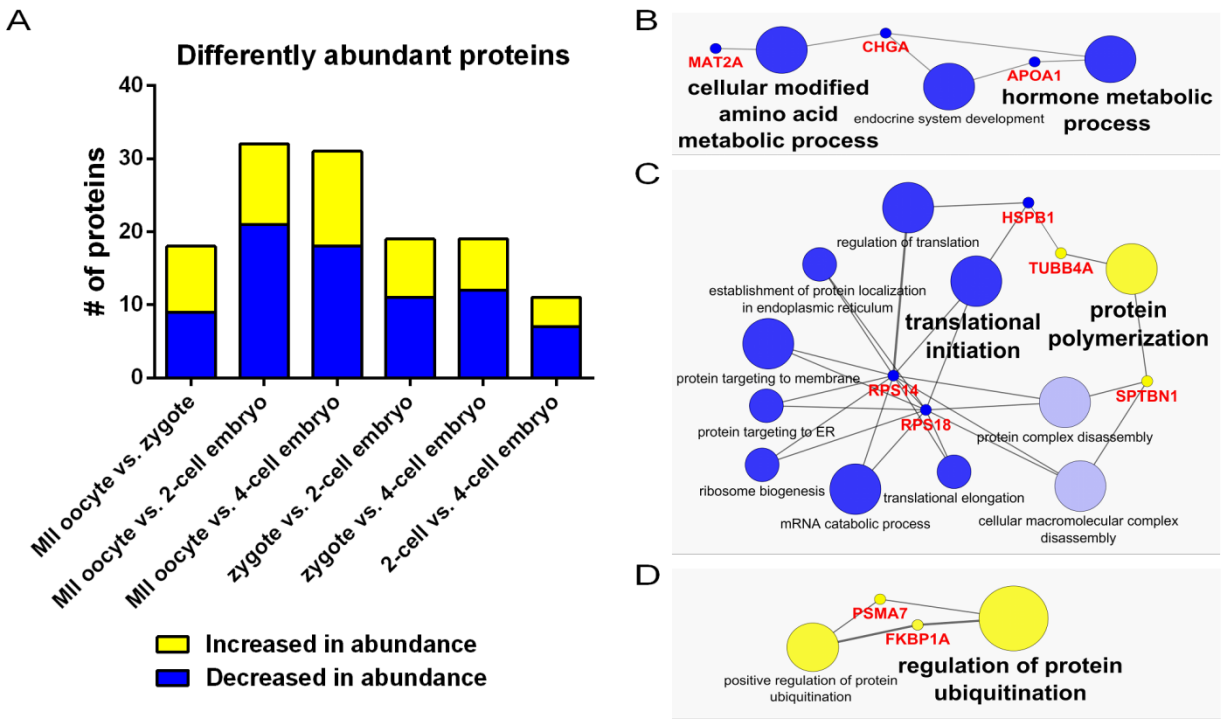

Figure 24. Differently abundant proteins in pair-wise comparisons between MII oocytes, zygotes, and two-cell and four-cell embryos. Yellow color: Proteins increasing in abundance during ongoing development. Blue color: Proteins decreasing in abundance during development. **A:** Number of differently abundant proteins between all six pair-wise comparisons. **B-D:** Cytoscape analyses of three pair-wise comparisons according to the GO term "biological process". In the functionally grouped network, terms and their associated genes (colored in red) are linked based on a κ score (≥ 0.3) and the edge thickness indicates the association strength. The node size corresponds to the statistical significance of each term. **B:** MII oocytes vs. zygotes, **C:** zygotes vs. two-cell embryos and **D:** two-cell vs. four-cell embryos.

3.3.3 Verification of iTRAQ data by 5-plex SRM

To verify protein profiles obtained by the holistic LC-MS/MS approach, SRM assays for a subset of five proteins relevant for early embryogenesis were established. Selection of targeted proteins was based on literature research of biological functions, signal intensities of corresponding peptides and protein profiles determined by the iTRAQ approach. To cover different abundance alteration profiles, proteins from several SOTA clusters were chosen which are highlighted in blue in Figure 22. Three proteins were selected from SOTA cluster 1: Astacin-like metalloendopeptidase (ASTL), tudor and KH domain-containing protein (TDRKH) and vimentin (VIM). Additionally, one protein was selected from SOTA cluster 2, heat shock protein beta-1 (HSPB1), and another one from SOTA cluster 3, wee1-like protein kinase 2 (WEE2). Table 7 shows two characteristic peptides along with the corresponding top 3 transitions selected for relative quantification of the selected proteins. The protein amounts were determined simultaneously in pools of 10 oocytes or embryos each, using synthetic stable isotope-labeled (SI) peptides as internal standards for each endogenous peptide. Four biological replicates were analyzed. Whenever possible, the most intense transition of each peptide was used for relative quantification, and abundance alteration was determined via the intensity ratio of the transition obtained from the endogenous peptide and the corresponding SI peptide. Alterations in protein abundance between groups were expressed as log2 fold change compared to MII oocytes. The two peptides used for quantitation of each protein provided high signal to noise ratios of at least 14. The quantified protein profiles obtained in the SRM experiment by peptide 1 and 2 proved to be consistent in all cases with those acquired in the iTRAQ experiment (Figure 25), demonstrating the reliability of the iTRAQ data.

Table 7. Top three transitions for each of the two peptides per protein selected for validation by SRM.[a]

gene symbol	peptide sequence	precurser ion (m/z)	top three transitions (m/z)	charge / fragment ions	CE (V)
ASTL	SQLQQLLK	479.29	742.48	2+ / y6	20
			629.40	2+ / y5	20
			501.34	2+ / y4	23
	NGGVVEVPFLLSSK	723.40	1118.65	2+ / y10	31
			328.16	2+ / b4	31
			229.09	2+ / b3	40
HSPB1	LFDQAFGLPR	582.31	903.47	2+ / y8	28
			589.35	2+ / y5	28
			660.38	2+ / y6	31
	ALPAAAIEGPAYNR	707.38	677.34	2+ / y6	30
			495.29	2+ / b6	30
			424.26	2+ / b5	36
TDRKH	IDVDTEDIGDER	688.81	1049.44	2+ / y9	32
			934.41	2+ / y8	35
			704.32	2+ / y6	32
	NLDIGLELVR	571.33	686.42	2+ / y6	27
			343.16	2+ / b3	24
			799.50	2+ / y7	27
VIM	TLYTSSPGGVYATR	736.87	1095.54	2+ / y11	37
			820.43	2+ / y8	34
			994.50	2+ / y10	37
	FADLSEAANR	547.27	647.31	2+ / y6	26
			875.42	2+ / y8	23
			334.14	2+ / b3	29
WEE2	IGVGDFGTVYK	578.31	886.43	2+ / y8	27
			1042.52	2+ / y10	24
			714.38	2+ / y6	30
	IGDLGHVTSISNPK	719.39	746.40	2+ / y7	40
			593.30	2+ / b6	40
			692.37	2+ / b7	40

[a]Precursor ions and top three transitions in decreasing intensity order are listed with their mass to charge (m/z) ratios. CE represents the collision energy in Volt.

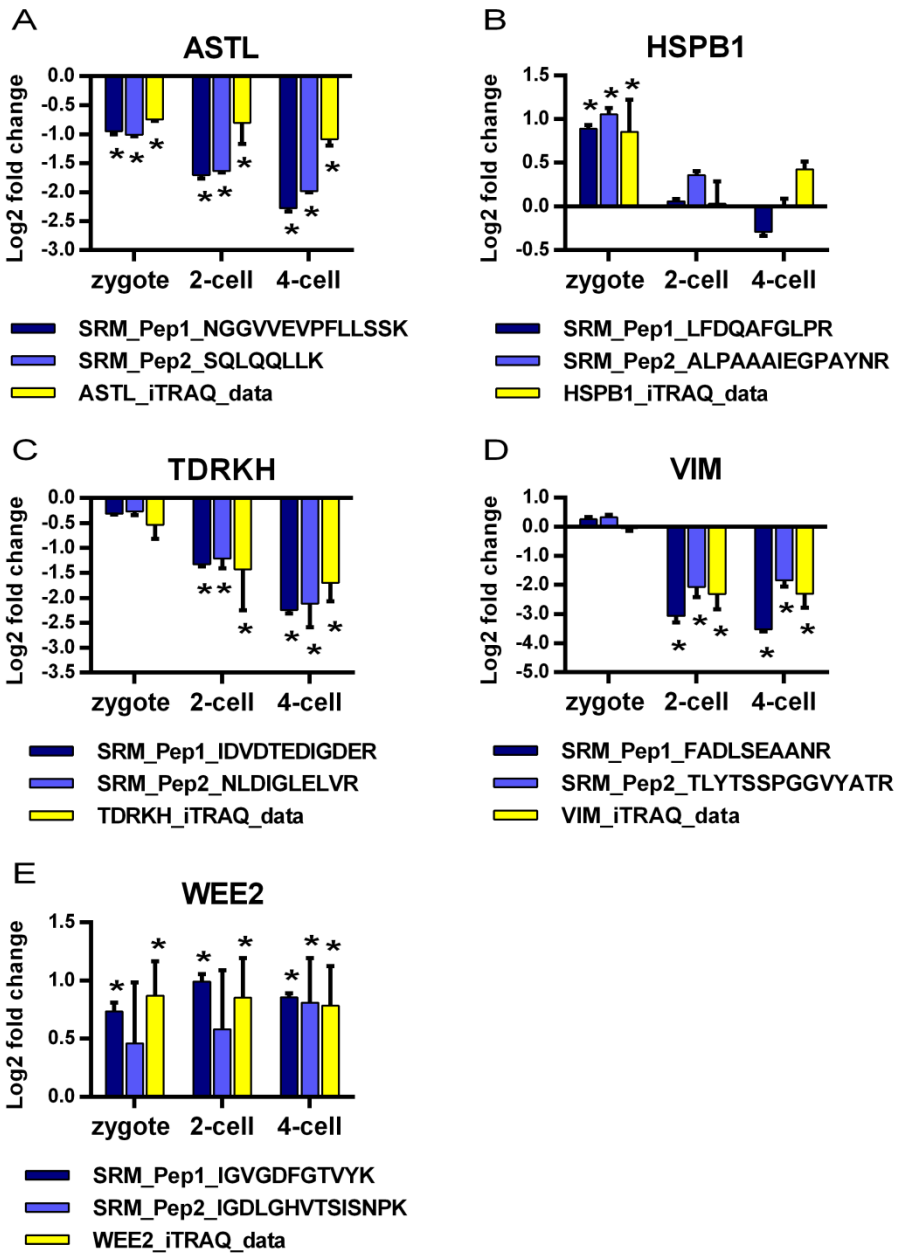

Figure 25. Comparison of protein profiles obtained by either SRM or iTRAQ based quantitation for 5 selected proteins. The log2 fold changes outlined at the y-axis were determined by comparing protein abundances against MII oocytes for each stage ± SD (n = 4). The two peptides used for quantitation of each protein by SRM are outlined separately by dark and bright blue bars and iTRAQ data is outlined by yellow bars. Pep1 = Peptide 1; Pep2 = Peptide 2. **A:** ASTL (SOTA cluster 1), **B:** HSPB1 (SOTA cluster 2), **C:** TDRKH (SOTA cluster 1), **D:** VIM (SOTA cluster 1) and **E:** WEE2 (SOTA cluster 3). *Significant difference in protein abundance compared to MII oocytes (Log2 fold change ≥ $\left|0.6\right|$ and t-test with a significance level of $p \leq 0.05$).

3.3.4 Principle component analysis of iTRAQ and SRM data

To test if the subset of 5 proteins chosen for SRM analysis enables discrimination between oocytes, zygotes, two-cell and four-cell embryos, analysis of variance (ANOVA) was performed on iTRAQ intensities and SRM data. Subsequently, the significantly altered proteins of the iTRAQ data were subjected to principle component analysis (PCA) that led to a clear discrimination of the four groups (Figure 26A). The ANOVA and PCA conducted on the relative quantitation of ASTL, HSPB1, TDRKH, VIM and WEE2 by multiplexed SRM also enabled clear distinction between the four developmental stages (Figure 26B). This indicates the capability of these proteins to be parameters which enable discrimination between MII oocytes, zygotes, and two-cell and four-cell embryos on the abundance level of a few proteins.

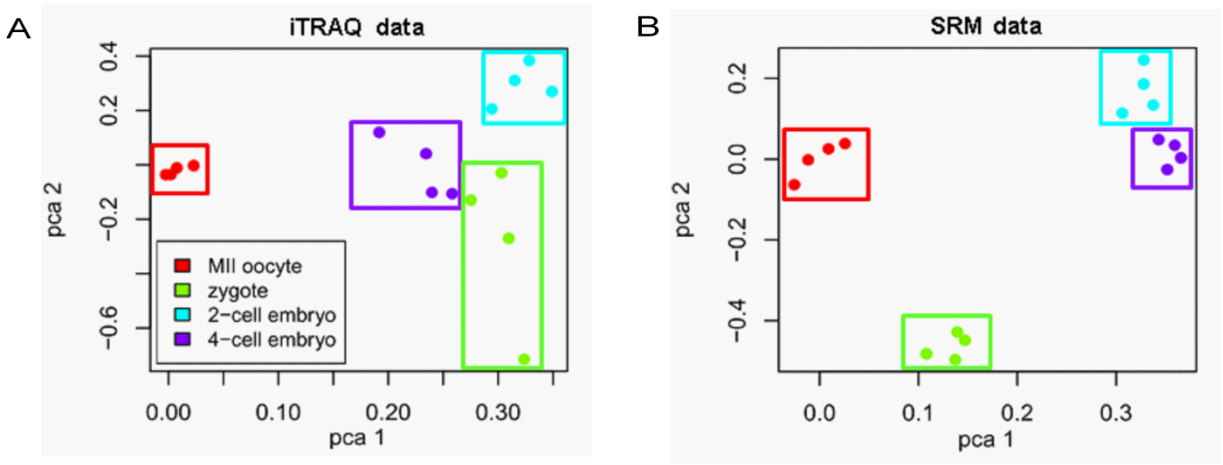

Figure 26. Principal component analysis (PCA) of iTRAQ and SRM data. A: Analysis of variance (ANOVA) was performed on iTRAQ data (n = 4) followed by principal component analysis of the significant differences in protein abundance. **B:** ANOVA and PCA was conducted on the targeted, SRM-based relative quantitation of ASTL, HSPB1, TDRKH, VIM and WEE2 (n = 4). ANOVA and PCA analysis was performed in collaboration with Kathrin Otte.

3.3.5 Localization of WEE2 by LSM

WEE2 protein was found to increase between MII oocytes and two-cell embryos by a log2 fold change of about 0.9 (Figure 25E). Immunofluorescence and LSM was used to study the localization of WEE2 in two-cell embryos. Staining for WEE2 protein revealed it to be localized inside of the nucleus (Figure 27).

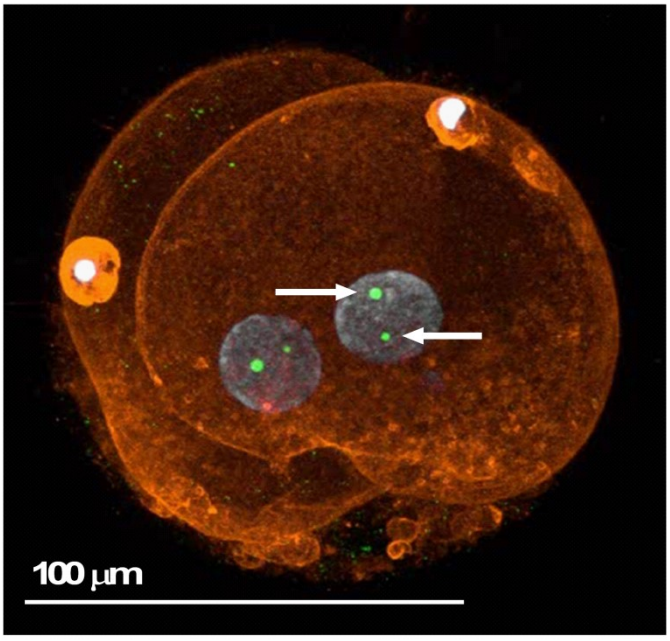

Figure 27. LSM analysis of WEE2 in a two-cell embryo. WEE2 staining is shown in green, DNA staining with DAPI is in white and f-actin filaments (phalloidin-TRITC) staining is shown in red. Arrows indicate the localization of WEE2 in the nucleus of one blastomere of the two-cell embryo. Scale bar represents 100 µm. Image capturing and interpretation was performed in collaboration with Dr. Felix Habermann.

3.4 Targeted proteome analysis by multiplexed SRM

3.4.1 General remarks

The multiplexed SRM assay consisting of ASTL, HSPB1, TDRKH, VIM and WEE2 was further extended to cover a larger set of biologically relevant proteins. Target proteins were selected based on their significant differences in abundance during oocyte maturation (Table 2 and 3) and early embryogenesis (Table 5 and 6), as well as from previous proteomic experiments of our lab and literature research of biological functions. In total, 27 proteins were chosen for the multiplexed SRM assay, which are listed in Table 8. The 54 peptides of the 27 selected proteins and their corresponding SI peptides (324 transitions) were measured simultaneously in a scheduled SRM assay. In Figure 28, an exemplary SRM chromatogram from the measurement of 10 zygotes is depicted. Zygotes were selected, because the abundance of some analyzed proteins was very low in GV and MII oocytes. To improve quantification, the added amounts of SI peptides were optimized to closely reflect the amounts of the endogenous peptides in the sample. The complete SRM method can be viewed in Supplementary Table 10.

Table 8. Proteins for which SRM assays were established.

Study of origin: a: iTRAQ study of oocyte maturation; b: iTRAQ study of embryogenesis; c: previous proteomic experiments of the lab.

protein name	gene name	peptide sequences	Study of origin
Zygote arrest 1 variant 1	ZAR1	TLAVYSPVTSR DAAVQVNPFR	a
Heat shock protein 70	HSP70	NQVALNPQNTVFDAK LYQGAGGPGAGGFGAQGP K	a
Importin subunit alpha-8	KPNA7	IGQVVDTGVLPR LIVDAGLIPR	a
Clusterin	CLU	GSLFFNPK LLLSSLEEAK	a
Retinol-binding protein 4	RBP4	DPSGFSPEVQK YWGVASFLQK	a
Gametocyte specific factor 1	GTSF1	LATCPFNAR SCIEQDVVNQTR	a
Tudor and KH domain-containing protein	TDRKH	IDVDTEDIGDER NLDIGLELVR	b
Heat shock protein beta-1	HSPB1	ALPAAAIEGPAYNR LFDQAFGLPR	b
Protein regulator of cytokinesis 1	PRC1	LQIPAEER VEVAQYWDR	b
Astacin-like metalloendopeptidase	ASTL	NGGVVEVPFLLSSK SQLQQLLK	b
Programmed cell death protein 5	PDCD5	VSEQGLIEILEK NSILAQVLDQSAR	c
Phosphatidylethanolamine-binding protein 1	PEBP1	LYEQLSGK YGGAEVDELGK	c
Ubiquitin-40S ribosomal protein S27a	RPS27A	ESTLHLVLR TLSDYNIQK	c
Thioredoxin-dependent peroxide reductase, mitochondrial	PRDX3	GLFIIDPNGVIK HLSVNDLPVGR	c
Glutathione S-transferase mu 3	GSTM3	YLEQLPGQLK YSWFAGEK	c
Lysosomal-associated membrane protein 2	LAMP2	IPLNDIFR EKEVFTVNNR	c
10 kDa heat shock protein, mitochondrial	HSPE1	VLLPEYGGTK VLQATVVAVGSGSK	c
Pterin-4-alpha-carbinolamine dehydratase	PCBD1	AVGWNELEGR DQLLPNLR	c
ACC synthase-like protein 2	ACCSL	NTLGYINLGTSENK FGALYTHNR	a, b
Wee1-like protein kinase 2	WEE2	IGVGDFGTVYK IGDLGHVTSISNPK	a, b
E3 ubiquitin-protein ligase UHRF1	UHRF1	YAPIEGNR LNDTIQLLVR	a, b
Stathmin	STMN1	ASGQAFELILSPR AIEENNNFSK	a, b
Aurora kinase A	AURKA	TAVPLSDGPK IADFGWSVHAPSSR	a, b
Vimentin	VIM	FADLSEAANR TLYTSSPGGVYATR	a, b
Transforming acidic coiled-coil-containing protein 3	TACC3	QASEEIAQVR ICDDLISK	a, b
Y-box-binding protein	YBX2	TPGNPATAASGTPAPLAR GAEAANVTGPGGVPVK	a, c
Hyaluronan and proteoglycan link protein 3	HAPLN3	SNCGALEPGVR LTLAEAR	b, c

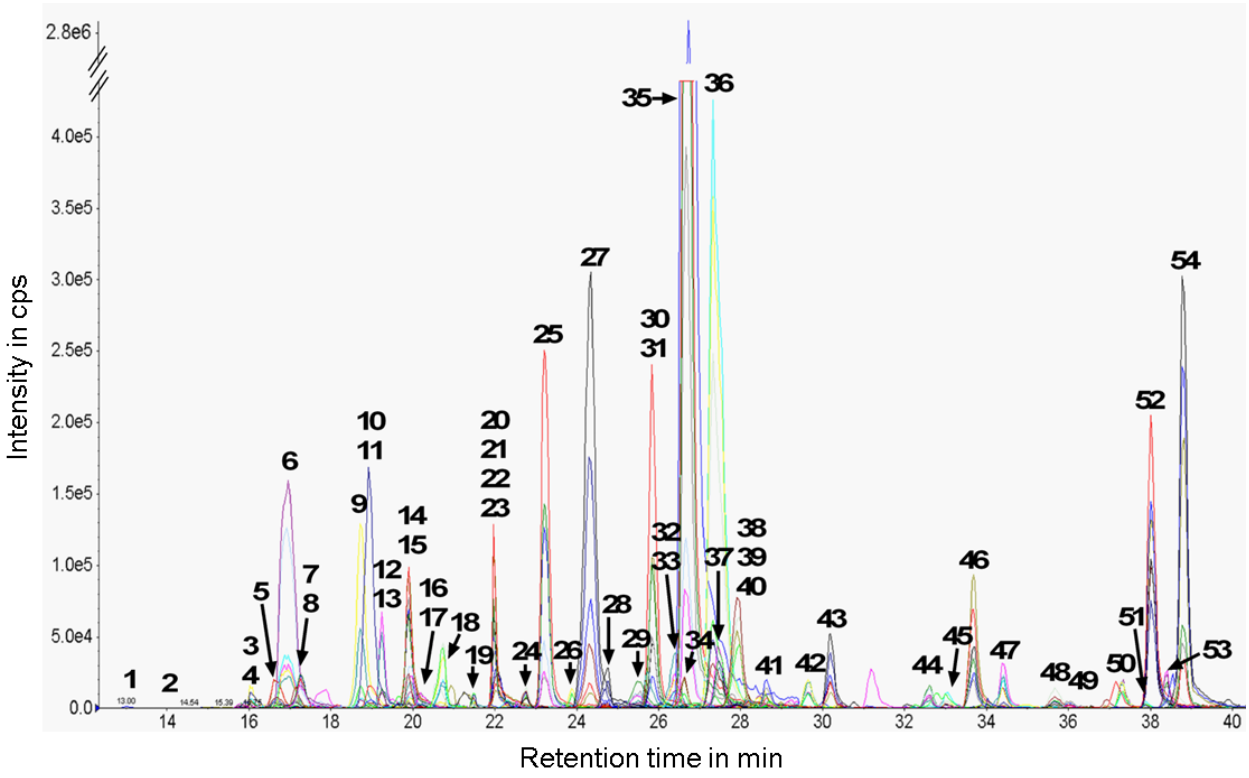

Figure 28. SRM chromatogram obtained from the analysis of ten zygotes by LC-ESI-MS/MS. The light and heavy form of 54 peptides corresponding to 27 proteins were analyzed. Peak assignments: 1, UHRF1_YAPIEGNR; 2, STMN1_AIEENNNFSK; 3, TACC3_QASEEIAQVR; 4, HAPLN3_SNCGALEPGVR; 5, LAMP2_EKEVFTVNNR; 6, PEBP1_LYEQLSGK3; 7, HAPLN3_LTLAEAR; 8, ACCSL_FGALYTHNR; 9, AURKA_TAVPLSDGPK; 10, RPS27A_TLSDYNIQK; 11, RBP4_DPSGFSPEVQK; 12, YBX2_GAEAANVTGPGGVPVK; 13, PRC1_LQIPAEER; 14, PEBP1_YGGAEVDELGK; 15, TACC3_ICDDLISK; 16, GTSF1_LATCPFNAR; 17, VIM_FADLSEAANR; 18, YBX2_TPGNPATAASGTPAPLAR; 19, WEE2_IGDLGHVTSISNPK; 20, GTSF1_ SCIEQDVVNQTR; 21, HSP70_LYQGAGGPGAGGFGAQGPK; 22, HSPE1_VLQATVVAVGSGSK; 23, VIM_TLYTSSPGGVYATR; 24, TDRKH_IDVDTEDIGDER; 25, PRDX3_HLSVNDLPVGR; 26, ZAR1_TLAVYSPVTSR; 27, HSPE1_VLLPEYGGTK; 28, RPS27A_ESTLHLVLR; 29, HSPB1_ALPAAAIEGPAYNR; 30, ZAR1_DAAVQVNPFR; 31, ASTL_SQLQQLLK; 32, KPNA7_IGQVVDTGVLPR; 33, PRC1_VEVAQYWDR; 34, PCBD1_AVGWNELEGR; 35, GSTM3_YLEQLPGQLK; 36, GSTM3_YSWFAGEK; 37, HSP70_NQVALNPQNTVFDAK; 38, ACCSL_NTLGYINLGTSENK; 39, PCBD1_DQLLPNLR; 40, CLU_GSLFFNPK; 41, AURKA_IADFGWSVHAPSSR; 42, WEE2_IGVGDFGTVYK; 43, CLU_LLLSSLEEAK; 44, KPNA7_LIVDAGLIPR; 45, UHRF1_LNDTIQLLVR; 46, LAMP2_IPLNDIFR; 47, HSPB1_LFDQAFGLPR; 48, STMN1_ASGQAFELILSPR; 49, TDRKH_NLDIGLELVR; 50, PDCD5_NSILAQVLDQSAR; 51, RBP4_YWGVASFLQK; 52, ASTL_NGGVVEVPFLLSSK; 53, PDCD5_VSEQGLIEILEK; 54, PRDX3_GLFIIDPNGVIK.

3.4.2 Reproducibility of the 27-plex SRM assay

The reproducibility of the 27-plex SRM assay was validated by iterative analysis of twelve aliquots comprising ten zygotes each. The zygote stage was selected for this assay, because the abundance of some analyzed proteins was very low in GV and MII oocytes. The mean coefficient of variation (CV) was 10.1 % for all transitions (quantifier + both qualifiers) (Figure 29A) and the mean CV for the quantifier transition only was 7.8 % (Figure 29B). The reproducibility of the retention time of each peptide was also tested and the mean CV was

0.5 %. The elution times of the peptides were well separated and evenly distributed over the chromatographic gradient (Figure 29C).

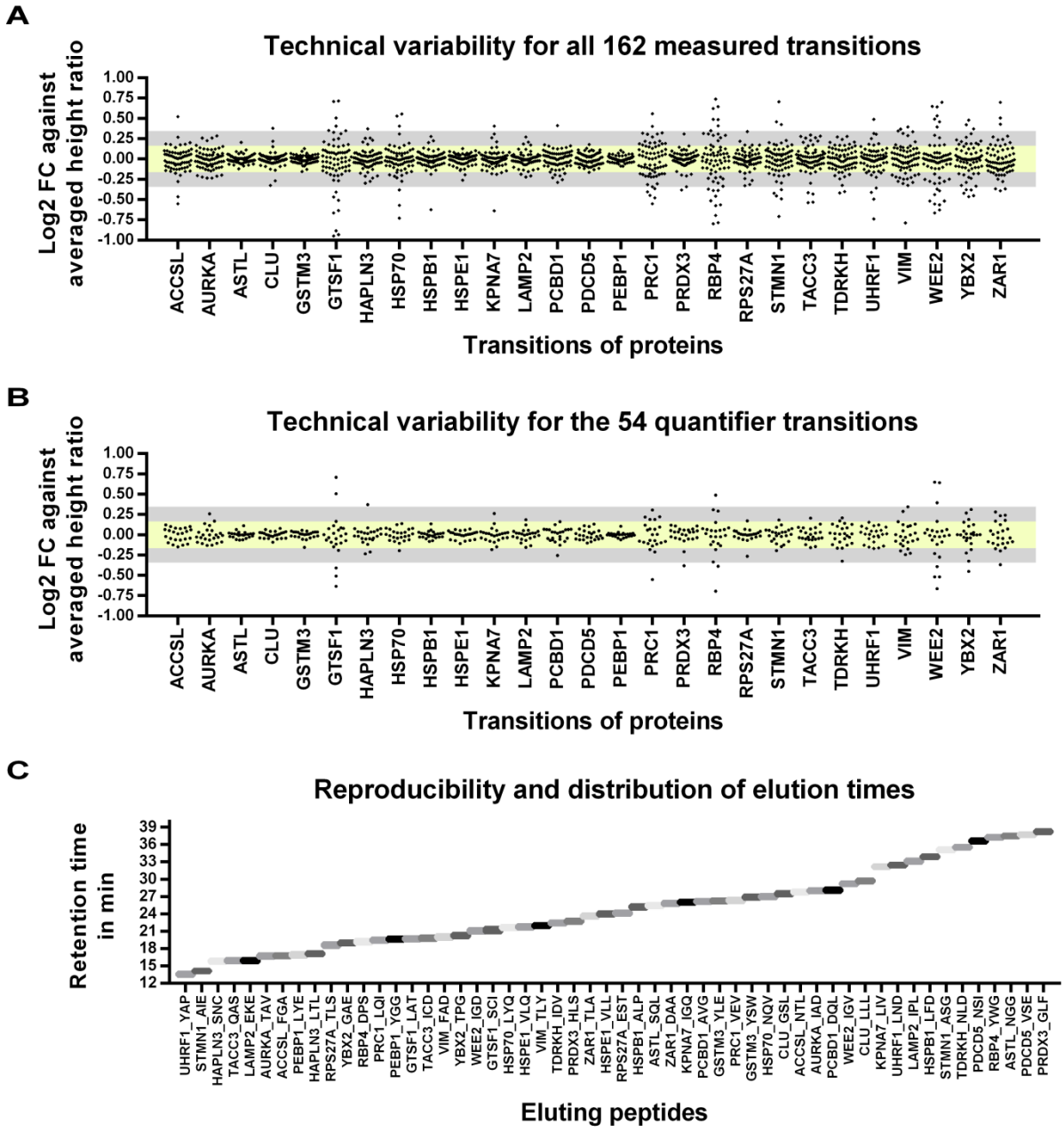

Figure 29. Reproducibility of the 27-plex SRM assay. Yellow bar: 10 % variation; Grey bar: 25 % variation; FC = Fold change. **A:** Technical variability of the SRM measurement of all 162 transitions (quantifier + qualifier) corresponding to 27 proteins. **B:** Technical variability of the SRM measurement of the 54 quantifier transitions corresponding to 27 proteins. **C:** Reproducibility and distribution of the elution times over the chromatographic gradient of all 54 analyzed peptides.

3.4.3 Targeted quantification of 27 proteins in oocytes and embryos

3.4.3.1 Relative quantification of 27 proteins

Protein amounts were determined simultaneously in six biological replicates consisting of pools of ten oocytes or embryos each. All oocytes and embryos were evaluated microscopically prior to collection. Oocytes were studied at the GV and at the MII stage. The studied embryonic stages comprised embryos at zygote, two-cell, four-cell, eight- to 16-cell, morula and blastocyst stage. Embryos at the blastocyst stage were collected at day 7 and 8 post insemination. At day 8 post insemination, only hatched blastocysts were collected. Relative quantification was done via the intensity ratio of the quantifier transition of the endogenous peptide (light peptide) to SI peptide and alterations in protein abundance between groups were expressed as mean log2 fold change compared to the dataset mean of each peptide (Figure 30). Intensity values were only considered valid with a signal to noise ratio ≥ 10. Significance criteria for quantification were a log2 fold change ≥ $\left|0.6\right|$ and $p < 0.05$. In about 70 % of all significant cases, the calculated log2 fold change of peptide 1 differed less than 25°% from peptide 2. Further, in about 5 % of all significant cases, the calculated log2 fold change of peptide 1 differed more than 100 % from peptide 2. Peptide 1 and 2 used for quantification of each protein are illustrated in Supplementary Figure 33.

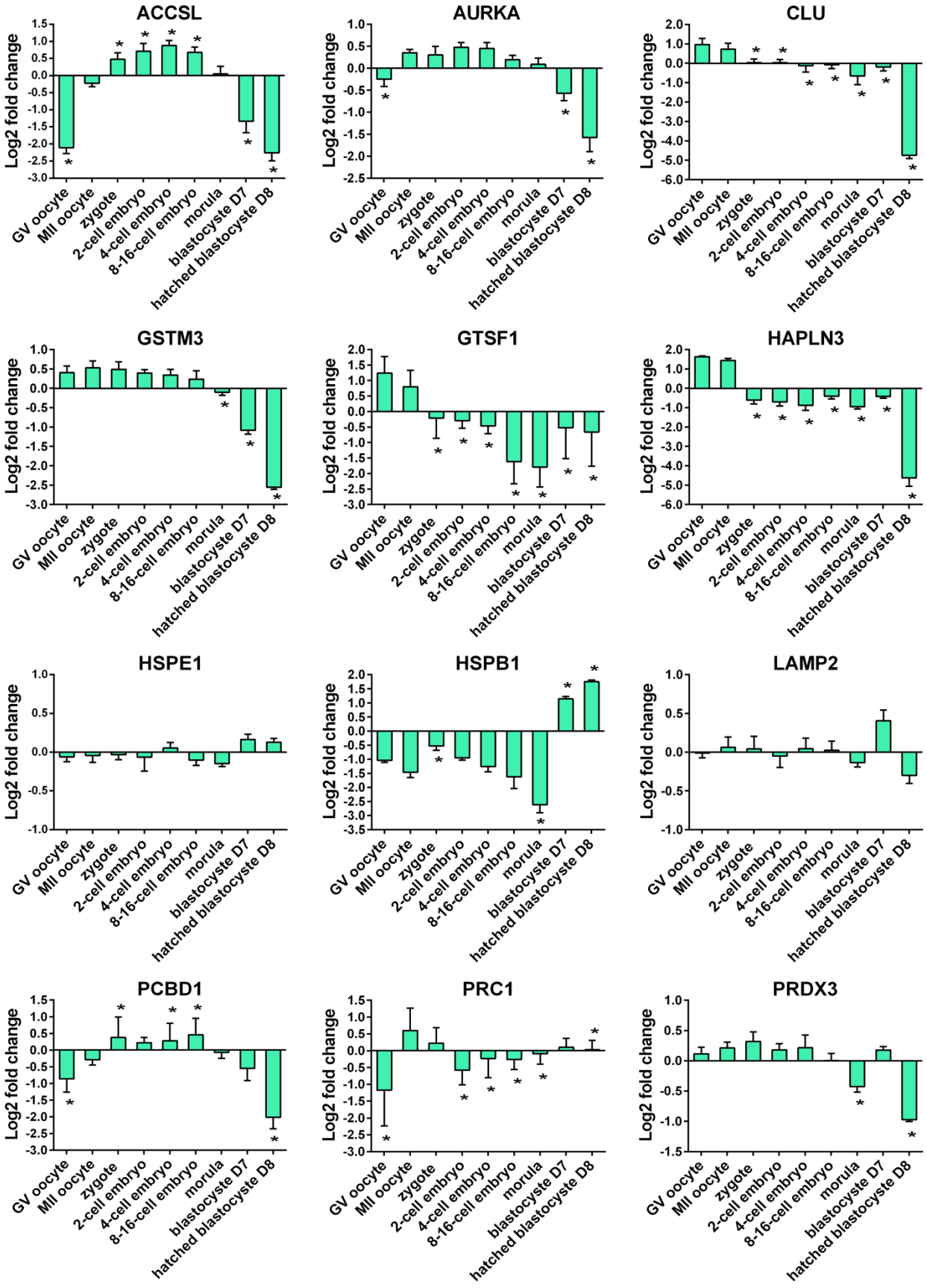
ACCSL
AURKA
CLU
GSTM3
GTSF1
HAPLN3
HSPE1
HSPB1
LAMP2
PCBD1
PRC1
PRDX3
Log2 fold change
GV oocyte
MII oocyte
zygote
2-cell embryo
4-cell embryo
8-16-cell embryo
morula
blastocyste D7
hatched blastocyste D8

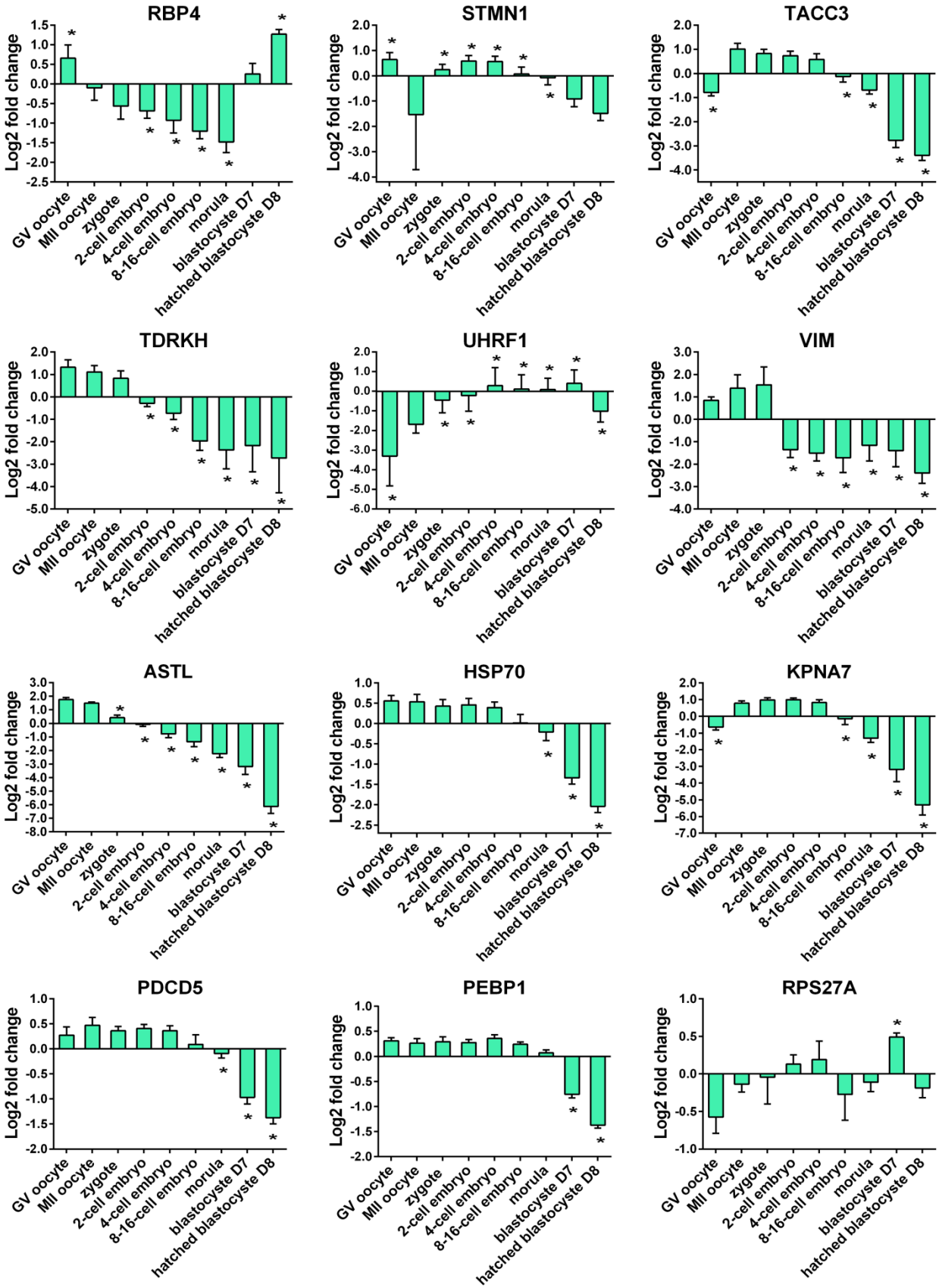
RBP4
STMN1
TACC3
TDRKH
UHRF1
VIM
ASTL
HSP70
KPNA7
PDCD5
PEBP1
RPS27A
Log2 fold change
GV oocyte
MII oocyte
zygote
2-cell embryo
4-cell embryo
8-16-cell embryo
morula
blastocyste D7
hatched blastocyste D8

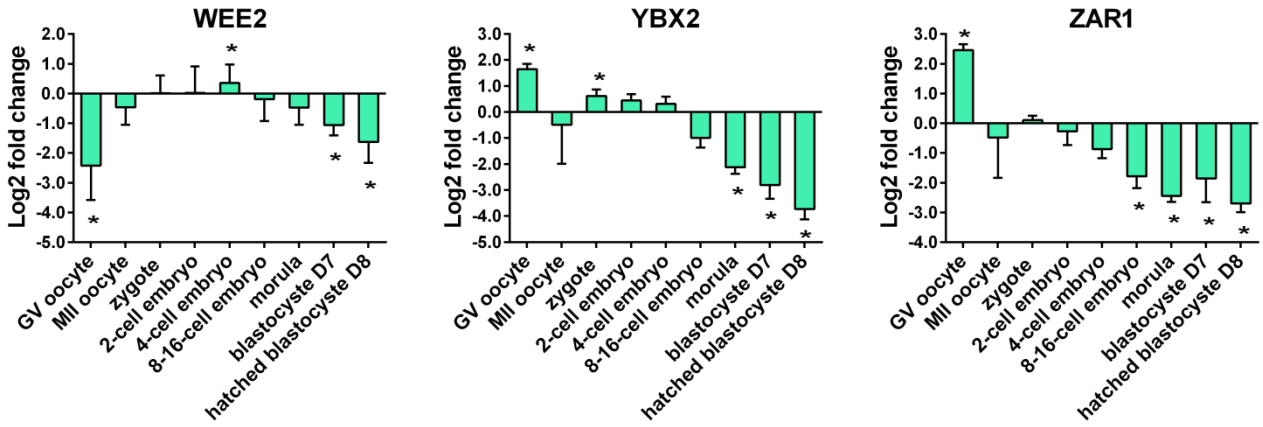

Figure 30. Relative quantification of 27 proteins in oocytes and embryos by SRM. Values are expressed as mean log2 fold change ± SD (n=6) compared to the dataset mean of each peptide. D7 = day 7; D8 = day 8. *Significant changes of protein abundance compared to MII oocytes: $p < 0.05$ and log2 fold change $\geq |0.6|$.

3.4.3.2 Comparison between iTRAQ data and SRM data

Sixteen proteins of the 27-plex SRM assay also showed significant abundance alterations in at least one of the two previously performed iTRAQ studies covering GV oocytes, zygotes, two-cell embryos and four-cell embryos compared to MII oocytes (see chapter 3.2 and 3.3). The quantitative values obtained by iTRAQ and SRM analysis were outlined and compared (Table 9). In 31 out of 34 cases, highlighted in blue in Table 9, a significant value ($p \leq 0.05$ and log2 fold change $\geq |0.6|$) was obtained by SRM analysis which confirmed the value obtained by iTRAQ analysis. In three out of 34 cases, highlighted in orange in Table 9, no significant quantitative value was obtained by SRM analysis.

Table 9. Comparison of significant abundance alterations obtained by either iTRAQ or SRM analysis.

Only significant quantitative values of each stage compared to MII oocytes (Log2 FC $\geq |0.6|$ and $p \leq 0.05$) are listed. Positive and negative values represent an increase or decrease of protein abundance in the indicated group compared to MII oocytes, respectively. N/A: No quantitative value available. N/S: No significant quantitative value available.

		GV oocyte		Zygote		two-cell embryo		four-cell embryo	
		[Log2 FC]		[Log2 FC]		[Log2 FC]		[Log2 FC]	
Quantified Proteins	**Gene Symbol**	**iTRAQ**	**SRM**	**iTRAQ**	**SRM**	**iTRAQ**	**SRM**	**iTRAQ**	**SRM**
Probable inactive 1-aminocyclopropane-1-carboxylate synthase-like protein 2	ACCSL	-1.49	-1.89	0.72	0.70	0.99	0.93	1.11	1.10
Astacin-like metalloendopeptidase	ASTL	N/S	N/S	-0.75	-1.06	-0.81	-1.56	-1.09	-2.26
Aurora kinase A	AURKA	-0.79	-0.60	N/S	N/S	N/S	N/S	N/S	N/S
Gametocyte-specific factor 1	GTSF1	0.66	N/S	N/S	-1.01	N/S	-1.09	N/S	-1.26
Hyaluronan and proteoglycan link protein 3	HAPLN3	N/S	N/S	-1.48	-2.05	-1.49	-2.14	-1.32	-2.31
Heat shock 27kDa protein 1	HSPB1	N/S	N/S	0.86	0.93	N/S	N/S	N/S	N/S
Importin subunit alpha-8	KPNA7	-0.96	-1.43	N/S	N/S	N/S	N/S	N/S	N/S
Protein regulator of cytokinesis 1	PRC1	N/A	-1.77	N/S	N/S	-1.17	-1.18	-1.08	-0.83
Retinol-binding protein 4	RBP4	0.80	0.76	N/S	N/S	N/S	N/S	N/S	-0.83
Stathmin	STMN1	2.73	2.17	2.09	1.77	2.44	2.11	2.38	2.09
Transforming acidic coiled-coil-containing protein 3	TACC3	-1.25	-1.80	N/S	N/S	N/S	N/S	N/S	N/S
Tudor and KH domain-containing protein	TDRKH	N/S	N/S	N/S	N/S	-1.43	-1.40	-1.70	-1.83
E3 ubiquitin-protein ligase UHRF1	UHRF1	-1.53	-1.61	0.88	1.24	0.90	1.48	1.22	1.98
Vimentin	VIM	N/S	N/S	N/A	N/S	-2.32	-2.75	-2.30	-2.91
Wee1-like protein kinase 2	WEE2	-2.90	-1.96	0.87	N/S	0.85	N/S	0.78	0.82
Zygote arrest protein 1	ZAR1	1.09	2.95	N/A	N/S	N/A	N/S	N/A	N/S

3.4.3.3 Absolute quantification of nine proteins

For absolute quantification of nine proteins, two synthetic SI “AQUA™” peptides were used as internal standard for each protein. These AQUA™ peptides are provided in solution and the concentration it determined at a precision of ± 5% by the manufacturer, which enables the calculation of absolute protein contents. They were added to the sample prior to digestion at pre-defined concentrations which are listed in Supplementary Table 10.

3.4.3.3.1 Determination of the limit of detection (LOD) and the limit of quantification (LOQ) for all nine proteins

For each of the 18 AQUA™ peptides, the LOD and LOQ were determined. The AQUA™ peptides were added to the samples consisting of three aliquots of five GV oocytes each in concentrations ranging from 50 amol to 100 fmol per sample. For the LOD, the signal to noise ratio had to be ≥ 3 and for the LOQ, the signal to noise ratio had to be ≥ 10. The responses were linear over several orders of magnitude for all peptides (Figure 31). The LOQ and LOD of the 18 SI peptides used for absolute quantification by SRM are listed in Supplementary Table 11.

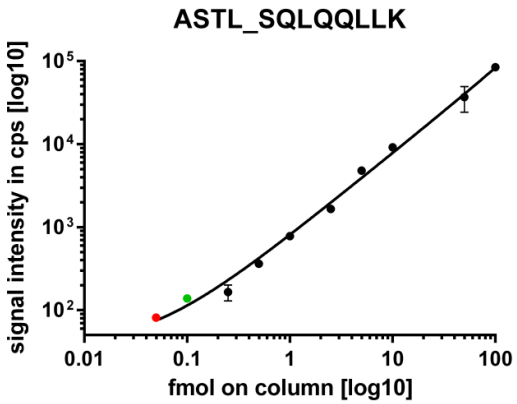
ASTL_SQLQQLLK
signal intensity in cps [log10]
fmol on column [log10]

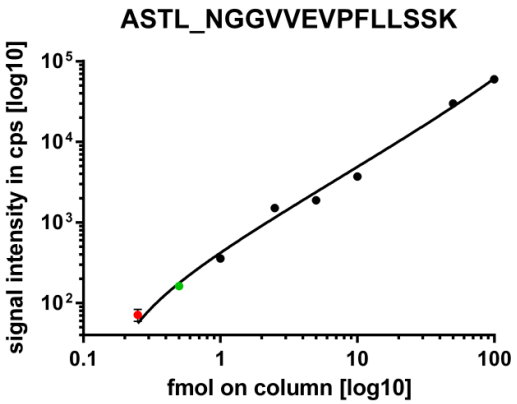
ASTL_NGGVVEVPFLLSSK
signal intensity in cps [log10]
fmol on column [log10]

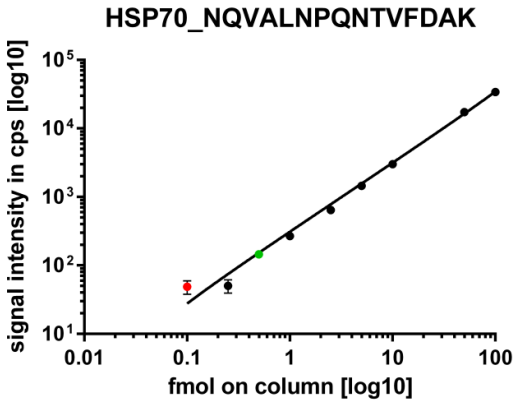
HSP70_NQVALNPQNTVFDAK
signal intensity in cps [log10]
fmol on column [log10]

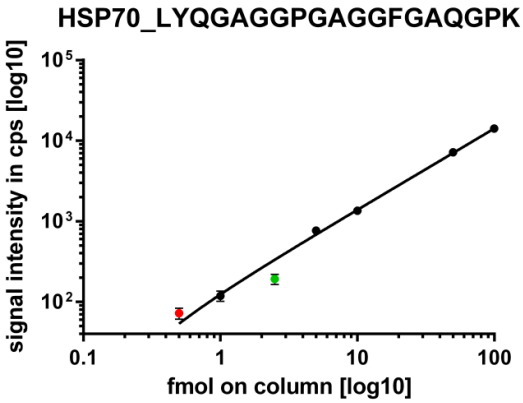
HSP70_LYQGAGGPGAGGFGAQGPK
signal intensity in cps [log10]
fmol on column [log10]

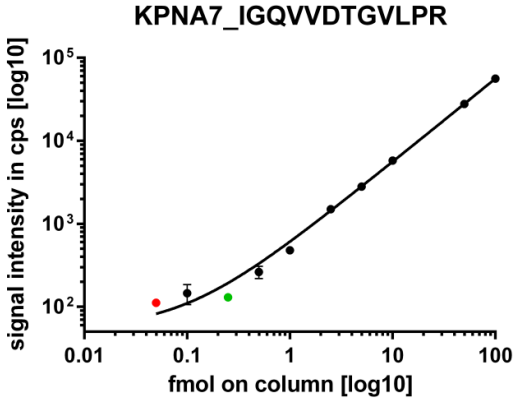
KPNA7_IGQVVDTGVLPR
signal intensity in cps [log10]
fmol on column [log10]

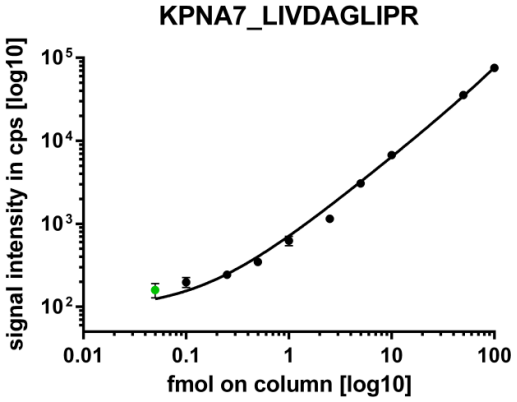
KPNA7_LIVDAGLIPR
signal intensity in cps [log10]
fmol on column [log10]

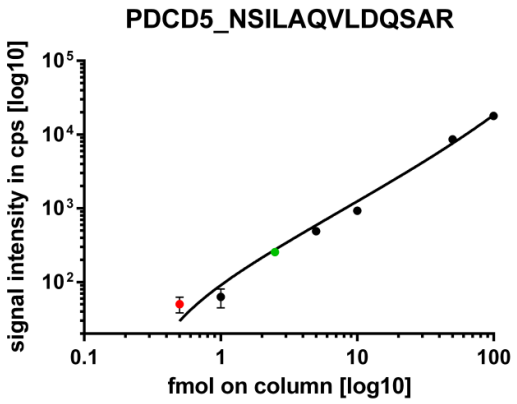
PDCD5_NSILAQVLDQSAR
signal intensity in cps [log10]
fmol on column [log10]

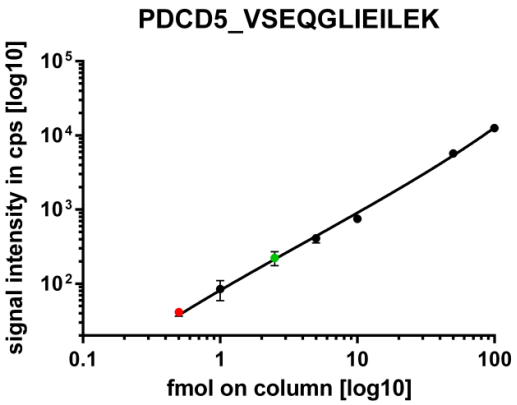
PDCD5_VSEQGLIEILEK
signal intensity in cps [log10]
fmol on column [log10]

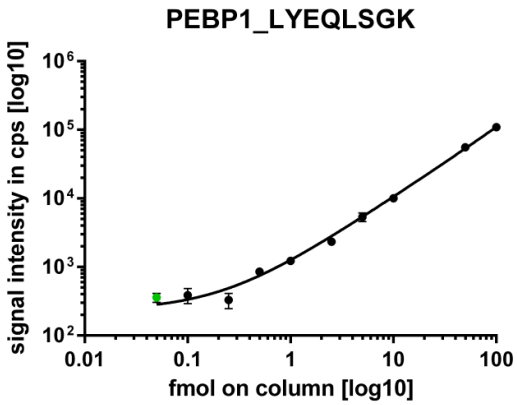
PEBP1_LYEQLSGK
signal intensity in cps [log10]
fmol on column [log10]

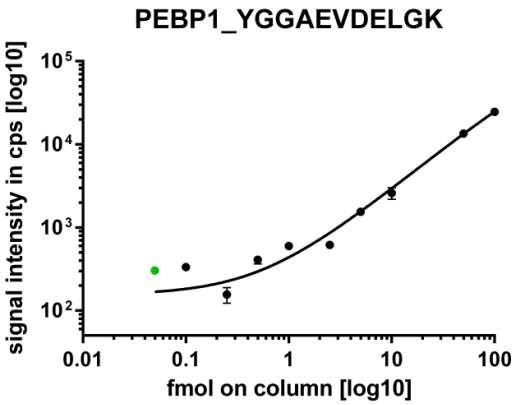
PEBP1_YGGAEVDELGK
signal intensity in cps [log10]
fmol on column [log10]

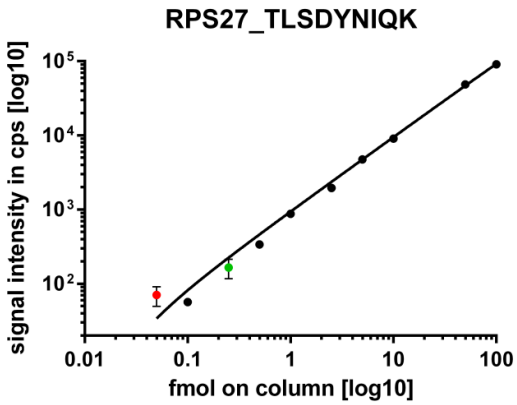
RPS27_TLSDYNIQK
signal intensity in cps [log10]
fmol on column [log10]

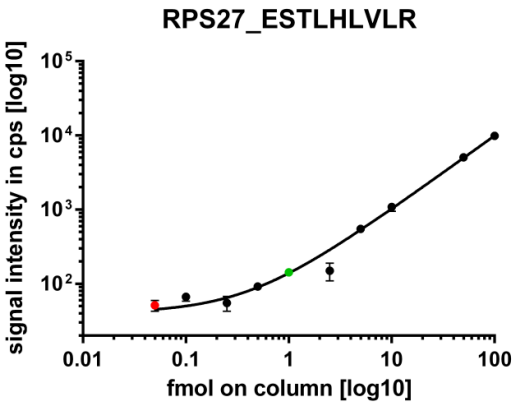
RPS27_ESTLHLVLR
signal intensity in cps [log10]
fmol on column [log10]

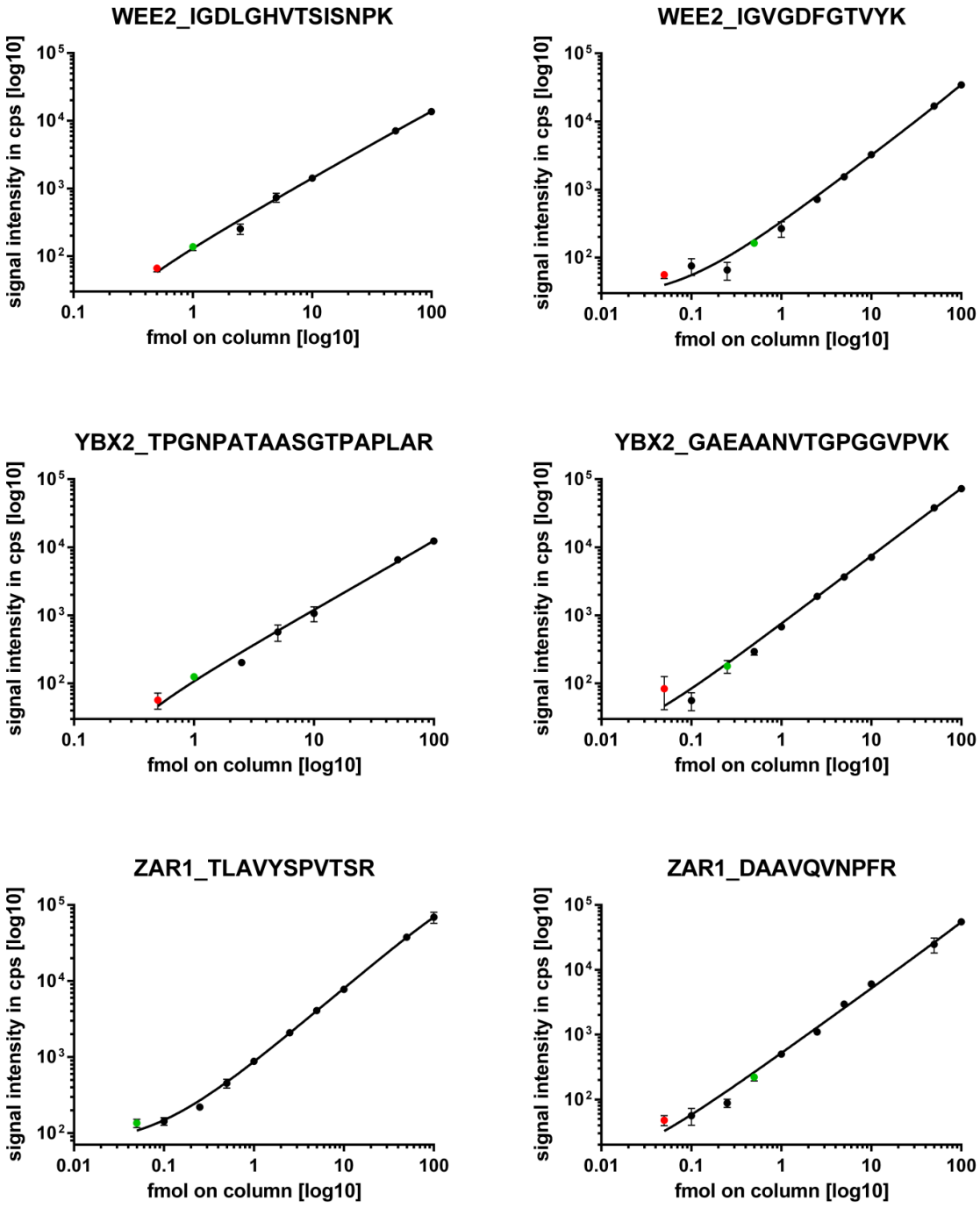

Figure 31. Determination of the LOQ and LOD of the 18 AQUA™ peptides by SRM. Five GV oocytes were used as background. Values are depicted as mean signal intensity in cps [log10] ± SD (n=3). Red data point: LOD; Green data point: LOQ.

3.4.3.3.2 Absolute quantification of nine proteins in oocytes and embryos

Protein amounts were determined simultaneously in six biological replicates consisting of pools of ten oocytes or embryos each as described in chapter 3.4.3.1. For absolute quantification, the intensity ratios of the quantifier transition of the light and the heavy peptide were used and the protein abundance was expressed as mean amol or fmol per oocyte or embryo (Figure 32). Intensity values were only considered valid with a signal to noise ratio ≥ 10. Significance criteria for quantification were a log2 fold change ≥ $|0.6|$ and $p < 0.05$. Peptide 1 and 2 used for quantification of each protein are illustrated in Supplementary Figure 34.

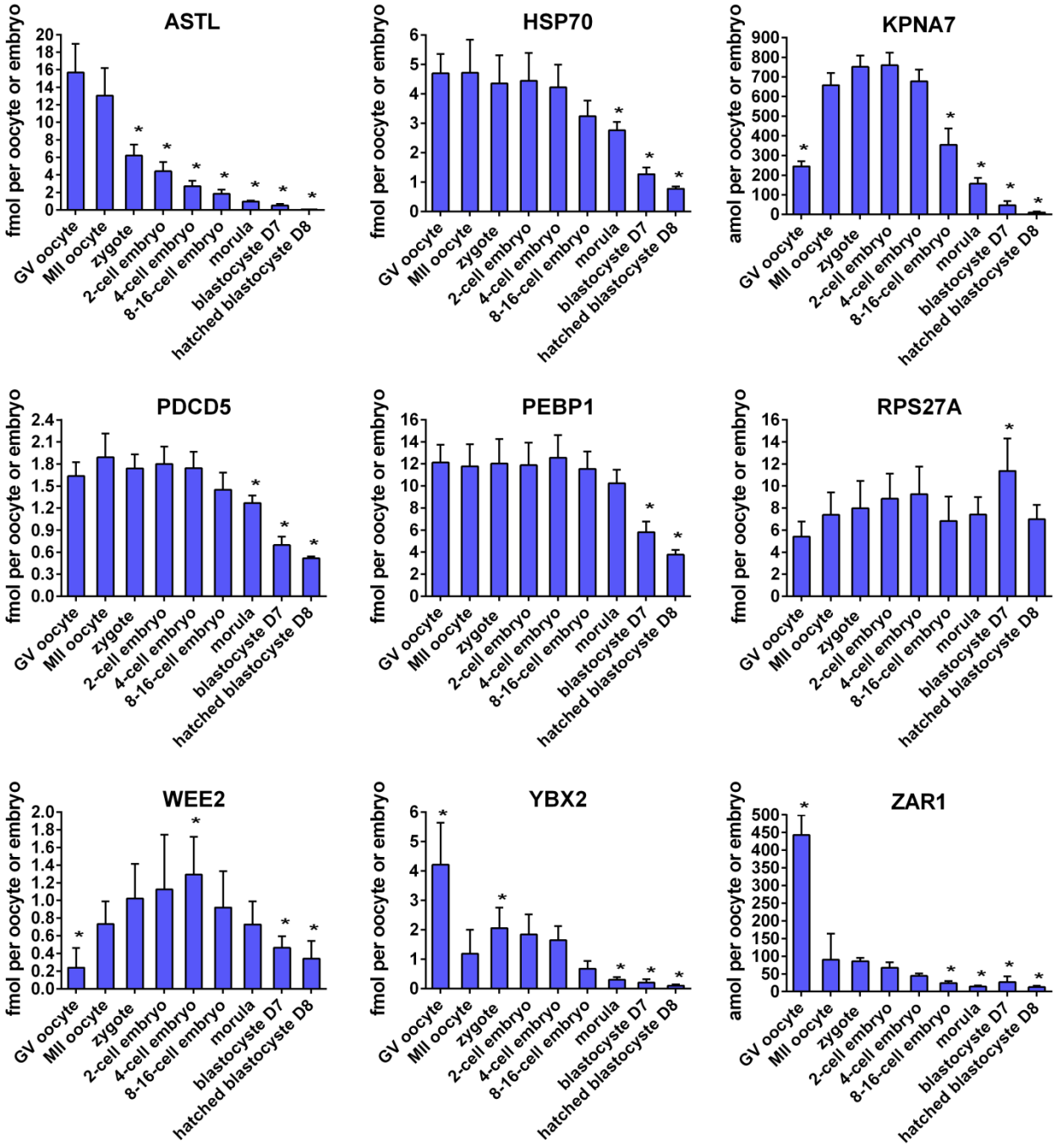

Figure 32. Absolute quantification of nine proteins in oocytes and embryos. Values are expressed as mean fmol or amol per oocyte or embryo ± SD (n=6). D7 = day 7; D8 = day 8. *comparison with MII oocytes as reference group: $p < 0.05$ and log2 fold change ≥ $|0.6|$.

4. Discussion

4.1 General aspects

The first aim of this thesis was the establishment of proteome profiles of oocyte maturation and early embryogenesis by a holistic proteomic approach. Among the variety of different holistic proteomic methods available to reach that goal, isotope labeling based quantification is generally regarded as more precise compared to label free methods. Non-radioactive stable isotope labels (SIL) can be introduced metabolically during cell culture, e.g., SILAC [64]. However, this approach was no option due to the low metabolism during oocyte maturation and the few cleavage cycles of the studied embryos. Chemical labeling at the level of proteins, such as ICAT [65], enables only a comparison of two samples. Chemical labeling of peptides using iTRAQ [66], however, offers the possibility to quantitatively compare four sample and was therefore the method of choice. The 4-plex iTRAQ method was applied for the simultaneous analysis of the proteomes of GV oocytes and MII oocytes matured *in vitro* according to three different maturation protocols. MII oocytes are usually matured with supplementation of ECS and LH/FSH in our lab. To assess the influence of the exogenous hormone supplementation of LH/FSH, one group was matured with ECS only. Growth hormones such as GH are also frequently used in oocyte maturation and a group matured with LH/FSH/GH supplementation was included in the study. The 4-plex iTRAQ method also enabled a simultaneous analysis of the proteomes of zygotes, two-cell embryos, four-cell embryos and an internal standard consisting of MII oocytes for the establishment of proteome profiles of early mammalian embryogenesis. A further advantage of the iTRAQ method is that the multiplexed approach downsizes the total number of necessary LC-MS runs, and minimizes technical variances due to stable isotope labeling of peptide mixtures prior to LC-MS analysis.

A common problem of bottom-up proteomics is under sampling. Under sampling usually occurs during analysis of complex biological samples. The high number of components to be

analyzed exceeds the data acquisition capacity of the instrument, causing loss of information [97]. Therefore, a pre-fractionation step was included in the workflow. Several methods are available, such as OFFGEL [98], SDS-PAGE and strong cation exchange (SCX) chromatography, which were all tested in pilot studies (data not shown). The largest number of identified proteins was achieved with pre-fractionation by SCX, which is in line with results previously reported [99, 100]. The combination of SCX chromatography and iTRAQ offers the possibility of first-dimension separation and simultaneous cleanup of excess iTRAQ reagents, salts and other interfering compounds [101]. Furthermore, SCX is performed after isotope labeling of the samples, which minimizes technical variances. The sample is eluted from the SCX column stepwise, using different concentration of KCl. In the iTRAQ study of oocyte maturation, six salt steps were applied which was previously reported by Demant *et al.* (unpublished data). The salt steps were further optimized (data not shown) and in the iTRAQ study of early embryogenesis, eight salt steps were applied. The analytical depth was further enhanced by splitting each SCX fraction into two or three aliquots to be iteratively analyzed by LC-MS/MS with manually established exclusion lists applied in the following runs. These exclusion lists instructed the mass spectrometer to ignore masses already acquired, thus enhancing data acquisition. The number of protein identifications could be substantially increased which is in agreement with previously reported studies about technical replication of LC-MS/MS analysis [102]. In the study of oocyte maturation, the largest increase in protein identification was already achieved after application of the first exclusion list. Therefore, only one exclusion list was applied in the follow-up study of early embryogenesis. Due to these optimizations, the sample amount could be substantially decreased from 4 x 150 oocytes per replicate, which corresponds to the protein amount of 50 µg usually applied in iTRAQ studies, to 4 x 100 oocytes/embryos in the second iTRAQ study reaching comparable results. This lessened the problem of the more challenging generation of embryos compared to oocytes.

The last aim of this thesis was to use the data derived from these holistic proteomic approaches for the establishment of SRM assays which enabled targeted protein quantification of selected proteins for verification of results as well as for targeted protein

quantification in additional embryonic stages. Ten oocytes/embryos were pooled per sample, corresponding to about 1 µg total protein, which facilitate a reproducible quantification. For relative quantification, crude stable isotope-labeled (SI) peptides were sufficient; however, for absolute quantification of proteins, SI peptides in highly accurate concentrations were required. Therefore, due to the high cost, absolute values were established for a subset of nine proteins throughout nine developmental stages. These absolute protein contents are of additional value, because they can be used as independent references and as read out for functional assays.

4.2 Proteome signatures of bovine oocyte *in vitro* maturation

4.2.1 Fundamental events of oocyte maturation are reflected on the level of proteins

To become a fully competent oocyte, a multitude of fundamental events have to occur and must be precisely regulated during maturation, e.g. inhibition and induction of meiosis, interaction with cumulus cells, chromatin condensation, organelle redistribution and cytoskeletal changes [103]. Several of these processes were found to be reflected on the level of proteins. In total, 1115 proteins were identified with high confidence (FDR < 1%) from six biological replicates, and 53 quantitative differences were detected in the six pair-wise comparisons between all groups (Table 2 and 3). Functional analysis using Cytoscape of the 26 proteins differentially abundant between GV oocytes and MII oocytes matured according to the standard protocol with FSH/LH supplementation revealed proteins related to “protein import”, “regulation of protein transport” and “microtubule cytoskeleton organization”, which may hint to the rearrangement processes during GV breakdown in maturation (Figure 14). Among these proteins is importin subunit alpha-8 (KPNA7), a member of the importin family which mediate nuclear transport of, e.g. transcription and chromatin remodeling factors. Its abundance increases by a log2 fold change of 1 in MII oocytes compared to GV oocytes. KPNA7 has a particularly strong binding affinity for the nuclear protein nucleoplasmin 2, which is a core histone chaperone involved in chromatin reprogramming, especially important during fertilization and early embryonic development [104,105]. By PCR and Western blot analysis, it was demonstrated that KPNA7 mRNA and protein abundance is high in bovine GV oocytes and slightly increased in MII oocytes [105] and this trend in protein abundance was confirmed by the results presented here.

Furthermore, the functional analysis with Cytoscape of proteins increased in abundance in MII oocytes revealed an enrichment of proteins important for cell cycle progression, e.g. GO terms “mitosis”, “spindle organization”, “centrosome cycle” and “M phase” (Figure 14). Among them are aurora kinase A (AURKA), cyclin-dependent kinase 1 (CDK1), transforming acidic coiled-

coil-containing protein 3 (TACC3) and wee1-like protein kinase 2 (WEE2). AURKA is a serine/threonine kinase involved in many processes essential for mitosis and its abundance increases by a log2 fold change of 0.8 in MII oocytes compared to GV oocytes (Table 2). It regulates centrosome maturation and separation, followed by assembly of a bipolar spindle, trigger of mitotic entry, alignment of chromosomes in metaphase, cytokinesis and the return to G1 [106]. A substrate of AURKA is TACC3, which supports the centrosome-dependent microtubule assembly in mitosis [107]. The abundance of TACC3 increased strongly during maturation by a log2 fold change of 1.3. Furthermore, the activation of the CDK1/cyclin B complex is also supported by AURKA, which allows nuclear entry [108]. Interestingly, the abundance of WEE2 was also found to strongly increase by a log2 fold change of 2.9 in MII oocytes compared to GV oocytes. WEE2 is a downstream substrate of protein kinase A and known to be responsible for phosphorylation of the CDK1 inhibitory site and thereby maintaining meiotic arrest in oocytes [109]. High levels of WEE2 are probably needed for a tight control of the cell cycle during the upcoming cleavage cycles.

4.2.2 Differences in the proteome signature of oocyte maturation caused by exogenous hormone supplementation of FSH, LH and GH

In vitro oocyte maturation is obtained by simulating the pre-ovulatory follicle environment. Therefore, all three maturation media were supplemented with ECS, which is taken from the female cow on day 0 of the estrous cycle, at estrus and shortly before ovulation. ECS has been shown to increase developmental capacity of oocytes compared to supplementation with fetal calf serum (FCS) [110]. Gonadotropins, especially LH and FSH, are frequently added to the maturation media in view of their natural role as promoter of *in vivo* oocyte maturation, cumulus cell expansion and ovulation [103, 111]. Due to endogenous LH/FSH levels in ECS, exogenous addition may be needless but compensates fluctuating endogenous levels. LH/FSH has been shown to impact oocyte *in vitro* maturation, cumulus cell expansion and

developmental competence [36, 112, 113]. By assessing gene expression activity, it was postulated, that the *in vitro* FSH-response of cumulus cells is similar to the *in vivo* LH-response [114]. The effects of LH are mediated by epidermal growth (EGF)-like family members, which are secreted by granulosa cells and activate the EGF receptor on cumulus cells [115]. An influence of LH and FSH on the cumulus cells was also observed in this study by microscopic evaluation of COCs, where exogenous LH/FSH supplementation caused increased expansion of COCs. However, the effects of especially LH during IVM were discussed controversial and there are studies reporting no influence on the developmental capacity of oocytes [39]. The aim of this study was to assess the influence of these hormones on the proteome of oocytes undergoing maturation. All maturation protocols resulted in the same biological outcome, i.e. matured MII oocytes which developed until the blastocyst stage with comparable rates (Figure 11). This is in line with the result, that the abundance of about 35 out of 42 altered proteins was changed in the same way by addition of LH/FSH or LH/FSH/GH (Table 2). A total of 18 significant differences in protein abundance were detected between the three maturation protocols comprising maturation without exogenous hormones, LH/FSH and LH/FSH/GH supplementation, respectively (Table 3). Of those, nine differences in protein abundance were detected between MII oocytes matured with ECS only and ECS + LH/FSH. LH and FSH were supplemented in a concentration of 8 and 10 µg/mL (0.0125 and 0.025 IU/mL), respectively, which are in the range of normally adopted concentrations [116-118]. However, these concentrations are about hundred fold higher than preovulatory surge levels of LH (100 ng/mL) and FSH (50 ng/mL) in the serum of estrus cows [5]. These strongly increased concentrations may cause the reported differences in protein abundance (Figure 15). Supplementation with LH/FSH led to an enrichment of the HSP70 cochaperone (HSPBP1) by a log2 fold change of 0.8 in MII oocytes compared to GV oocytes. Molecular chaperones are essential during growth, development, and for dealing with accumulated non-native proteins under stress, thereby exerting pro-survival functions. HSPBP1, in particular, inhibits the ubiquitination and proteasomal degradation of anti-apoptotic, inducible heat shock 70 kDa proteins (HSP70), which mediate the folding of newly translated polypeptides and recognize nonnative conformations of proteins [119]. HSP70 proteins are important for

embryonic development [120,121]. One may therefore conclude that LH/FSH addition to the maturation media, although it was not reflected in the blastocyst rate, is beneficial for embryonic viability.

GH has been employed in IVM medium for cattle and has been shown to increase the percentage of oocytes that reached the MII stage, developed to blastocysts and hatched [122] by accelerating nuclear maturation of cumulus enclosed bovine oocytes [41]. GH was also shown to act as survival factor during *in vitro* culture, to reduce apoptosis by altering the BAX to BCL-2 ratio during early embryogenesis [123] and to alter the structure and the pore size of the zona pellucida of blastocysts [124]. However, it is not routinely applied in IVM. In this study, the effects of GH on the level of proteins were investigated by using a GH concentration of 100 ng/mL as previously reported [122, 125]. By microscopic evaluation, it was observed that GH addition led to increased cumulus cell expansion, which is in line with the results previously reported [125]. Effects on the protein level varied. On the one hand, an increase of heat shock 70 kDa protein 1B (HSPA1B) was detected under GH addition, which may hint towards an enhanced embryonic viability. Contrariwise, the abundance of proteins important for mitosis such as CDK1 and nucleosome assembly protein 1-like 4 (NAP1L4) [126] were decreased by GH addition (Figure 16). In the case of NAP1L4, the increase in protein abundance caused by LH/FSH was even negated.

Noteworthy, abundance of vimentin (VIM) was found to strongly increase (over 2-fold) in the presence of GH (Table 3 and Figure 17) in MII oocytes compared to GV oocytes and was selected for a further study by LSM. Vimentins are class-III intermediate filaments attached to the nucleus, endoplasmic reticulum, and mitochondria [127] and a role for VIM in the attainment of genomic union during fertilization in mammals was suggested [128]. Interestingly, LSM analysis revealed VIM to be localized in large amounts in the cytoplasmic extensions of the cumulus cells, which protrude into the zona pellucida of the oocyte, and to accumulate at the gap junctions towards the oocyte (Figure 18). It was concluded, that the increase in VIM protein abundance was actually caused by the remaining cytoplasmic extension of the cumulus cells. GH probably triggers VIM production by the cumulus cells or

re-localization, which is in line with the observed influence of GH on cumulus cells, leading to increased cumulus cell expansion.

In conclusion, numerous proteins important for oocyte maturation were identified and quantified, and protein profiles for key players previously described were contributed. Bioinformatics analysis revealed proteins increased in abundance related to rearrangement of the cytoskeleton, protein transport and cell cycle progression. It was demonstrated, that supplementation of oocyte maturation media with hormones led to few prominent abundance alterations in the proteome of MII oocytes. FSH/LH supplementation resulted in an increase of developmentally important proteins, but had no influence on subsequent embryonic development. Addition of GH also did not influence developmental rates and had diverse and opposing effects on the abundance of proteins during oocyte maturation.

4.3 Proteome signatures of early bovine embryo development

4.3.1 The proteomes of two-cell and four-cell embryos differed most from the reference MII oocyte

The six pair-wise comparisons of embryonic stages (Figure 24A) revealed that 32 and 31 abundance alterations were detected between the proteomes of two-cell and four-cell embryos, respectively, compared to MII oocytes. Eighteen differences were found between MII oocytes and zygotes, among them are proteins associated with the GO terms “cellular modified amino acid metabolic process” and “hormone metabolic process” which became less abundant in zygotes (MAT2A, CHGA, APOA1) (Figure 24B). In the first cleavage forming a two-cell embryo, the abundance of RPS14, RPS18 and HSPB1 decreased (Figure 24C) while proteins belonging to the GO term “protein polymerization” (TUBB4A/TUBB5, SPTBN1) increased, compared to zygotes. Only few changes were detected between the proteomes of two-cell and four-cell embryos (Figure 24A). Among these, two proteins of the ontology group “regulation of protein ubiquitination” were found with about 2-fold increased abundance in four-cell embryos compared to two-cell embryos. One of the two proteins was proteasome subunit alpha type-7 (PSMA7) which is part of the 20S proteasome core complex. This complex is responsible for protein degradation through the ubiquitin-proteasome pathway and is involved in numerous cellular processes like cell cycle control, cell proliferation and differentiation and regulation of transcription and is therefore describes as a potential biomarker [129]. An increase of PSMA7 in four-cell embryos might be related to degradation of maternal proteins during the process of MET. The second protein showing an increased abundance in four-cell embryos was peptidyl-prolyl cis-trans isomerase (FKBP1A). FKBP1A, which has not been reported in the context of mammalian embryogenesis, is an immunophilin known to be important for immunoregulation and cellular processes like protein assembly, folding and trafficking [130, 131], all of which are vital processes during the rapid cleavage divisions of the embryo.

4.3.2 Evidence for a major role of the p53 pathway during early embryogenesis

Functional analysis with Cytoscape of SOTA cluster 1 (Figure 22A), which consisted of proteins gradually decreased abundance, revealed an enrichment of proteins linked to “translation” and related terms such as “maturation of SSU-rRNA” (small subunit ribosomal RNA), which is vital for translation of mRNAs into proteins [132], and “protein transport” (PPA1, LSM14B, PATL2, KPNA2, RPS14, RPS18, RPS8, ABCE1, TOMM70A, EIF4ENIF1, NUP93, APOA1 and PABPC4). This may reflect the attenuated translation before the major activation of the embryonic genome at the eight-cell stage. Interestingly, a recently published transcriptome study by Graf and co-workers [52] demonstrated the genes *RPS14* and *RPS18* connected to the GO term “translation” to be activated at the four-cell stage. Both proteins are components of the small 40S subunit of the ribosome which is the molecular machine that translates mRNAs into proteins [132]. Little is known about RPS18 besides its ribosomal functions, but excess free S14 protein was proposed to be a negative effector of *RPS14* mRNA transcription [133]. The observed decrease in abundance of S14 protein during embryogenesis in our study therefore might enable the subsequent activation of the *RPS14* gene. Furthermore, RPS14 is involved in various cellular processes. It negates c-Myc function [134] and plays a key role in erythropoiesis [135] as well as in the ribosomal stress-p53 pathway where overexpression of RPS14 leads to elevated p53 activity via inactivation of MDM2 and subsequently to G1 or G2 arrest and growth inhibition [136]. Another member of the p53 pathway is HNRNPK, for which a 1.8-fold increase in abundance until the four-cell stage compared to MII oocytes was demonstrated (Figure 22B). It is also one of the genes found to be transcriptionally activated at the four-cell stage by Graf *et al.* [52] which is related to the GO term “RNA processing”. This ribonucleoprotein is a DNA/RNA-binding protein participating in numerous processes such as chromatin remodeling, transcription, splicing and translation [137]. In response to DNA damage, it activates transcription of cell-cycle arrest genes as a cofactor of p53 [138], which leads to DNA repair, cell-cycle arrest or apoptosis [139]. The abundance alterations of HNRNPK and RPS14 together with activation of their

genes before the major EGA suggest a major role of the p53 pathway during early embryogenesis.

4.3.3 Proteins involved in energy and lipid metabolism are increased in embryo development

Complex I-75kD (NDUFS1), belonging to the respiratory chain, and the enzymes citrate synthase (CS) and succinate dehydrogenase (SDHA) of the tricarboxylic acid (TCA) cycle, became less abundant until the four-cell stage (Figure 23A). These might be the first signs of the switch in energy generation by ATP synthesis from oxidation of acetate in the TCA cycle to energy generation by glycolysis, which has been demonstrated to occur at the blastocyst stage in mice [140]. ATP formation via TCA cycle takes place in mitochondria, which are maternally inherited. A 100-fold increase in oocyte mitochondrial DNA as compared to somatic cells has been found in bovine oocytes [141] and human oocytes contain between 240,000 and 1.55 million mitochondria which do not start to replicate before embryonic differentiation [142, 143]. Therefore, it is no surprise that functional analyses with DAVID of oocyte and embryo proteomes revealed a high percentage (18.1%) of mitochondrion proteins (Figure 21) and three mitochondrion related annotation clusters (Table 4) with enrichment scores of 25.5, 11.5 and 1.7. Failures in mitochondria redistribution, differentiation or transcription are thus associated to the efficiency of respiration in human and bovine oocytes. This efficiency of respiration has been shown to be closely correlated to the developmental capacity after *in vitro* fertilization [144, 145]. Major substrates used for ATP production in the mitochondrial TCA cycle are lipids. Proteins involved in assembly of high-density lipoprotein particles were found to decrease during embryo development (Figure 23A). Previous studies demonstrated the presence of a high amount of lipid droplets in the cytoplasm of bovine oocytes and early embryos until the blastocyst stage, at which they were significantly reduced [146], which is in line with the results presented here. Lipid droplets are supposed to facilitate increased ATP production required for blastocyst formation [147] and an accumulation of

lipids in the cytoplasm of oocytes has been suggested to reflect good developmental capacity [148]. However, abnormally increased accumulation of cytoplasmic lipids caused by supplementation of culture medium with serum during *in vitro* production of embryos is supposed to impair cryotolerance [149, 150], and can lead to immature or even abnormal mitochondria [151]. There are also some studies stating serum supplementation resulting in a higher blastocyst rate [152] and a generally improved embryonic development in cattle [153, 154]. Obviously, lipid metabolism is crucial for embryogenesis and therefore proteins of this pathway represent interesting targets for future studies. Especially interesting is apolipoprotein A1 (APOA1), which has previously been shown to be produced by human preimplantation embryos. Increased APOA1 secretion was associated with blastocysts of a higher morphologic grade, suggesting a role in embryonic development [155]. Therefore, the 1.6-fold decrease in APOA1 abundance in the data presented here (SOTA cluster 1) may results from growing secretion of this protein in the culture medium during ongoing embryogenesis and increases evidence for an important role of APOA1 in embryo development.

4.3.4 Protein abundance profiles of key players in mitosis and meiosis were established

Four proteins were detected showing a strong, at least 2-fold, increase in abundance in the zygote stage, followed by a decrease until the four-cell stage to the basal level measured in MII oocytes (Figure 22D). Among them is beta-II spectrin (SPTBN1), which is related to “protein polymerization” (Figure 23D). It has been demonstrated to be a functional partner of ankyrin-G in de novo membrane biogenesis during mitosis of epithelial cells, where both are required for the delivery of proteins and phospholipids to the membrane [156, 157]. SPTBN1 has already been shown to be required for compaction of early mouse embryos [157]. Furthermore, PPP1CC was quantified, which is the catalytic subunit of protein phosphatase 1, as well as rab GTPase-activating protein 1 (RABGAP1), which are both crucial for cell division [158, 159]. PPP1CC is a key player of spermiogenesis [160] while RABGAP1 has not been

connected to mammalian reproduction yet so far. The results presented here suggest these proteins to be particularly important for either formation of the diploid zygote and/or early steps of mitosis in bovine embryogenesis.

The majority of proteins increasing in abundance of SOTA cluster 2 (Figure 22B) and 3 (Figure 22C) are necessary for organization of cellular components, which is in line with the fundamental morphological reorganization of the entire structure of the cell during mitosis. The detected proteins were related to the GO terms “regulation of organelle organization”, “cellular macromolecular complex assembly” (Figure 23B), “protein transport” and “M phase” (Figure 23C). The structural changes were found to be accompanied by an increase of metabolically active proteins which were associated with the GO terms “cellular amino acid metabolic process” and “purine ribonucleotide metabolic process” (Figure 23B). The main regulator of M phase, cyclin-dependent kinase 1 (CDK1), was found to be unaltered in abundance in the proteome data while one of its substrates, stathmin (STMN1/Op18), was becoming 5.2-fold more abundant in zygotes compared to MII oocytes. STMN1 is a microtubule-destabilizing, cytosolic phosphoprotein of which a threshold level is required for progression through mitosis [161-163]. WEE2 was also detected, which was shown to deter meiosis by inhibiting cyclin B/CDK1 [164] and to function downstream of cAMP in the rhesus macaque [165]. Interestingly, *WEE2* mRNA was found to be exclusively expressed in mouse MII oocytes and to abruptly decrease after fertilization [166], while the data presented here showed WEE2 protein to become 1.7-fold more abundant until the four-cell stage compared to MII oocytes, demonstrating the disparity between transcript and protein abundance during embryogenesis. Furthermore, WEE2 was already found to be altered in abundance in oocyte maturation and therefore selected for an additional localization study. By immunofluorescence and LSM in two-cell embryos, WEE2 protein was localized inside of the nucleus of the two blastomeres of the embryo (Figure 27). This result is in line with those of Hanna *et al*. [165] who demonstrated a specific nuclear localization of WEE2 protein in both growing and fully grown GV oocytes of rhesus macaque monkeys.

4.3.5 Activation of "The unfolded protein response" may be an indicator for low success rates of *in vitro* embryo production

Comparing the GO networks of proteins with increased and decreased abundances in the four-cell stage compared to MII oocytes (Figure 23A and Figure 23B), resulted in a quite striking observation. Proteins involved in "protein folding" (PFDN2, CCT6A, PPID, ERP44 and FKBP4) decreased while at the same time proteins associated with the "response to unfolded protein" became more abundant (MANF, GFPT1, SEC31A, CHORDC1, PGLS, FKBP1A, HSPB1, PGLS and ATP2A2). Proteins are usually folded and assembled in the endoplasmic reticulum (ER). In the case of an accumulation of unfolded proteins in the lumen of the ER (ER stress), intracellular signal transduction pathways are activated which are collectively termed the unfolded protein response (UPR). The aim of the UPR is the protection of the cell against proteotoxicity or the induction of apoptosis if the ER stress cannot be mitigated [167]. These results suggest an accumulation of defects in protein folding during early embryogenesis which might be one of the reasons for the still low success rate of in vitro embryo production The UPR may be caused by the artificial environment during in vitro maturation of oocytes and culture of embryos. It would be interesting to see, if new approaches to *in vitro* maturation are beneficial to protein folding, such as simulated physiological oocyte maturation (SPOM), which mimics some characteristics of *in vivo* oocyte maturation. It delays the completion of meiosis which promotes gap junctional communication between the oocyte and the cumulus cells [168]. Besides, it is possible that the UPR is a normal phenomenon and also occurs in oocytes and embryos generated *in vivo*.

4.4 Targeted protein quantification by SRM

4.4.1 iTRAQ data was successfully verified by 5-plex SRM in a pilot study

In a pilot study, a 5-plex SRM assay was established which was used to verify the iTRAQ data of early embryogenesis. This SRM assay also represents the first step towards an approach facilitating molecular staging of early embryos based on quantitative protein assays. Developmentally interesting proteins, namely ASTL, HSPB1, TDRKH, VIM and WEE2, were selected based on their differential abundance determined in the iTRAQ approach. ASTL is an astacin-like metalloendopeptidase supposed to be involved in the hatching process. It is also called ovastacin due to its predominant expression in ovarian tissue, especially in unfertilized oocytes. ASTL has been studied in the murine system, where transcript levels have been found to strongly increase in superovulated mice, suggesting a hormonal control [169]. Moreover, Burkart and co-workers [170] demonstrated zona pellucida sperm-binding protein 2 (ZP2) to be a direct substrate of ASTL. Proteolytic cleavage of ZP2 after gamete fusion is important for the postfertilization block to sperm binding which warrants monospermic fertilization and thereby successful embryogenesis in mice. Burkart *et al* [170] detected ASTL only before fertilization, which is consistent with the strong 2.2-fold decrease of ASTL protein abundance until the four-cell stage in the data set presented here. The small heat shock protein HSP27 was chosen (HSPB1) which was demonstrated to co-localize with mitotic spindles, especially with tubulin and microtubules, in HeLa cells [171] and to add to chaperone capacity by binding unfolded proteins [172]. HSPB1 protein abundance was demonstrated to increase 1.8-fold until the zygote stage compared to MII oocytes, and to decrease again until the four-cell stage, suggesting a role in fertilization and/or zygote formation. Furthermore, VIM was selected which strongly decreased by a fold change of 4.9 until the four-cell stage compared to MII oocytes in the iTRAQ data. The domains of tudor and KH domain-containing protein (TDRKH/TDRD2) are supposed to mediate protein-RNA interactions by binding RNA and are involved in cellular RNA metabolism [173, 174]. TDRKH, in particular, is known to be involved in spermatogenesis and in piRNA biogenesis in the

germLine [175] and became 3.2-fold less abundant in four-cell embryos. The fifth protein of the SRM assay was the oocyte-specific key regulator of meiosis WEE2, the nuclear localization of which has been determined by LSM analysis (Figure 27). iTRAQ analysis revealed that WEE2 abundance increased by a fold change of 1.7 until the zygote stage compared to MII oocytes, and stayed on this level until the four-cell stage. Quantitative values obtained by iTRAQ were verified by SRM in all cases in pools of only ten oocytes or embryos each which demonstrates the performance of the SRM method.

To prove the applicability of these proteins for molecular staging of early embryos, a PCA analysis was performed to test if they enable clear separation of MII oocytes, zygotes and 2- and four-cell embryos (Figure 26). As a proof of principle, a PCA based on the proteins significantly differing in abundance in the iTRAQ approach was performed (Figure 26A). This dataset led to a clear separation of the analyzed embryonic stages. Moreover, subjecting SRM-derived quantification of the five proteins mentioned above to PCA analysis resulted in an even better separation of the embryonic stages (Figure 26B). This demonstrates the possibility to characterize early embryos on a much more precise level throughout their development at the level of proteins.

4.4.2 Nine interesting developmental stages were analyzed by 27-plex SRM

The results of the SRM pilot study suggested expanding the panel used for multiplexed SRM analysis. SRM offers the possibility to study distinctively more developmental interesting stages than the iTRAQ approach, due to the significantly lower sample amounts required. This is particularly advantageous when studying more developed embryos, such as the morula or blastocyst stage, which are difficult to generate. Therefore, the pursued strategy involved the use of easier generated developmental stages for discovery of promising candidate proteins by iTRAQ which were then studied further by SRM in a multitude of biological stages. Fourteen additional proteins known from the two iTRAQ studies (see chapter 3.2 and 3.3) were included which have partly been discussed above. Furthermore,

eight proteins known from previous proteomic studies of the lab for which SRM assays had already been established were included (Table 8). Among the not yet mentioned proteins are PRC1, GTSF1, UHRF1, CLU, YBX2 and ZAR1. Protein regulator of cytokinesis 1 (PRC1) controls spindle polarization and recruitment of cytokinetic factors during monopolar cytokinesis [176]. Gametocyte-specific factor 1 (GTSF1) is highly expressed in embryonic male and female mouse gonads, in the cytoplasm of all stages of postnatal oocyte maturation, and in prespermatogonia during early postnatal testicular development. An essential role for GTFS1 in germ cell development was suggested [177]. E3 ubiquitin-protein ligase UHRF1 (UHRF1) is associated with regulation of the immune system and has previously been reported in bovine endometrium [178]. Clusterin (CLU) is involved in complement inactivation and has been found to play a role in reproductive complications [179]. *CLU* mRNA has also been found to be delivered to porcine oocytes by spermatozoa, suggesting a contribution to zygotic and embryonic development [180]. Y-box-binding protein 2 (YBX2) has been reported to have an important role in storage and translational regulation of maternal mRNAs during bovine *in vitro* embryogenesis [181]. Zygote arrest protein 1 (ZAR1) is a maternal-effect gene involved in the oocyte-to-embryo transition and essential for female fertility [182].

Quantification of proteins by SRM can be performed by selecting and quantifying at least one proteotypic peptide per protein. However, the targeted peptide may be affected by post-translation modifications (PTM) which interfere with the MS analysis by causing mass shifts of the peptide or miscleavages during trypsin digestion, thus leading to erroneous quantitative values. Possible PTMs are attachment of biochemically functional groups (e.g. phosphorylation), changing of the chemical nature of an amino acid (e.g. conversion of arginine to citrulline) and proteolytic cleavage [183-185]. Furthermore, one peptide can correspond to unknown protein isoforms which abundances are affected in different ways throughout biological processes as has been previously demonstrated for the protein “similar to GSTM5” [76]. In this thesis, reliability of quantification was improved by selection of two proteotypic peptides per protein and using corresponding stable isotope-labeled (SI) peptides for each analyzed peptide as internal standard. The final SRM assay comprised 54

endogenous and 54 SI peptides, corresponding to 27 proteins, listed in Supplementary Table 10. Noteworthy, in the resulting SRM chromatogram, maxima of the eluting peptides are fairly equally distributed over the entire elution time (Figure 28). The number of analytes to be studied simultaneously was reduced by using “scheduled” SRM which instructs the instrument to acquire data of each peptide only in a pre-specified time frame of 240 seconds around the expected elution time. The design of the multiplex SRM thus facilitated data acquisition from a sufficient number of individual data points for each of the 108 monitored analytes along their individual elution periods. Quantification using the multiplexed SRM was highly reproducible, as evident from the results of technical replicates (Figure 29). Relative abundance, i.e., the intensity ratio endogenous/SI peptide, was determined with a median coefficient of variation (CV) of 7.8 %, and the CV of the elution times was 0.5 %. This corresponds to results previously reported for SRMs studies concerning protein quantification in plasma [186] and urine [187].

Due to the low sample amount of only ten oocytes or embryos required, it was possible to analyze six replicates of nine different developmental stages starting with GV oocytes and ending with hatched day 8 blastocysts (Figure 30). Quantitative profiles of 27 proteins were established which represents the first comprehensive approach to an exact protein quantification covering such a high number of developmental stages. Distinct protein profiles were uncovered, e.g., the protein abundance of ACCSL increased strongly, about four-fold, from the GV until the MII oocyte stage, continued to increase until the four-cell stage, and then decreased strongly, about 4-fold, until development to the blastocyst stage. A similar abundance profile was discovered for AURKA, KPNA7, WEE2, TACC3 and PCBD1. In contrast, the abundance of HSPE1 and LAMP2 stayed fairly constant throughout all developmental stages analyzed. The abundance of PDCD5, PEBP1, GSTM3 and HSP70 also remained broadly at the same level until the four-cell stage or the eight- to 16-cell stage, and declined from than onward, which may be caused by the embryonic-genome activation. Two proteins, ASTL and TDRKH, became steadily less abundant until the blastocyst stage. Interestingly, the abundance of the majority of analyzed proteins started to decline at one

point until the blastocyst stage, despite the increased *de-novo* translation after the activation of the embryonic genome at the eight-cell stage. In the iTRAQ study of early embryogenesis, the protein PSMA7 was found to increase in abundance until the four-cell stage. PSMA7 is responsible for protein degradation through the ubiquitin-proteasome pathway and thus an increase of PSMA7 is in line with the decreasing protein abundances in the SRM study. Only HSPB1 and RBP4 became more abundant in hatched day 8 blastocysts.

The criteria for significant quantification were a log2 fold change of at least 0.6, which equals a fold change of 50 % in protein abundance, and $p < 0.05$ in each stage compared to MII oocytes. For 16 proteins showing significant abundance alteration in the iTRAQ analysis of oocyte maturation and early embryogenesis, i.e., GV oocytes, zygotes, two-cell embryos and four-cell embryos using MII oocytes as a reference group, corresponding SRM data were acquired. SRM results verified the corresponding iTRAQ ratios in all cases. Only in three out of 34 cases, the obtained SRM values were not significant and could therefore not be used for comparison with the iTRAQ data (Table 9), that demonstrates the power of SRM for verification of protein abundance.

In the 27-plex SRM assay, two peptides per protein were used for quantification and in about 70 % of all significant quantifications, the value obtained by peptide 1 differed less than 25 % from the value obtained by peptide 2. However, in about 5 % of all significant cases, quantitative values obtained by peptide 1 differed more than 100 % of those obtained by peptide 2 (Supplementary Figure 33). Possible reasons for this have been outlined above. To obtain reliable quantitative values in these cases, the synthesis of additional proteotypic peptides for the establishment of further SRM assays and repetition of the study would be necessary. If the quantitative values obtained by peptide 1 and 2 differed from each other only in single developmental stages, as is the case for e.g. ZAR1, also outliers can be assumed and the SRM assay can still be regarded as valid.

SRM also offers the option to determine very precise protein concentrations, by far exceeding the possibilities offered by staining techniques such as immunohistochemistry. For a subset of

nine proteins, additional absolute protein values were established which has rarely been done in embryos so far. The limits of detection and quantification were determined for each of the selected 18 peptides (Figure 31) and absolute quantitative values were obtained for nine developmental stages using pools of ten oocytes or embryos each (Figure 32). For the protein ASTL, e.g., a protein concentration of about 16 fmol per GV oocyte was determined. Assuming an oocyte diameter of 100 µm and thus a volume of 5.2×10^{-10} L, 16 fmol ASTL per GV oocyte correspond to 32 µmol/L. This protein concentration decreased gradually to about 1 fmol per embryo at the blastocyst stage (≈ 2 µmol/L) The high amount of ASTL in GV oocytes and the decreasing abundance of ASTL are consistent with the function of this protein as an oocyte-specific oolemmal receptor involved in sperm and egg adhesion and fertilization [170]. PEBP1 had a constant concentration of about 12 fmol per oocyte or embryo (≈ 24 µmol/L) from the GV oocyte stage until the morula stage which decreased to about 6 fmol per embryo at the blastocyst stage (≈ 12 µmol/L). For PEBP1, an involvement in defective sperm physiology has been reported [188] but the role of PEBP1 in mammalian embryogenesis still needs to be elucidated. For these absolute values, no reference group is required and they can therefore be used as independent reference values for further experiments or in other laboratories. Additionally, knowledge of protein concentrations as a function of cellular state is critical for mathematic models and system biology [189].

In conclusion, the approaches described demonstrate the power of modern proteomic techniques and approaches to effectively discover and quantify proteins crucial for mammalian reproduction. By SRM analysis of nine developmental stages, considerable dynamics in the occurrence of proteins with even low abundances at stages of embryogenesis were demonstrated which - from a morphological point of view - seem to only redistribute the molecular environment of the inner cell mass to increasing numbers of blastomeres. Highly sensitive, multiplexed SRM quantification can facilitate the detection of developmental disturbances and disorders, e.g., during different conditions of *in vitro* production of embryos, and provide first insights into the underlying molecular pathways. Protein concentrations for nine proteins in nine developmental stages were determined and represent the first dataset of

this magnitude which can be used as reference values for other laboratories and for further functional assays, e.g., concentrations of metabolites can be calculated and the influence of hormones and inhibitors on a system can be assessed. With respect to mammalian reproduction, the ultimate ambition of comprehensive proteomic analysis in single oocytes and embryos will soon be affordable, leading to significantly increased and rapid understanding of the processes in early development.

5. Summary

One of the most critical periods in mammalian development is early embryogenesis. Its timing and morphology have been well studied, but molecular processes are still poorly understood. Several transcriptomic studies have addressed these molecular events. However, development of early embryonic stages before activation of the embryonic genome depends on sufficiently stored products of the maternal genome and adequate de/activation and relocation of proteins. Therefore, this thesis addresses early mammalian development, i.e., oocyte maturation and the first steps of embryogenesis, by holistic iTRAQ-based discovery approaches and by a targeted approach based on SRM. Numerous proteins important for oocyte maturation and embryogenesis so far not described in the mammalian system were identified and quantified, and protein profiles for key players previously described in the literature were contributed. In oocyte maturation, bioinformatics analysis revealed proteins increasing in abundance involved in rearrangement of the cytoskeleton, protein transport and cell cycle progression. Supplementation of oocyte maturation media with the gonadotropins follicle stimulation hormone and luteinizing hormone resulted in an increase of developmentally important proteins, but did not change developmental rates. Addition of growth hormone during oocyte maturation led to diverse and opposing effects at the level of proteins and also did not influence subsequent embryo development. During early embryogenesis, a considerable fraction of proteins continuously increased in abundance, despite a strongly attenuated rate of translation reported for this period. Bioinformatics analysis revealed particularly interesting proteins involved in the p53 pathway, lipid metabolism and mitosis. Activation of the unfolded protein response is demonstrated, which may be an indicator of the still lower success rates of *in vitro* versus *in vivo* embryo production. Relevant differences between transcript and protein abundance levels were detected, e.g., for WEE2, which highlights the importance of innovative proteomic tools and workflows to complement transcriptome data of early embryogenesis.

iTRAQ results of early embryogenesis were successfully verified by targeted 5-plex SRM analysis. By principal component analysis, SRM quantifications comprising a panel of only five proteins were shown to discriminate between all four developmental stages analyzed. Using an expanded 27-plex SRM assay, proteins were quantified in nine developmentally interesting stages and absolute protein contents were established for nine proteins. SRM is a highly sensitive tool for detection of disturbances and disorders of embryonic development at the molecular level, thus complementing morphological analyses by high resolution microscopy.

6. References

1. Li, R.; Albertini, D. F., The road to maturation: somatic cell interaction and self-organization of the mammalian oocyte. *Nature reviews. Molecular cell biology* **2013,** 14, 141-52.

2. Pauerstein, C. J.; Eddy, C. A.; Croxatto, H. D.; Hess, R.; Siler-Khodr, T. M.; Croxatto, H. B., Temporal relationships of estrogen, progesterone, and luteinizing hormone levels to ovulation in women and infrahuman primates. *American journal of obstetrics and gynecology* **1978,** 130, 876-86.

3. Akbar, A. M.; Reichert, L. E., Jr.; Dunn, T. G.; Kaltenbach, C. C.; Niswender, G. D., Serum levels of follicle-stimulating hormone during the bovine estrous cycle. *Journal of animal science* **1974,** 39, 360-5.

4. Peters, A.; Lamming, E., Hormone patterns and reproduction in cattle. *In practice* **1983,** 5, 153-8.

5. Gordon, I. R., Laboratory production of cattle embryos, 2nd edition. *Google Books Result* **2003,** Biotechnology in Agriculture Series, No. 27.

6. Gilbert, S. F., *Developmental Biology*. Tenth Edition ed.; Sinauer Associates: 2013.

7. Yip, K. S.; Suvorov, A.; Connerney, J.; Lodato, N. J.; Waxman, D. J., Changes in mouse uterine transcriptome in estrus and proestrus. *Biol Reprod* **2013,** 89, 13.

8. Pelton, T. A.; Bettess, M. D.; Lake, J.; Rathjen, J.; Rathjen, P. D., Developmental complexity of early mammalian pluripotent cell populations in vivo and in vitro. *Reprod Fertil Dev* **1998,** 10, 535-49.

9. Tadros, W.; Lipshitz, H. D., The maternal-to-zygotic transition: a play in two acts. *Development (Cambridge, England)* **2009,** 136, 3033-42.

10. Crosby, I. M.; Gandolfi, F.; Moor, R. M., Control of protein synthesis during early cleavage of sheep embryos. *J Reprod Fertil* **1988,** 82, 769-75.

11. Walser, C. B.; Lipshitz, H. D., Transcript clearance during the maternal-to-zygotic transition. *Current opinion in genetics & development* **2011,** 21, 431-43.

12. Kanka, J.; Nemcova, L.; Toralova, T.; Vodickova-Kepkova, K.; Vodicka, P.; Jeseta, M.; Machatkova, M., Association of the transcription profile of bovine oocytes and embryos with developmental potential. *Animal Reproduction Science* **2012,** 134, 29-35.

13. Sirard, M. A., Factors affecting oocyte and embryo transcriptomes. *Reprod Domest Anim* **2012,** 47 Suppl 4, 148-55.

14. Braude, P.; Bolton, V.; Moore, S., Human gene expression first occurs between the four- and eight-cell stages of preimplantation development. *Nature* **1988,** 332, 459-61.

15. Memili, E.; First, N. L., Control of gene expression at the onset of bovine embryonic development. *Biol Reprod* **1999,** 61, 1198-207.

16. Memili, E.; Dominko, T.; First, N. L., Onset of transcription in bovine oocytes and preimplantation embryos. *Mol Reprod Dev* **1998,** 51, 36-41.

17. Johnson, M. H.; Ziomek, C. A., The foundation of two distinct cell lineages within the mouse morula. *Cell* **1981,** 24, 71-80.

18. Tosti, E., Dynamic roles of ion currents in early development. *Mol Reprod Dev* **2010,** 77, 856-67.

19. Watson, A. J.; Barcroft, L. C., Regulation of blastocyst formation. *Frontiers in bioscience : a journal and virtual library* **2001,** 6, D708-30.

20. Wang, H.; Dey, S. K., Roadmap to embryo implantation: clues from mouse models. *Nature reviews. Genetics* **2006,** 7, 185-99.

21. Fong, C. Y.; Bongso, A.; Ng, S. C.; Kumar, J.; Trounson, A.; Ratnam, S., Blastocyst transfer after enzymatic treatment of the zona pellucida: improving in-vitro fertilization and understanding implantation. *Hum Reprod* **1998,** 13, 2926-32.

22. Pauklin, S.; Pedersen, R. A.; Vallier, L., Mouse pluripotent stem cells at a glance. *Journal of cell science* **2011,** 124, 3727-32.

23. Lee, K. Y.; DeMayo, F. J., Animal models of implantation. *Reproduction* **2004,** 128, 679-95.

24. Wilcox, A. J.; Baird, D. D.; Weinberg, C. R., Time of implantation of the conceptus and loss of pregnancy. *The New England journal of medicine* **1999,** 340, 1796-9.

25. Forde, N.; McGettigan, P. A.; Mehta, J. P.; O'Hara, L.; Mamo, S.; Bazer, F. W.; Spencer, T. E.; Lonergan, P., Proteomic analysis of uterine fluid during the pre-implantation period of pregnancy in cattle. *Reproduction* **2014,** 147, 575-87.

26. Mamo, S.; Rizos, D.; Lonergan, P., Transcriptomic changes in the bovine conceptus between the blastocyst stage and initiation of implantation. *Anim Reprod Sci* **2012,** 134, 56-63.

27. Yamakoshi, S.; Bai, R.; Chaen, T.; Ideta, A.; Aoyagi, Y.; Sakurai, T.; Konno, T.; Imakawa, K., Expression of mesenchymal-related genes by the bovine trophectoderm following conceptus attachment to the endometrial epithelium. *Reproduction* **2012,** 143, 377-87.

28. Menezo, Y. J.; Herubel, F., Mouse and bovine models for human IVF. *Reproductive biomedicine online* **2002,** 4, 170-5.

29. Adams, G. P.; Pierson, R. A., Bovine model for study of ovarian follicular dynamics in humans. *Theriogenology* **1995,** 43, 113-120.

30. Hewitson, L.; Simerly, C.; Schatten, G., Cytoskeletal aspects of assisted fertilization. *Seminars in reproductive medicine* **2000,** 18, 151-9.

31. Navara, C. S.; First, N. L.; Schatten, G., Microtubule organization in the cow during fertilization, polyspermy, parthenogenesis, and nuclear transfer: the role of the sperm aster. *Developmental biology* **1994,** 162, 29-40.

32. Anderiesz, C.; Ferraretti, A.; Magli, C.; Fiorentino, A.; Fortini, D.; Gianaroli, L.; Jones, G. M.; Trounson, A. O., Effect of recombinant human gonadotrophins on human, bovine and murine oocyte meiosis, fertilization and embryonic development in vitro. *Hum Reprod* **2000,** 15, 1140-8.

33. Wrenzycki, C.; Herrmann, D.; Keskintepe, L.; Martins, A., Jr.; Sirisathien, S.; Brackett, B.; Niemann, H., Effects of culture system and protein supplementation on mRNA expression in pre-implantation bovine embryos. *Hum Reprod* **2001,** 16, 893-901.

34. Mihm, M.; Evans, A. C., Mechanisms for dominant follicle selection in monovulatory species: a comparison of morphological, endocrine and intraovarian events in cows, mares and women. *Reprod Domest Anim* **2008,** 43 Suppl 2, 48-56.

35. Hall, V.; Hinrichs, K.; Lazzari, G.; Betts, D. H.; Hyttel, P., Early embryonic development, assisted reproductive technologies, and pluripotent stem cell biology in domestic mammals. *The Veterinary Journal* **2013,** 197, 128-142.

36. Choi, Y. H.; Carnevale, E. M.; Seidel, G. E., Jr.; Squire, E. L., Effects of gonadotropins on bovine oocytes matured in TCM-199. *Theriogenology* **2001,** 56, 661-70.

37. Younis, A. I.; Brackett, B. G.; Fayrer-Hosken, R. A., Influence of serum and hormones on bovine oocyte maturation and fertilization in vitro. *Gamete research* **1989,** 23, 189-201.

38. Gervasio, C. G.; Bernuci, M. P.; Silva-de-Sa, M. F.; Rosa, E. S. A. C., The role of androgen hormones in early follicular development. *ISRN obstetrics and gynecology* **2014,** 2014, 818010.

39. Ali, A.; Sirard, M. A., The effects of 17beta-estradiol and protein supplement on the response to purified and recombinant follicle stimulating hormone in bovine oocytes. *Zygote (Cambridge, England)* **2002,** 10, 65-71.

40. Izadyar, F.; Colenbrander, B.; Bevers, M. M., In vitro maturation of bovine oocytes in the presence of growth hormone accelerates nuclear maturation and promotes subsequent embryonic development. *Mol Reprod Dev* **1996,** 45, 372-7.

41. Bevers, M. M.; Izadyar, F., Role of growth hormone and growth hormone receptor in oocyte maturation. *Molecular and cellular endocrinology* **2002,** 197, 173-8.

42. Izadyar, F.; Van Tol, H. T.; Hage, W. G.; Bevers, M. M., Preimplantation bovine embryos express mRNA of growth hormone receptor and respond to growth hormone addition during in vitro development. *Mol Reprod Dev* **2000,** 57, 247-55.

43. Mio, Y., Morphological Analysis of Human Embryonic Development Using Time-Lapse Cinematography. *Journal of Mammalian Ova Research* **2006,** 23, 27-35.

44. Ebner, T.; Moser, M.; Sommergruber, M.; Tews, G., Selection based on morphological assessment of oocytes and embryos at different stages of preimplantation development: a review. *Human reproduction update* **2003,** 9, 251-62.

45. Bachvarova, R., Synthesis, turnover, and stability of heterogeneous RNA in growing mouse oocytes. *Developmental biology* **1981,** 86, 384-92.

46. Schultz, R. M.; Wassarman, P. M., Biochemical studies of mammalian oogenesis: Protein synthesis during oocyte growth and meiotic maturation in the mouse. *Journal of cell science* **1977,** 24, 167-94.

47. Jeanblanc, M.; Salvaing, J.; Mason, K.; Debey, P.; Beaujean, N., [Embryonic genome activation]. *Gynecologie, obstetrique & fertilite* **2008,** 36, 1126-32.

48. Telford, N. A.; Watson, A. J.; Schultz, G. A., Transition from maternal to embryonic control in early mammalian development: a comparison of several species. *Mol Reprod Dev* **1990,** 26, 90-100.

49. Korf, U.; Lobke, C.; Haller, F.; Sultmann, H.; Poustka, A., Infrared-based protein detection arrays for quantitative proteomics. *Expert opinion on drug discovery* **2008,** 3, 273-83.

50. Vigneault, C.; Gravel, C.; Vallee, M.; McGraw, S.; Sirard, M. A., Unveiling the bovine embryo transcriptome during the maternal-to-embryonic transition. *Reproduction* **2009,** 137, 245-57.

51. Kues, W. A.; Sudheer, S.; Herrmann, D.; Carnwath, J. W.; Havlicek, V.; Besenfelder, U.; Lehrach, H.; Adjaye, J.; Niemann, H., Genome-wide expression profiling reveals distinct clusters of transcriptional regulation during bovine preimplantation development in vivo. *Proc Natl Acad Sci U S A* **2008,** 105, 19768-73.

52. Graf, A.; Krebs, S.; Zakhartchenko, V.; Schwalb, B.; Blum, H.; Wolf, E., Fine mapping of genome activation in bovine embryos by RNA sequencing. *Proc Natl Acad Sci U S A* **2014**.

53. Schmid, M.; Jensen, T. H., SnapShot: nuclear RNAPII transcript modification. *Cell* **2014,** 157, 1244; 1244.e1-2.

54. Schwanhausser, B.; Busse, D.; Li, N.; Dittmar, G.; Schuchhardt, J.; Wolf, J.; Chen, W.; Selbach, M., Global quantification of mammalian gene expression control. *Nature* **2011,** 473, 337-42.

55. Snider, N. T.; Omary, M. B., Post-translational modifications of intermediate filament proteins: mechanisms and functions. *Nature reviews. Molecular cell biology* **2014,** 15, 163-77.

56. Klose, J., Protein mapping by combined isoelectric focusing and electrophoresis of mouse tissues. A novel approach to testing for induced point mutations in mammals. *Humangenetik* **1975,** 26, 231-43.

57. O'Farrell, P. H., High resolution two-dimensional electrophoresis of proteins. *J.Biol.Chem.* **1975,** 250, 4007-4021.

58. Frohlich, T.; Arnold, G. J., Proteome research based on modern liquid chromatography - tandem mass spectrometry: separation, identification and quantification. *Journal of Neural Transmission* **2006,** 113, 973-994.

59. Hayes, R. N.; Gross, M. L., Collision-induced dissociation. *Methods Enzymol.* **1990,** 193, 237-263.

60. McLuckey, S. A., Principles of collisional activation in analytical mass spectrometry. *Journal of the American Society for Mass Spectrometry* **1992,** 3, 599-614.

61. Arnold, G. J.; Frohlich, T., Dynamic proteome signatures in gametes, embryos and their maternal environment. *Reprod Fertil Dev* **2011,** 23, 81-93.

62. Cox, J.; Mann, M., MaxQuant enables high peptide identification rates, individualized p.p.b.-range mass accuracies and proteome-wide protein quantification. *Nature biotechnology* **2008,** 26, 1367-72.

63. Carvalho, P. C.; Hewel, J.; Barbosa, V. C.; Yates, J. R., 3rd, Identifying differences in protein expression levels by spectral counting and feature selection. *Genetics and molecular research : GMR* **2008,** 7, 342-56.

64. Ong, S. E.; Blagoev, B.; Kratchmarova, I.; Kristensen, D. B.; Steen, H.; Pandey, A.; Mann, M., Stable isotope labeling by amino acids in cell culture, SILAC, as a simple and accurate approach to expression proteomics. *Mol.Cell Proteomics.* **2002,** 1, 376-386.

65. Gygi, S. P.; Rist, B.; Gerber, S. A.; Turecek, F.; Gelb, M. H.; Aebersold, R., Quantitative analysis of complex protein mixtures using isotope-coded affinity tags. *Nat.Biotechnol.* **1999,** 17, 994-999.

66. Ross, P. L.; Huang, Y. N.; Marchese, J. N.; Williamson, B.; Parker, K.; Hattan, S.; Khainovski, N.; Pillai, S.; Dey, S.; Daniels, S.; Purkayastha, S.; Juhasz, P.; Martin, S.; Bartlet-Jones, M.; He, F.; Jacobson, A.; Pappin, D. J., Multiplexed protein quantitation in Saccharomyces cerevisiae using amine-reactive isobaric tagging reagents. *Mol Cell Proteomics* **2004,** 3, 1154-69.

67. Zieske, L. R., A perspective on the use of iTRAQ reagent technology for protein complex and profiling studies. *Journal of experimental botany* **2006,** 57, 1501-8.

68. Frohlich, T.; Arnold, G. J., Quantifying attomole amounts of proteins from complex samples by nano-LC and selected reaction monitoring. *Methods in molecular biology (Clifton, N.J.)* **2011,** 790, 141-64.

69. Lange, V.; Picotti, P.; Domon, B.; Aebersold, R., Selected reaction monitoring for quantitative proteomics: a tutorial. *Mol Syst Biol* **2008,** 4, 222.

70. Picotti, P.; Rinner, O.; Stallmach, R.; Dautel, F.; Farrah, T.; Domon, B.; Wenschuh, H.; Aebersold, R., High-throughput generation of selected reaction-monitoring assays for proteins and proteomes. *Nature methods* **2010,** 7, 43-6.

71. Barnidge, D. R.; Dratz, E. A.; Martin, T.; Bonilla, L. E.; Moran, L. B.; Lindall, A., Absolute quantification of the G protein-coupled receptor rhodopsin by LC/MS/MS using proteolysis product peptides and synthetic peptide standards. *Analytical chemistry* **2003,** 75, 445-51.

72. Bhojwani, M.; Rudolph, E.; Kanitz, W.; Zuehlke, H.; Schneider, F.; Tomek, W., Molecular analysis of maturation processes by protein and phosphoprotein profiling during in vitro maturation of bovine oocytes: a proteomic approach. *Cloning Stem Cells* **2006,** 8, 259-74.

73. Fan, H. Y.; Sun, Q. Y., Involvement of mitogen-activated protein kinase cascade during oocyte maturation and fertilization in mammals. *Biol Reprod* **2004,** 70, 535-47.

74. Kishimoto, T., Cell-cycle control during meiotic maturation. *Current opinion in cell biology* **2003,** 15, 654-63.

75. Tomek, W.; Melo Sterza, F. A.; Kubelka, M.; Wollenhaupt, K.; Torner, H.; Anger, M.; Kanitz, W., Regulation of translation during in vitro maturation of bovine oocytes: the role of MAP kinase, eIF4E (cap binding protein) phosphorylation, and eIF4E-BP1. *Biol Reprod* **2002,** 66, 1274-82.

76. Berendt, F. J.; Frohlich, T.; Bolbrinker, P.; Boelhauve, M.; Gungor, T.; Habermann, F. A.; Wolf, E.; Arnold, G. J., Highly sensitive saturation labeling reveals changes in

abundance of cell cycle-associated proteins and redox enzyme variants during oocyte maturation in vitro. *Proteomics* **2009,** 9, 550-64.

77. Yang, J.; Winkler, K.; Yoshida, M.; Kornbluth, S., Maintenance of G2 arrest in the Xenopus oocyte: a role for 14-3-3-mediated inhibition of Cdc25 nuclear import. *The EMBO journal* **1999,** 18, 2174-83.

78. Yurttas, P.; Morency, E.; Coonrod, S. A., Use of proteomics to identify highly abundant maternal factors that drive the egg-to-embryo transition. *Reproduction* **2010,** 139, 809-23.

79. You, J.; Lee, E.; Bonilla, L.; Francis, J.; Koh, J.; Block, J.; Chen, S.; Hansen, P. J., Treatment with the proteasome inhibitor MG132 during the end of oocyte maturation improves oocyte competence for development after fertilization in cattle. *PLoS One* **2012,** 7, e48613.

80. You, J.; Kim, J.; Lee, H.; Hyun, S. H.; Hansen, P. J.; Lee, E., MG132 treatment during oocyte maturation improves embryonic development after somatic cell nuclear transfer and alters oocyte and embryo transcript abundance in pigs. *Mol Reprod Dev* **2012,** 79, 41-50.

81. Tanaka, K., The proteasome: from basic mechanisms to emerging roles. *The Keio journal of medicine* **2013,** 62, 1-12.

82. Karabinova, P.; Kubelka, M.; Susor, A., Proteasomal degradation of ubiquitinated proteins in oocyte meiosis and fertilization in mammals. *Cell and tissue research* **2011,** 346, 1-9.

83. Krisher, R. L.; Bavister, B. D., Enhanced glycolysis after maturation of bovine oocytes in vitro is associated with increased developmental competence. *Mol Reprod Dev* **1999,** 53, 19-26.

84. Rivera, R. M.; Kelley, K. L.; Erdos, G. W.; Hansen, P. J., Reorganization of microfilaments and microtubules by thermal stress in two-cell bovine embryos. *Biol Reprod* **2004,** 70, 1852-62.

85. Frei, R. E.; Schultz, G. A.; Church, R. B., Qualitative and quantitative changes in protein synthesis occur at the 8-16-cell stage of embryogenesis in the cow. *J Reprod Fertil* **1989,** 86, 637-41.

86. Memili, E.; First, N. L., Zygotic and embryonic gene expression in cow: a review of timing and mechanisms of early gene expression as compared with other species. *Zygote (Cambridge, England)* **2000,** 8, 87-96.

87. Massicotte, L.; Coenen, K.; Mourot, M.; Sirard, M. A., Maternal housekeeping proteins translated during bovine oocyte maturation and early embryo development. *Proteomics* **2006,** 6, 3811-20.

88. Berg, U.; Brem, G., In vitro Production of Bovine Blastocysts by in vitro Maturation and Fertilization of Oocytes and Subsequent in vitro Culture. *Reproduction in Domestic Animals* **1989,** 24, 134-139.

89. Parrish, J. J.; Susko-Parrish, J. L.; Leibfried-Rutledge, M. L.; Critser, E. S.; Eyestone, W. H.; First, N. L., Bovine in vitro fertilization with frozen-thawed semen. *Theriogenology* **1986,** 25, 591-600.

90. Perkins, D. N.; Pappin, D. J.; Creasy, D. M.; Cottrell, J. S., Probability-based protein identification by searching sequence databases using mass spectrometry data. *Electrophoresis* **1999,** 20, 3551-67.

91. Huang da, W.; Sherman, B. T.; Lempicki, R. A., Systematic and integrative analysis of large gene lists using DAVID bioinformatics resources. *Nat Protoc* **2009,** 4, 44-57.

92. Huang da, W.; Sherman, B. T.; Lempicki, R. A., Bioinformatics enrichment tools: paths toward the comprehensive functional analysis of large gene lists. *Nucleic acids research* **2009,** 37, 1-13.

93. Herrero, J.; Valencia, A.; Dopazo, J., A hierarchical unsupervised growing neural network for clustering gene expression patterns. *Bioinformatics (Oxford, England)* **2001,** 17, 126-36.

94. Bindea, G.; Mlecnik, B.; Hackl, H.; Charoentong, P.; Tosolini, M.; Kirilovsky, A.; Fridman, W. H.; Pages, F.; Trajanoski, Z.; Galon, J., ClueGO: a Cytoscape plug-in to decipher functionally grouped gene ontology and pathway annotation networks. *Bioinformatics (Oxford, England)* **2009,** 25, 1091-3.

95. Bindea, G.; Galon, J.; Mlecnik, B., CluePedia Cytoscape plugin: pathway insights using integrated experimental and in silico data. *Bioinformatics (Oxford, England)* **2013,** 29, 661-3.

96. Cline, M. S.; Smoot, M.; Cerami, E.; Kuchinsky, A.; Landys, N.; Workman, C.; Christmas, R.; Avila-Campilo, I.; Creech, M.; Gross, B.; Hanspers, K.; Isserlin, R.; Kelley, R.; Killcoyne, S.; Lotia, S.; Maere, S.; Morris, J.; Ono, K.; Pavlovic, V.; Pico, A. R.; Vailaya, A.; Wang, P. L.; Adler, A.; Conklin, B. R.; Hood, L.; Kuiper, M.; Sander, C.; Schmulevich, I.; Schwikowski, B.; Warner, G. J.; Ideker, T.; Bader, G. D., Integration of biological networks and gene expression data using Cytoscape. *Nat Protoc* **2007,** 2, 2366-82.

97. Liu, H.; Sadygov, R. G.; Yates, J. R., 3rd, A model for random sampling and estimation of relative protein abundance in shotgun proteomics. *Analytical chemistry* **2004,** 76, 4193-201.

98. Moreda-Pineiro, A.; Garcia-Otero, N.; Bermejo-Barrera, P., A review on preparative and semi-preparative offgel electrophoresis for multidimensional protein/peptide assessment. *Analytica chimica acta* **2014,** 836c, 1-17.

99. Barnea, E.; Sorkin, R.; Ziv, T.; Beer, I.; Admon, A., Evaluation of prefractionation methods as a preparatory step for multidimensional based chromatography of serum proteins. *Proteomics* **2005,** 5, 3367-75.

100. Luczak, M.; Marczak, L.; Stobiecki, M., Optimization of Plasma Sample Pretreatment for Quantitative Analysis Using iTRAQ Labeling and LC-MALDI-TOF/TOF. *PLoS One* **2014,** 9, e101694.

101. Lau, E.; Lam, M. P.; Siu, S. O.; Kong, R. P.; Chan, W. L.; Zhou, Z.; Huang, J.; Lo, C.; Chu, I. K., Combinatorial use of offline SCX and online RP-RP liquid chromatography for iTRAQ-based quantitative proteomics applications. *Mol Biosyst* **2011,** 7, 1399-408.

102. Tabb, D. L.; Vega-Montoto, L.; Rudnick, P. A.; Variyath, A. M.; Ham, A. J.; Bunk, D. M.; Kilpatrick, L. E.; Billheimer, D. D.; Blackman, R. K.; Cardasis, H. L.; Carr, S. A.; Clauser, K. R.; Jaffe, J. D.; Kowalski, K. A.; Neubert, T. A.; Regnier, F. E.; Schilling, B.; Tegeler, T. J.; Wang, M.; Wang, P.; Whiteaker, J. R.; Zimmerman, L. J.; Fisher, S. J.; Gibson, B. W.; Kinsinger, C. R.; Mesri, M.; Rodriguez, H.; Stein, S. E.; Tempst, P.;

Paulovich, A. G.; Liebler, D. C.; Spiegelman, C., Repeatability and reproducibility in proteomic identifications by liquid chromatography-tandem mass spectrometry. *J Proteome Res* **2010,** 9, 761-76.

103. Coticchio, G.; Dal-Canto, M.; Guglielmo, M. C.; Mignini-Renzini, M.; Fadini, R., Human oocyte maturation in vitro. *The International journal of developmental biology* **2012,** 56, 909-18.

104. Platonova, O.; Akey, I. V.; Head, J. F.; Akey, C. W., Crystal structure and function of human nucleoplasmin (npm2): a histone chaperone in oocytes and embryos. *Biochemistry* **2011,** 50, 8078-89.

105. Tejomurtula, J.; Lee, K. B.; Tripurani, S. K.; Smith, G. W.; Yao, J., Role of importin alpha8, a new member of the importin alpha family of nuclear transport proteins, in early embryonic development in cattle. *Biol Reprod* **2009,** 81, 333-42.

106. Nikonova, A. S.; Astsaturov, I.; Serebriiskii, I. G.; Dunbrack, R. L., Jr.; Golemis, E. A., Aurora A kinase (AURKA) in normal and pathological cell division. *Cellular and molecular life sciences : CMLS* **2013,** 70, 661-87.

107. Kinoshita, K.; Noetzel, T. L.; Pelletier, L.; Mechtler, K.; Drechsel, D. N.; Schwager, A.; Lee, M.; Raff, J. W.; Hyman, A. A., Aurora A phosphorylation of TACC3/maskin is required for centrosome-dependent microtubule assembly in mitosis. *The Journal of cell biology* **2005,** 170, 1047-55.

108. De Souza, C. P.; Ellem, K. A.; Gabrielli, B. G., Centrosomal and cytoplasmic Cdc2/cyclin B1 activation precedes nuclear mitotic events. *Experimental cell research* **2000,** 257, 11-21.

109. Liu, C.; Liu, Y.; Liu, Y.; Wu, D.; Luan, Z.; Wang, E.; Yu, B., Ser 15 of WEE1B is a potential PKA phosphorylation target in G2/M transition in one-cell stage mouse embryos. *Molecular medicine reports* **2013,** 7, 1929-37.

110. Schellander, K.; Fuhrer, F.; Brackett, B. G.; Korb, H.; Schleger, W., In vitro fertilization and cleavage of bovine oocytes matured in medium supplemented with estrous cow serum. *Theriogenology* **1990,** 33, 477-85.

111. Richards, J. S.; Russell, D. L.; Ochsner, S.; Espey, L. L., Ovulation: new dimensions and new regulators of the inflammatory-like response. *Annual review of physiology* **2002,** 64, 69-92.

112. Wang, X.; Tsai, T.; Qiao, J.; Zhang, Z.; Feng, H. L., Impact of gonadotropins on oocyte maturation, fertilisation and developmental competence in vitro. *Reprod Fertil Dev* **2014,** 26, 752-7.

113. Mito, T.; Yoshioka, K.; Noguchi, M.; Yamashita, S.; Hoshi, H., Recombinant human follicle-stimulating hormone and transforming growth factor-alpha enhance in vitro maturation of porcine oocytes. *Mol Reprod Dev* **2013,** 80, 549-60.

114. Assidi, M.; Richard, F. J.; Sirard, M. A., FSH in vitro versus LH in vivo: similar genomic effects on the cumulus. *Journal of ovarian research* **2013,** 6, 68.

115. Conti, M.; Hsieh, M.; Park, J. Y.; Su, Y. Q., Role of the epidermal growth factor network in ovarian follicles. *Mol Endocrinol* **2006,** 20, 715-23.

116. Leidenfrost, S.; Boelhauve, M.; Reichenbach, M.; Gungor, T.; Reichenbach, H. D.; Sinowatz, F.; Wolf, E.; Habermann, F. A., Cell arrest and cell death in mammalian

preimplantation development: lessons from the bovine model. *PLoS One* **2011,** 6, e22121.

117. Hiendleder, S.; Wirtz, M.; Mund, C.; Klempt, M.; Reichenbach, H. D.; Stojkovic, M.; Weppert, M.; Wenigerkind, H.; Elmlinger, M.; Lyko, F.; Schmitz, O. J.; Wolf, E., Tissue-specific effects of in vitro fertilization procedures on genomic cytosine methylation levels in overgrown and normal sized bovine fetuses. *Biol Reprod* **2006,** 75, 17-23.

118. Stojkovic, M.; Machado, S. A.; Stojkovic, P.; Zakhartchenko, V.; Hutzler, P.; Goncalves, P. B.; Wolf, E., Mitochondrial distribution and adenosine triphosphate content of bovine oocytes before and after in vitro maturation: correlation with morphological criteria and developmental capacity after in vitro fertilization and culture. *Biol Reprod* **2001,** 64, 904-9.

119. Rogon, C.; Ulbricht, A.; Hesse, M.; Alberti, S.; Vijayaraj, P.; Best, D.; Adams, I. R.; Magin, T. M.; Fleischmann, B. K.; Hohfeld, J., HSP70 Binding Protein HSPBP1 Regulates Chaperone Expression at a Posttranslational Level and is Essential for Spermatogenesis. *Molecular biology of the cell* **2014**.

120. Neuer, A.; Mele, C.; Liu, H. C.; Rosenwaks, Z.; Witkin, S. S., Monoclonal antibodies to mammalian heat shock proteins impair mouse embryo development in vitro. *Hum Reprod* **1998,** 13, 987-90.

121. Rupik, W.; Jasik, K.; Bembenek, J.; Widłak, W., The expression patterns of heat shock genes and proteins and their role during vertebrate's development. *Comparative Biochemistry and Physiology Part A: Molecular & Integrative Physiology* **2011,** 159, 349-366.

122. Mtango, N. R.; Varisanga, M. D.; Dong, Y. J.; Rajamahendran, R.; Suzuki, T., Growth factors and growth hormone enhance in vitro embryo production and post-thaw survival of vitrified bovine blastocysts. *Theriogenology* **2003,** 59, 1393-402.

123. Kolle, S.; Stojkovic, M.; Boie, G.; Wolf, E.; Sinowatz, F., Growth hormone inhibits apoptosis in in vitro produced bovine embryos. *Mol Reprod Dev* **2002,** 61, 180-6.

124. Kolle, S.; Stojkovic, M.; Reese, S.; Reichenbach, H. D.; Wolf, E.; Sinowatz, F., Effects of growth hormone on the ultrastructure of bovine preimplantation embryos. *Cell and tissue research* **2004,** 317, 101-8.

125. Kolle, S.; Stojkovic, M.; Boie, G.; Wolf, E.; Sinowatz, F., Growth hormone-related effects on apoptosis, mitosis, and expression of connexin 43 in bovine in vitro maturation cumulus-oocyte complexes. *Biol Reprod* **2003,** 68, 1584-9.

126. Okuwaki, M.; Kato, K.; Nagata, K., Functional characterization of human nucleosome assembly protein 1-like proteins as histone chaperones. *Genes to cells : devoted to molecular & cellular mechanisms* **2010,** 15, 13-27.

127. Challa, A. A.; Stefanovic, B., A novel role of vimentin filaments: binding and stabilization of collagen mRNAs. *Molecular and cellular biology* **2011,** 31, 3773-89.

128. Payne, C.; Rawe, V.; Ramalho-Santos, J.; Simerly, C.; Schatten, G., Preferentially localized dynein and perinuclear dynactin associate with nuclear pore complex proteins to mediate genomic union during mammalian fertilization. *Journal of cell science* **2003,** 116, 4727-38.

129. Du, H.; Huang, X.; Wang, S.; Wu, Y.; Xu, W.; Li, M., PSMA7, a potential biomarker of diseases. *Protein and peptide letters* **2009,** 16, 486-9.

130. Mustafi, S. M.; Chen, H.; Li, H.; Lemaster, D. M.; Hernandez, G., Analysing the visible conformational substates of the FK506-binding protein FKBP12. *The Biochemical journal* **2013,** 453, 371-80.

131. Sugata, H.; Matsuo, K.; Nakagawa, T.; Takahashi, M.; Mukai, H.; Ono, Y.; Maeda, K.; Akiyama, H.; Kawamata, T., A peptidyl-prolyl isomerase, FKBP12, accumulates in Alzheimer neurofibrillary tangles. *Neuroscience letters* **2009,** 459, 96-9.

132. Pratte, D.; Singh, U.; Murat, G.; Kressler, D., Mak5 and Ebp2 act together on early pre-60S particles and their reduced functionality bypasses the requirement for the essential pre-60S factor Nsa1. *PLoS One* **2013,** 8, e82741.

133. Tasheva, E. S.; Roufa, D. J., Regulation of human RPS14 transcription by intronic antisense RNAs and ribosomal protein S14. *Genes & development* **1995,** 9, 304-16.

134. Zhou, X.; Hao, Q.; Liao, J. M.; Liao, P.; Lu, H., Ribosomal protein S14 negatively regulates c-Myc activity. *J Biol Chem* **2013**.

135. Wang, L.; Luo, J.; Nian, Q.; Xiao, Q.; Yang, Z.; Liu, L., Ribosomal protein S14 silencing inhibits growth of acute myeloid leukemia transformed from myelodysplastic syndromes via activating p53. *Hematology (Amsterdam, Netherlands)* **2013**.

136. Zhou, X.; Hao, Q.; Liao, J.; Zhang, Q.; Lu, H., Ribosomal protein S14 unties the MDM2-p53 loop upon ribosomal stress. *Oncogene* **2013,** 32, 388-96.

137. Bomsztyk, K.; Denisenko, O.; Ostrowski, J., hnRNP K: one protein multiple processes. *BioEssays : news and reviews in molecular, cellular and developmental biology* **2004,** 26, 629-38.

138. Pelisch, F.; Pozzi, B.; Risso, G.; Munoz, M. J.; Srebrow, A., DNA damage-induced heterogeneous nuclear ribonucleoprotein K sumoylation regulates p53 transcriptional activation. *J Biol Chem* **2012,** 287, 30789-99.

139. Moumen, A.; Masterson, P.; O'Connor, M. J.; Jackson, S. P., hnRNP K: an HDM2 target and transcriptional coactivator of p53 in response to DNA damage. *Cell* **2005,** 123, 1065-78.

140. Gardner, D. K.; Leese, H. J., Non-invasive measurement of nutrient uptake by single cultured pre-implantation mouse embryos. *Hum Reprod* **1986,** 1, 25-7.

141. Michaels, G. S.; Hauswirth, W. W.; Laipis, P. J., Mitochondrial DNA copy number in bovine oocytes and somatic cells. *Developmental biology* **1982,** 94, 246-51.

142. Cummins, J. M., The role of mitochondria in the establishment of oocyte functional competence. *European journal of obstetrics, gynecology, and reproductive biology* **2004,** 115 Suppl 1, S23-9.

143. Barritt, J. A.; Kokot, M.; Cohen, J.; Steuerwald, N.; Brenner, C. A., Quantification of human ooplasmic mitochondria. *Reproductive biomedicine online* **2002,** 4, 243-7.

144. Torner, H.; Brussow, K. P.; Alm, H.; Ratky, J.; Pohland, R.; Tuchscherer, A.; Kanitz, W., Mitochondrial aggregation patterns and activity in porcine oocytes and apoptosis in surrounding cumulus cells depends on the stage of pre-ovulatory maturation. *Theriogenology* **2004,** 61, 1675-89.

145. Au, H. K.; Yeh, T. S.; Kao, S. H.; Tzeng, C. R.; Hsieh, R. H., Abnormal mitochondrial structure in human unfertilized oocytes and arrested embryos. *Annals of the New York Academy of Sciences* **2005,** 1042, 177-85.

146. Crosier, A. E.; Farin, P. W.; Dykstra, M. J.; Alexander, J. E.; Farin, C. E., Ultrastructural morphometry of bovine blastocysts produced in vivo or in vitro. *Biol Reprod* **2001,** 64, 1375-85.

147. Tarazona, A. M.; Rodriguez, J. I.; Restrepo, L. F.; Olivera-Angel, M., Mitochondrial activity, distribution and segregation in bovine oocytes and in embryos produced in vitro. *Reprod Domest Anim* **2006,** 41, 5-11.

148. Nagano, M.; Katagiri, S.; Takahashi, Y., Relationship between bovine oocyte morphology and in vitro developmental potential. *Zygote (Cambridge, England)* **2006,** 14, 53-61.

149. Abe, H.; Hoshi, H., Evaluation of bovine embryos produced in high performance serum-free media. *The Journal of reproduction and development* **2003,** 49, 193-202.

150. Abe, H.; Otoi, T.; Tachikawa, S.; Yamashita, S.; Satoh, T.; Hoshi, H., Fine structure of bovine morulae and blastocysts in vivo and in vitro. *Anatomy and embryology* **1999,** 199, 519-27.

151. Shamsuddin, M.; Rodriguez-Martinez, H., Fine structure of bovine blastocysts developed either in serum-free medium or in conventional co-culture with oviduct epithelial cells. *Zentralblatt fur Veterinarmedizin. Reihe A* **1994,** 41, 307-16.

152. Pinyopummintr, T.; Bavister, B. D., In vitro-matured/in vitro-fertilized bovine oocytes can develop into morulae/blastocysts in chemically defined, protein-free culture media. *Biol Reprod* **1991,** 45, 736-42.

153. Lonergan, P.; Carolan, C.; Mermillod, P., Development of bovine embryos in vitro following oocyte maturation under defined conditions. *Reproduction, nutrition, development* **1994,** 34, 329-39.

154. Van Langendonckt, A.; Donnay, I.; Schuurbiers, N.; Auquier, P.; Carolan, C.; Massip, A.; Dessy, F., Effects of supplementation with fetal calf serum on development of bovine embryos in synthetic oviduct fluid medium. *J Reprod Fertil* **1997,** 109, 87-93.

155. Mains, L. M.; Christenson, L.; Yang, B.; Sparks, A. E.; Mathur, S.; Van Voorhis, B. J., Identification of apolipoprotein A1 in the human embryonic secretome. *Fertil Steril* **2011,** 96, 422-427.e2.

156. Kizhatil, K.; Yoon, W.; Mohler, P. J.; Davis, L. H.; Hoffman, J. A.; Bennett, V., Ankyrin-G and beta2-spectrin collaborate in biogenesis of lateral membrane of human bronchial epithelial cells. *J Biol Chem* **2007,** 282, 2029-37.

157. Kizhatil, K.; Davis, J. Q.; Davis, L.; Hoffman, J.; Hogan, B. L.; Bennett, V., Ankyrin-G is a molecular partner of E-cadherin in epithelial cells and early embryos. *J Biol Chem* **2007,** 282, 26552-61.

158. Miserey-Lenkei, S.; Couedel-Courteille, A.; Del Nery, E.; Bardin, S.; Piel, M.; Racine, V.; Sibarita, J. B.; Perez, F.; Bornens, M.; Goud, B., A role for the Rab6A' GTPase in the inactivation of the Mad2-spindle checkpoint. *The EMBO journal* **2006,** 25, 278-89.

159. Lee, J. H.; You, J.; Dobrota, E.; Skalnik, D. G., Identification and characterization of a novel human PP1 phosphatase complex. *J Biol Chem* **2010,** 285, 24466-76.

160. Varmuza, S.; Jurisicova, A.; Okano, K.; Hudson, J.; Boekelheide, K.; Shipp, E. B., Spermiogenesis is impaired in mice bearing a targeted mutation in the protein phosphatase 1cgamma gene. *Developmental biology* **1999,** 205, 98-110.

161. Holmfeldt, P.; Larsson, N.; Segerman, B.; Howell, B.; Morabito, J.; Cassimeris, L.; Gullberg, M., The catastrophe-promoting activity of ectopic Op18/stathmin is required for disruption of mitotic spindles but not interphase microtubules. *Molecular biology of the cell* **2001,** 12, 73-83.

162. Koppel, J.; Rehak, P.; Baran, V.; Vesela, J.; Hlinka, D.; Manceau, V.; Sobel, A., Cellular and subcellular localization of stathmin during oocyte and preimplantation embryo development. *Mol Reprod Dev* **1999,** 53, 306-17.

163. Rana, S.; Maples, P. B.; Senzer, N.; Nemunaitis, J., Stathmin 1: a novel therapeutic target for anticancer activity. *Expert review of anticancer therapy* **2008,** 8, 1461-70.

164. Han, S. J.; Chen, R.; Paronetto, M. P.; Conti, M., Wee1B is an oocyte-specific kinase involved in the control of meiotic arrest in the mouse. *Current biology : CB* **2005,** 15, 1670-6.

165. Hanna, C. B.; Yao, S.; Patta, M. C.; Jensen, J. T.; Wu, X., WEE2 is an oocyte-specific meiosis inhibitor in rhesus macaque monkeys. *Biol Reprod* **2010,** 82, 1190-7.

166. Nakanishi, M.; Ando, H.; Watanabe, N.; Kitamura, K.; Ito, K.; Okayama, H.; Miyamoto, T.; Agui, T.; Sasaki, M., Identification and characterization of human Wee1B, a new member of the Wee1 family of Cdk-inhibitory kinases. *Genes to cells : devoted to molecular & cellular mechanisms* **2000,** 5, 839-47.

167. Walter, P.; Ron, D., The unfolded protein response: from stress pathway to homeostatic regulation. *Science* **2011,** 334, 1081-6.

168. Albuz, F. K.; Sasseville, M.; Lane, M.; Armstrong, D. T.; Thompson, J. G.; Gilchrist, R. B., Simulated physiological oocyte maturation (SPOM): a novel in vitro maturation system that substantially improves embryo yield and pregnancy outcomes. *Hum Reprod* **2010,** 25, 2999-3011.

169. Quesada, V.; Sanchez, L. M.; Alvarez, J.; Lopez-Otin, C., Identification and characterization of human and mouse ovastacin: a novel metalloproteinase similar to hatching enzymes from arthropods, birds, amphibians, and fish. *J Biol Chem* **2004,** 279, 26627-34.

170. Burkart, A. D.; Xiong, B.; Baibakov, B.; Jimenez-Movilla, M.; Dean, J., Ovastacin, a cortical granule protease, cleaves ZP2 in the zona pellucida to prevent polyspermy. *The Journal of cell biology* **2012,** 197, 37-44.

171. Hino, M.; Kurogi, K.; Okubo, M. A.; Murata-Hori, M.; Hosoya, H., Small heat shock protein 27 (HSP27) associates with tubulin/microtubules in HeLa cells. *Biochem Biophys Res Commun* **2000,** 271, 164-9.

172. Bryantsev, A. L.; Kurchashova, S. Y.; Golyshev, S. A.; Polyakov, V. Y.; Wunderink, H. F.; Kanon, B.; Budagova, K. R.; Kabakov, A. E.; Kampinga, H. H., Regulation of stress-induced intracellular sorting and chaperone function of Hsp27 (HspB1) in mammalian cells. *The Biochemical journal* **2007,** 407, 407-17.

173. Ponting, C. P., Tudor domains in proteins that interact with RNA. *Trends in biochemical sciences* **1997,** 22, 51-2.

174. Dejgaard, K.; Leffers, H., Characterisation of the nucleic-acid-binding activity of KH domains. Different properties of different domains. *European journal of biochemistry / FEBS* **1996,** 241, 425-31.

175. Saxe, J. P.; Chen, M.; Zhao, H.; Lin, H., Tdrkh is essential for spermatogenesis and participates in primary piRNA biogenesis in the germline. *The EMBO journal* **2013,** 32, 1869-85.

176. Shrestha, S.; Wilmeth, L. J.; Eyer, J.; Shuster, C. B., PRC1 controls spindle polarization and recruitment of cytokinetic factors during monopolar cytokinesis. *Molecular biology of the cell* **2012,** 23, 1196-207.

177. Krotz, S. P.; Ballow, D. J.; Choi, Y.; Rajkovic, A., Expression and localization of the novel and highly conserved gametocyte-specific factor 1 during oogenesis and spermatogenesis. *Fertil Steril* **2009,** 91, 2020-4.

178. Beltman, M. E.; Forde, N.; Furney, P.; Carter, F.; Roche, J. F.; Lonergan, P.; Crowe, M. A., Characterisation of endometrial gene expression and metabolic parameters in beef heifers yielding viable or non-viable embryos on Day 7 after insemination. *Reprod Fertil Dev* **2010,** 22, 987-99.

179. Jarkovska, K.; Martinkova, J.; Liskova, L.; Halada, P.; Moos, J.; Rezabek, K.; Gadher, S. J.; Kovarova, H., Proteome mining of human follicular fluid reveals a crucial role of complement cascade and key biological pathways in women undergoing in vitro fertilization. *J Proteome Res* **2010,** 9, 1289-301.

180. Kempisty, B.; Antosik, P.; Bukowska, D.; Jackowska, M.; Lianeri, M.; Jaskowski, J. M.; Jagodzinski, P. P., Analysis of selected transcript levels in porcine spermatozoa, oocytes, zygotes and two-cell stage embryos. *Reprod Fertil Dev* **2008,** 20, 513-8.

181. Vigneault, C.; McGraw, S.; Sirard, M. A., Spatiotemporal expression of transcriptional regulators in concert with the maternal-to-embryonic transition during bovine in vitro embryogenesis. *Reproduction* **2009,** 137, 13-21.

182. Wu, X.; Viveiros, M. M.; Eppig, J. J.; Bai, Y.; Fitzpatrick, S. L.; Matzuk, M. M., Zygote arrest 1 (Zar1) is a novel maternal-effect gene critical for the oocyte-to-embryo transition. *Nature genetics* **2003,** 33, 187-91.

183. Yang, X. J.; Seto, E., Lysine acetylation: codified crosstalk with other posttranslational modifications. *Molecular cell* **2008,** 31, 449-61.

184. Glozak, M. A.; Sengupta, N.; Zhang, X.; Seto, E., Acetylation and deacetylation of non-histone proteins. *Gene* **2005,** 363, 15-23.

185. Khoury, G. A.; Baliban, R. C.; Floudas, C. A., Proteome-wide post-translational modification statistics: frequency analysis and curation of the swiss-prot database. *Sci. Rep.* **2011,** 1.

186. von Toerne, C.; Kahle, M.; Schafer, A.; Ispiryan, R.; Blindert, M.; Hrabe De Angelis, M.; Neschen, S.; Ueffing, M.; Hauck, S. M., Apoe, Mbl2, and Psp plasma protein levels correlate with diabetic phenotype in NZO mice--an optimized rapid workflow for SRM-based quantification. *J Proteome Res* **2013,** 12, 1331-43.

187. Selevsek, N.; Matondo, M.; Sanchez Carbayo, M.; Aebersold, R.; Domon, B., Systematic quantification of peptides/proteins in urine using selected reaction monitoring. *Proteomics* **2011,** 11, 1135-47.

188. D'Amours, O.; Frenette, G.; Fortier, M.; Leclerc, P.; Sullivan, R., Proteomic comparison of detergent-extracted sperm proteins from bulls with different fertility indexes. *Reproduction* **2010,** 139, 545-56.

189. Malmstrom, J.; Beck, M.; Schmidt, A.; Lange, V.; Deutsch, E. W.; Aebersold, R., Proteome-wide cellular protein concentrations of the human pathogen Leptospira interrogans. *Nature* **2009,** 460, 762-5.

7. Appendix

7.1 Abbreviations

ANOVA	Analysis of variance
ACN	Acetonitrile
ART	Assisted reproductive techniques
BSA	Bovine serum albumin
CE	Collision energy
CID	Collision induced dissociation
COC	Cumulus-oocyte complex
CV	Coefficient of variation
CXP	Collision exit potential
DAPI	4',6-diamidino-2-phenylindole
DP	Declustering potential
ECS	Estrous cow serum
e.g.	Exempli gratia (for example)
EGA	Embryonic genome activation
EP	Entrance potential
ER	Endoplasmic reticulum
FDR	False discovery rate
FSH	Follicle stimulating hormone
GH	Growth hormone
GO	Gene ontology
GV	Germinal vesicle
Hpi	Hours post insemination
HCD	Higher energy collision-induced dissociation
ICM	Inner cell mass
IVM	*in vitro* maturation
IVP	*in vitro* embryo production
iTRAQ	Isobaric tags for relative and absolute quantification
KCl	Potassium chloride

LC-MS/MS	Liqud chromatography tandem mass spectormetry
LH	Pituitary luteinizing hormone
LOD	Limit of detection
LOQ	Limit of quantification
LSM	Laser scanning microscopy
MALDI-TOF-MS	Matrix-Assisted-Laser-Desorption/Ionization-Time-Of-Flight-Mass-Spectrometry
MET	Maternal-to-embryonic transition
Mgf	Mascot generic format
MHKP	Maternal housekeeping proteins
MII	Metaphase II
m/z	mass to charge
PBS	Phosphate-buffered saline
PCA	Principle component analysis
PTM	Post-translation modification
RT	Room temperature
SCX	Strong cation exchange
SI	Stable isotope-labeled peptide
SOF	Synthetic oviduct fluid
SRM	Selected reaction monitoring
SSU-rRNA	Small subunit ribosomal ribobucleic acid
TCM	Tissue culture medium
TE	Trophectoderm
UPR	Unfolded protein response
Vs.	versus
2D-PAGE	Two-dimensional polyacrylamide gel electrophoresis

7.2 Supporting information

7.2.1 Details of the 27-plex SRM assay

Table 10. Details of the 27-plex SRM assay.

Light: Endogenous peptide. Heavy: Stable isotope labeled peptide. Blue color: Quantifier transition. Precursor ions and fragment ions are listed with their mass to charge (m/z) ratios. DP: Declustering potential: 100 Volt. EP: Entrance Potential: 10 Volt. CXP: Collision exit potential: 15 Volt. CE: Collision energy in Volt. Duration of the method: 64 min; 1280 cycles; MRM detection window: 240 s and target scan time: 3 s. Peptides are sorted by increasing retention time.

gene name	peptide sequence	light or heavy	charge / fragment ions	precurser ion (m/z)	fragment ion (m/z)	CE in volt	retention time in min	Amount heavy peptide in fmol/oocyte or embryo
UHRF1	YAPIEGNR	light	2+ / y6	460.24	685.36	22	13.8	/
UHRF1	YAPIEGNR	light	2+ / y5	460.24	588.31	28	13.8	/
UHRF1	YAPIEGNR	light	2+ / y4	460.24	475.23	28	13.8	/
UHRF1	YAPIEGNR	heavy	2+ / y6	465.24	695.36	22	13.8	12.4
UHRF1	YAPIEGNR	heavy	2+ / y5	465.24	598.31	28	13.8	12.4
UHRF1	YAPIEGNR	heavy	2+ / y4	465.24	485.23	28	13.8	12.4
STMN1	AIEENNNFSK	light	2+ / y8	583.28	981.43	25	14	/
STMN1	AIEENNNFSK	light	2+ / y6	583.28	723.34	28	14	/
STMN1	AIEENNNFSK	light	2+ / y7	583.28	852.38	25	14	/
STMN1	AIEENNNFSK	heavy	2+ / y8	587.28	989.43	25	14	8.8
STMN1	AIEENNNFSK	heavy	2+ / y6	587.28	731.34	28	14	8.8
STMN1	AIEENNNFSK	heavy	2+ / y7	587.28	860.38	25	14	8.8
TACC3	QASEEIAQVR	light	2+ / y4	565.79	473.28	30	16	/
TACC3	QASEEIAQVR	light	2+ / y6	565.79	715.41	30	16	/
TACC3	QASEEIAQVR	light	2+ / y8	565.79	931.48	30	16	/
TACC3	QASEEIAQVR	heavy	2+ / y4	570.79	483.28	30	16	7.0
TACC3	QASEEIAQVR	heavy	2+ / y6	570.79	725.41	30	16	7.0
TACC3	QASEEIAQVR	heavy	2+ / y8	570.79	941.48	30	16	7.0
HAPLN3	SNC[CAM]GALEPGVR	light	2+ / y4	580.28	428.26	35	16	/
HAPLN3	SNC[CAM]GALEPGVR	light	2+ / y6	580.28	670.39	31	16	/
HAPLN3	SNC[CAM]GALEPGVR	light	2+ / y8	580.28	798.45	31	16	/
HAPLN3	SNC[CAM]GALEPGVR	heavy	2+ / y4	585.28	438.26	35	16	17.8
HAPLN3	SNC[CAM]GALEPGVR	heavy	2+ / y6	585.28	680.39	31	16	17.8
HAPLN3	SNC[CAM]GALEPGVR	heavy	2+ / y8	585.28	808.45	31	16	17.8
LAMP2	EKEVFTVNNR	light	2+ / y8	618.32	978.50	29	18	/
LAMP2	EKEVFTVNNR	light	2+ / y6	618.32	750.39	35	18	/
LAMP2	EKEVFTVNNR	light	2+ / y7	618.32	849.46	32	18	/
LAMP2	EKEVFTVNNR	heavy	2+ / y8	623.32	988.50	29	18	15.0
LAMP2	EKEVFTVNNR	heavy	2+ / y6	623.32	760.39	35	18	15.0
LAMP2	EKEVFTVNNR	heavy	2+ / y7	623.32	859.46	32	18	15.0
AURKA	TAVPLSDGPK	light	2+ / y7	492.77	713.38	22	17.5	/
AURKA	TAVPLSDGPK	light	2+ / y5	492.77	503.25	33	17.5	/
AURKA	TAVPLSDGPK	light	2+ / y3	492.77	301.19	33	17.5	/
AURKA	TAVPLSDGPK	heavy	2+ / y7	496.77	721.38	22	17.5	3.1
AURKA	TAVPLSDGPK	heavy	2+ / y5	496.77	511.25	33	17.5	3.1
AURKA	TAVPLSDGPK	heavy	2+ / y3	496.77	309.19	33	17.5	3.1
PEBP1	LYEQLSGK	light	2+ / y6	469.25	661.35	23	17	/
PEBP1	LYEQLSGK	light	2+ / y7	469.25	824.41	20	17	/
PEBP1	LYEQLSGK	light	2+ / y5	469.25	532.31	23	17	/
PEBP1	LYEQLSGK	heavy	2+ / y6	473.25	669.35	23	17	10.0
PEBP1	LYEQLSGK	heavy	2+ / y7	473.25	832.41	20	17	10.0

PEBP1	LYEQLSGK	heavy	2+ / y5	473.25	540.31	23	17	10.0
HAPLN3	LTLAEAR	light	2+ / y5	387.23	559.32	19	17	/
HAPLN3	LTLAEAR	light	2+ / y4	387.23	446.24	25	17	/
HAPLN3	LTLAEAR	light	2+ / y6	387.23	660.37	22	17	/
HAPLN3	LTLAEAR	heavy	2+ / y5	392.23	569.32	19	17	7.8
HAPLN3	LTLAEAR	heavy	2+ / y4	392.23	456.24	25	17	7.8
HAPLN3	LTLAEAR	heavy	2+ / y6	392.23	670.37	22	17	7.8
ACCSL	FGALYTHNR	light	2+ / y5	539.78	690.33	29	17	/
ACCSL	FGALYTHNR	light	2+ / y4	539.78	527.27	29	17	/
ACCSL	FGALYTHNR	light	2+ / b3	539.78	276.13	31	17	/
ACCSL	FGALYTHNR	heavy	2+ / y5	544.78	700.33	29	17	2.5
ACCSL	FGALYTHNR	heavy	2+ / y4	544.78	537.27	29	17	2.5
ACCSL	FGALYTHNR	heavy	2+ / b3	544.78	276.13	31	17	2.5
RPS27A	TLSDYNIQK	light	2+ / y7	541.28	867.42	20	18.8	/
RPS27A	TLSDYNIQK	light	2+ / y6	541.28	780.39	20	18.8	/
RPS27A	TLSDYNIQK	light	2+ / y5	541.28	665.36	23	18.8	/
RPS27A	TLSDYNIQK	heavy	2+ / y7	545.28	875.42	20	18.8	7.8
RPS27A	TLSDYNIQK	heavy	2+ / y6	545.28	788.39	20	18.8	7.5
RPS27A	TLSDYNIQK	heavy	2+ / y5	545.28	673.36	23	18.8	7.5
RBP4	DPSGFSPEVQK	light	2+ / y6	595.79	687.37	31	19	/
RBP4	DPSGFSPEVQK	light	2+ / y8	595.79	891.46	31	19	/
RBP4	DPSGFSPEVQK	light	2+ / b3	595.79	300.12	28	19	/
RBP4	DPSGFSPEVQK	heavy	2+ / y6	599.79	695.37	31	19	2.7
RBP4	DPSGFSPEVQK	heavy	2+ / y8	599.79	899.46	31	19	2.7
RBP4	DPSGFSPEVQK	heavy	2+ / b3	599.79	300.12	28	19	2.7
YBX2	GAEAANVTGPGGVPVK	light	2+ / y3	712.38	343.23	33	19	/
YBX2	GAEAANVTGPGGVPVK	light	2+ / y9	712.38	811.47	35	19	/
YBX2	GAEAANVTGPGGVPVK	light	2+ / y10	712.38	910.54	35	19	/
YBX2	GAEAANVTGPGGVPVK	heavy	2+ / y3	716.38	351.23	33	19	5.0
YBX2	GAEAANVTGPGGVPVK	heavy	2+ / y9	716.38	819.47	35	19	5.0
YBX2	GAEAANVTGPGGVPVK	heavy	2+ / y10	716.38	918.54	35	19	5.0
PRC1	LQIPAEER	light	2+ / y5	478.26	601.29	23	19.5	/
PRC1	LQIPAEER	light	2+ / y6	478.26	714.38	23	19.5	/
PRC1	LQIPAEER	light	2+ / b3	478.26	355.23	20	19.5	/
PRC1	LQIPAEER	heavy	2+ / y5	483.26	611.29	23	19.5	0.8
PRC1	LQIPAEER	heavy	2+ / y6	483.26	724.38	23	19.5	0.8
PRC1	LQIPAEER	heavy	2+ / b3	483.26	355.23	20	19.5	0.8
PEBP1	YGGAEVDELGK	light	2+ / y10	569.27	974.48	24	20	/
PEBP1	YGGAEVDELGK	light	2+ / y9	569.27	917.46	24	20	/
PEBP1	YGGAEVDELGK	light	2+ / y7	569.27	789.40	24	20	/
PEBP1	YGGAEVDELGK	heavy	2+ / y10	573.27	982.48	24	20	10.0
PEBP1	YGGAEVDELGK	heavy	2+ / y9	573.27	925.46	24	20	10.0
PEBP1	YGGAEVDELGK	heavy	2+ / y7	573.27	797.40	24	20	10.0
TACC3	IC[CAM]DDLISK	light	2+ / y6	482.24	690.37	23	20	/
TACC3	IC[CAM]DDLISK	light	2+ / y7	482.24	850.40	20	20	/
TACC3	IC[CAM]DDLISK	light	2+ / b4	482.24	504.18	32	20	/
TACC3	IC[CAM]DDLISK	heavy	2+ / y6	486.24	698.37	23	20	4.9
TACC3	IC[CAM]DDLISK	heavy	2+ / y7	486.24	858.40	20	20	4.9
TACC3	IC[CAM]DDLISK	heavy	2+ / b4	486.24	504.18	32	20	4.9
GTSF1	LATC[CAM]PFNAR	light	2+ / y5	525.26	604.32	28	20	/
GTSF1	LATC[CAM]PFNAR	light	2+ / b8	525.26	875.41	22	20	/
GTSF1	LATC[CAM]PFNAR	light	2+ / y7	525.26	865.40	22	20	/
GTSF1	LATC[CAM]PFNAR	heavy	2+ / y5	530.26	614.32	28	20	26.7
GTSF1	LATC[CAM]PFNAR	heavy	2+ / b8	530.26	875.41	22	20	26.7
GTSF1	LATC[CAM]PFNAR	heavy	2+ / y7	530.26	875.40	22	20	26.7
VIM	FADLSEAANR	light	2+ / y6	547.27	647.31	26	21	/
VIM	FADLSEAANR	light	2+ / y8	547.27	875.42	23	21	/
VIM	FADLSEAANR	light	2+ / b3	547.27	334.14	29	21	/
VIM	FADLSEAANR	heavy	2+ / y6	552.27	657.31	26	21	3.2
VIM	FADLSEAANR	heavy	2+ / y8	552.27	885.42	23	21	3.2
VIM	FADLSEAANR	heavy	2+ / b3	552.27	334.14	29	21	3.2
YBX2	TPGNPATAASGTPAPLAR	light	2+ / y11	825.43	1011.56	46	21.5	/
YBX2	TPGNPATAASGTPAPLAR	light	2+ / y9	825.43	869.48	46	21.5	/
YBX2	TPGNPATAASGTPAPLAR	light	2+ / y10	825.43	940.52	43	21.5	/

YBX2	TPGNPATAASGTPAPLAR	heavy	2+ / y11	830.43	1021.56	46	21.5	5.0
YBX2	TPGNPATAASGTPAPLAR	heavy	2+ / y9	830.43	879.48	46	21.5	5.0
YBX2	TPGNPATAASGTPAPLAR	heavy	2+ / y10	830.43	950.52	43	21.5	5.0
HSP70	LYQGAGGPGAGGFGAQGPK	light	2+ / y14	845.42	1157.57	39	23.5	/
HSP70	LYQGAGGPGAGGFGAQGPK	light	2+ / y12	845.42	1043.53	39	23.5	/
HSP70	LYQGAGGPGAGGFGAQGPK	light	2+ / y13	845.42	1100.55	39	23.5	/
HSP70	LYQGAGGPGAGGFGAQGPK	heavy	2+ / y14	849.42	1165.57	39	23.5	4.0
HSP70	LYQGAGGPGAGGFGAQGPK	heavy	2+ / y12	849.42	1051.53	39	23.5	4.0
HSP70	LYQGAGGPGAGGFGAQGPK	heavy	2+ / y13	849.42	1108.55	39	23.5	4.0
GTSF1	SC[CAM]IEQDVVNQTR	light	2+ / y9	724.84	1088.53	37	22	/
GTSF1	SC[CAM]IEQDVVNQTR	light	2+ / y8	724.84	959.49	34	22	/
GTSF1	SC[CAM]IEQDVVNQTR	light	2+ / y7	724.84	831.43	31	22	/
GTSF1	SC[CAM]IEQDVVNQTR	heavy	2+ / y9	729.84	1098.53	37	22	24.9
GTSF1	SC[CAM]IEQDVVNQTR	heavy	2+ / y8	729.84	969.49	34	22	24.9
GTSF1	SC[CAM]IEQDVVNQTR	heavy	2+ / y7	729.84	841.43	31	22	24.9
WEE2	IGDLGHVTSISNPK	light	2+ / y7	719.39	746.40	40	22.8	/
WEE2	IGDLGHVTSISNPK	light	2+ / b6	719.39	593.30	40	22.8	/
WEE2	IGDLGHVTSISNPK	light	2+ / b7	719.39	692.37	40	22.8	/
WEE2	IGDLGHVTSISNPK	heavy	2+ / y7	723.39	754.40	40	22.8	1.5
WEE2	IGDLGHVTSISNPK	heavy	2+ / b6	723.39	593.30	40	22.8	1.5
WEE2	IGDLGHVTSISNPK	heavy	2+ / b7	723.39	692.37	40	22.8	1.5
HSPE1	VLQATVVAVGSGSK	light	2+ / y8	658.38	704.39	28	23	/
HSPE1	VLQATVVAVGSGSK	light	2+ / y11	658.38	975.55	28	23	/
HSPE1	VLQATVVAVGSGSK	light	2+ / y10	658.38	904.51	28	23	/
HSPE1	VLQATVVAVGSGSK	heavy	2+ / y8	662.38	712.39	28	23	16.7
HSPE1	VLQATVVAVGSGSK	heavy	2+ / y11	662.38	983.55	28	23	16.7
HSPE1	VLQATVVAVGSGSK	heavy	2+ / y10	662.38	912.51	28	23	16.7
VIM	TLYTSSPGGVYATR	light	2+ / y11	736.87	1095.54	37	23	/
VIM	TLYTSSPGGVYATR	light	2+ / y8	736.87	820.43	34	23	/
VIM	TLYTSSPGGVYATR	light	2+ / y10	736.87	994.50	37	23	/
VIM	TLYTSSPGGVYATR	heavy	2+ / y11	741.87	1105.54	37	23	4.2
VIM	TLYTSSPGGVYATR	heavy	2+ / y8	741.87	830.43	34	23	4.2
VIM	TLYTSSPGGVYATR	heavy	2+ / y10	741.87	1004.50	37	23	4.2
TDRKH	IDVDTEDIGDER	light	2+ / y9	688.81	1049.44	32	22.5	/
TDRKH	IDVDTEDIGDER	light	2+ / y8	688.81	934.41	35	22.5	/
TDRKH	IDVDTEDIGDER	light	2+ / y6	688.81	704.32	32	22.5	/
TDRKH	IDVDTEDIGDER	heavy	2+ / y9	693.81	1059.44	32	22.5	11.7
TDRKH	IDVDTEDIGDER	heavy	2+ / y8	693.81	944.41	35	22.5	11.7
TDRKH	IDVDTEDIGDER	heavy	2+ / y6	693.81	714.32	32	22.5	11.7
PRDX3	HLSVNDLPVGR	light	2+ / y9	603.83	956.52	32	24.5	/
PRDX3	HLSVNDLPVGR	light	2+ / b2	603.83	251.15	35	24.5	/
PRDX3	HLSVNDLPVGR	light	2+ / y5	603.83	541.35	38	24.5	/
PRDX3	HLSVNDLPVGR	heavy	2+ / y9	608.83	966.52	32	24.5	26.6
PRDX3	HLSVNDLPVGR	heavy	2+ / b2	608.83	251.15	35	24.5	26.6
PRDX3	HLSVNDLPVGR	heavy	2+ / y5	608.83	551.35	38	24.5	26.6
ZAR1	TLAVYSPVTSR	light	2+ / y7	597.33	809.42	28	24	/
ZAR1	TLAVYSPVTSR	light	2+ / y9	597.33	979.52	25	24	/
ZAR1	TLAVYSPVTSR	light	2+ / y6	597.33	646.35	28	24	/
ZAR1	TLAVYSPVTSR	heavy	2+ / y7	602.33	819.42	28	24	0.4
ZAR1	TLAVYSPVTSR	heavy	2+ / y9	602.33	989.52	25	24	0.4
ZAR1	TLAVYSPVTSR	heavy	2+ / y6	602.33	656.35	28	24	0.4
HSPE1	VLLPEYGGTK	light	2+ / y7	538.80	751.36	23	24	/
HSPE1	VLLPEYGGTK	light	2+ / y8	538.80	864.45	23	24	/
HSPE1	VLLPEYGGTK	light	2+ / y6	538.80	654.31	26	24	/
HSPE1	VLLPEYGGTK	heavy	2+ / y7	542.80	759.36	23	24	8.7
HSPE1	VLLPEYGGTK	heavy	2+ / y8	542.80	872.45	23	24	8.7
HSPE1	VLLPEYGGTK	heavy	2+ / y6	542.80	662.31	26	24	8.7
HSPB1	ALPAAAIEGPAYNR	light	2+ / y6	707.38	677.34	30	25.5	/
HSPB1	ALPAAAIEGPAYNR	light	2+ / b6	707.38	495.29	30	25.5	/

HSPB1	ALPAAAIEGPAYNR	light	2+ / b5	707.38	424.26	36	25.5	/
HSPB1	ALPAAAIEGPAYNR	heavy	2+ / y6	712.38	687.34	30	25.5	8.1
HSPB1	ALPAAAIEGPAYNR	heavy	2+ / b6	712.38	495.29	30	25.5	8.1
HSPB1	ALPAAAIEGPAYNR	heavy	2+ / b5	712.38	424.26	36	25.5	8.1
ZAR1	DAAVQVNPFR	light	2+ / y6	558.79	760.41	24	27	/
ZAR1	DAAVQVNPFR	light	2+ / y5	558.79	632.35	27	27	/
ZAR1	DAAVQVNPFR	light	2+ / y4	558.79	533.28	24	27	/
ZAR1	DAAVQVNPFR	heavy	2+ / y6	563.79	770.41	24	27	0.4
ZAR1	DAAVQVNPFR	heavy	2+ / y5	563.79	642.35	27	27	0.4
ZAR1	DAAVQVNPFR	heavy	2+ / y4	563.79	543.28	24	27	0.4
ASTL	SQLQQLLK	light	2+ / y6	479.29	742.48	20	27	/
ASTL	SQLQQLLK	light	2+ / y5	479.29	629.40	20	27	/
ASTL	SQLQQLLK	light	2+ / y4	479.29	501.34	23	27	/
ASTL	SQLQQLLK	heavy	2+ / y6	483.29	750.48	20	27	8.0
ASTL	SQLQQLLK	heavy	2+ / y5	483.29	637.40	20	27	8.0
ASTL	SQLQQLLK	heavy	2+ / y4	483.29	509.34	23	27	8.0
KPNA7	IGQVVDTGVLPR	light	2+ / y8	627.36	856.49	30	27	/
KPNA7	IGQVVDTGVLPR	light	2+ / y7	627.36	757.42	30	27	/
KPNA7	IGQVVDTGVLPR	light	2+ / b3	627.36	299.17	33	27	/
KPNA7	IGQVVDTGVLPR	heavy	2+ / y8	632.36	866.49	30	27	0.4
KPNA7	IGQVVDTGVLPR	heavy	2+ / y7	632.36	767.42	30	27	0.4
KPNA7	IGQVVDTGVLPR	heavy	2+ / b3	632.36	299.17	33	27	0.4
PCBD1	AVGWNELEGR	light	2+ / y8	565.78	960.45	21	27.4	/
PCBD1	AVGWNELEGR	light	2+ / y6	565.78	717.35	33	27.4	/
PCBD1	AVGWNELEGR	light	2+ / y7	565.78	903.43	30	27.4	/
PCBD1	AVGWNELEGR	heavy	2+ / y8	570.78	970.45	21	27.4	10.1
PCBD1	AVGWNELEGR	heavy	2+ / y6	570.78	727.35	33	27.4	10.1
PCBD1	AVGWNELEGR	heavy	2+ / y7	570.78	913.43	30	27.4	10.1
GSTM3	YLEQLPGQLK	light	2+ / y5	594.84	542.33	31	27.4	/
GSTM3	YLEQLPGQLK	light	2+ / y8	594.84	912.51	25	27.4	/
GSTM3	YLEQLPGQLK	light	2+ / y6	594.84	655.41	28	27.4	/
GSTM3	YLEQLPGQLK	heavy	2+ / y5	598.84	550.33	31	27.4	90.4
GSTM3	YLEQLPGQLK	heavy	2+ / y8	598.84	920.51	25	27.4	90.4
GSTM3	YLEQLPGQLK	heavy	2+ / y6	598.84	663.41	28	27.4	90.4
PRC1	VEVAQYWDR	light	2+ / y7	583.29	937.45	25	27.6	/
PRC1	VEVAQYWDR	light	2+ / y6	583.29	838.38	28	27.6	/
PRC1	VEVAQYWDR	light	2+ / b2	583.29	229.12	28	27.6	/
PRC1	VEVAQYWDR	heavy	2+ / y7	588.29	947.45	25	27.6	0.9
PRC1	VEVAQYWDR	heavy	2+ / y6	588.29	848.38	28	27.6	0.9
PRC1	VEVAQYWDR	heavy	2+ / b2	588.29	229.12	28	27.6	0.9
RPS27A	ESTLHLVLR	light	2+ / y5	534.31	637.41	32	26	/
RPS27A	ESTLHLVLR	light	2+ / y6	534.31	750.50	28	26	/
RPS27A	ESTLHLVLR	light	2+ / y7	534.31	851.55	38	26	/
RPS27A	ESTLHLVLR	heavy	2+ / y5	539.31	647.41	32	26	7.8
RPS27A	ESTLHLVLR	heavy	2+ / y6	539.31	760.50	28	26	7.5
RPS27A	ESTLHLVLR	heavy	2+ / y7	539.31	861.55	38	26	7.5
HSP70	NQVALNPQNTVFDAK	light	2+ / y9	829.93	1019.52	36	27.2	/
HSP70	NQVALNPQNTVFDAK	light	2+ / y10	829.93	1133.56	36	27.2	/
HSP70	NQVALNPQNTVFDAK	light	2+ / y8	829.93	922.46	36	27.2	/
HSP70	NQVALNPQNTVFDAK	heavy	2+ / y9	833.93	1027.52	36	27.2	4.0
HSP70	NQVALNPQNTVFDAK	heavy	2+ / y10	833.93	1141.56	36	27.2	4.0
HSP70	NQVALNPQNTVFDAK	heavy	2+ / y8	833.93	930.46	36	27.2	4.0
GSTM3	YSWFAGEK	light	2+ / y6	494.23	737.36	21	28.4	/
GSTM3	YSWFAGEK	light	2+ / y5	494.23	551.28	24	28.4	/
GSTM3	YSWFAGEK	light	2+ / y7	494.23	824.39	21	28.4	/
GSTM3	YSWFAGEK	heavy	2+ / y6	498.23	745.36	21	28.4	86.2
GSTM3	YSWFAGEK	heavy	2+ / y5	498.23	559.28	24	28.4	86.2
GSTM3	YSWFAGEK	heavy	2+ / y7	498.23	832.39	21	28.4	86.2
ACCSL	NTLGYINLGTSENK	light	2+ / y11	762.39	1195.60	33	29	/
ACCSL	NTLGYINLGTSENK	light	2+ / y6	762.39	635.30	39	29	/
ACCSL	NTLGYINLGTSENK	light	2+ / y8	762.39	862.43	33	29	/
ACCSL	NTLGYINLGTSENK	heavy	2+ / y11	766.39	1203.60	33	29	2.5
ACCSL	NTLGYINLGTSENK	heavy	2+ / y6	766.39	643.30	39	29	2.5
ACCSL	NTLGYINLGTSENK	heavy	2+ / y8	766.39	870.43	33	29	2.5
PCBD1	DQLLPNLR	light	2+ / b3	484.78	357.18	17	28.5	/
PCBD1	DQLLPNLR	light	2+ / y6	484.78	725.47	32	28.5	/
PCBD1	DQLLPNLR	light	2+ / b5	484.78	612.38	26	28.5	/

PCBD1	DQLLPNLR	heavy	2+ / b3	489.78	357.18	17	28.5	1.5
PCBD1	DQLLPNLR	heavy	2+ / y6	489.78	735.47	32	28.5	1.5
PCBD1	DQLLPNLR	heavy	2+ / b5	489.78	622.38	26	28.5	1.5
CLU	GSLFFNPK	light	2+ / y5	455.25	652.35	19	29	/
CLU	GSLFFNPK	light	2+ / y4	455.25	505.28	24	29	/
CLU	GSLFFNPK	light	2+ / b5	455.25	552.28	19	29	/
CLU	GSLFFNPK	heavy	2+ / y5	459.25	660.35	19	29	4.2
CLU	GSLFFNPK	heavy	2+ / y4	459.25	513.28	24	29	4.2
CLU	GSLFFNPK	heavy	2+ / b5	459.25	552.28	19	29	4.2
AURKA	IADFGWSVHAPSSR	light	3+ / y6	510.59	654.33	30	30	/
AURKA	IADFGWSVHAPSSR	light	3+ / y8	510.59	840.43	27	30	/
AURKA	IADFGWSVHAPSSR	light	3+ / y7	510.59	753.40	27	30	/
AURKA	IADFGWSVHAPSSR	heavy	3+ / y6	513.92	664.33	30	30	26.4
AURKA	IADFGWSVHAPSSR	heavy	3+ / y8	513.92	850.43	27	30	26.4
AURKA	IADFGWSVHAPSSR	heavy	3+ / y7	513.92	763.40	27	30	26.4
WEE2	IGVGDFGTVYK	light	2+ / y8	578.31	886.43	27	29.5	/
WEE2	IGVGDFGTVYK	light	2+ / y10	578.31	1042.52	24	29.5	/
WEE2	IGVGDFGTVYK	light	2+ / y6	578.31	714.38	30	29.5	/
WEE2	IGVGDFGTVYK	heavy	2+ / y8	582.31	894.43	27	29.5	1.5
WEE2	IGVGDFGTVYK	heavy	2+ / y10	582.31	1050.52	24	29.5	1.5
WEE2	IGVGDFGTVYK	heavy	2+ / y6	582.31	722.38	30	29.5	1.5
CLU	LLLSSLEEAK	light	2+ / y8	551.82	876.47	24	31	/
CLU	LLLSSLEEAK	light	2+ / y7	551.82	763.38	33	31	/
CLU	LLLSSLEEAK	light	2+ / y6	551.82	676.35	24	31	/
CLU	LLLSSLEEAK	heavy	2+ / y8	555.82	884.47	24	31	5.9
CLU	LLLSSLEEAK	heavy	2+ / y7	555.82	771.38	33	31	5.9
CLU	LLLSSLEEAK	heavy	2+ / y6	555.82	684.35	24	31	5.9
KPNA7	LIVDAGLIPR	light	2+ / y8	533.84	840.49	25	32.5	/
KPNA7	LIVDAGLIPR	light	2+ / y5	533.84	555.36	22	32.5	/
KPNA7	LIVDAGLIPR	light	2+ / y6	533.84	626.40	31	32.5	/
KPNA7	LIVDAGLIPR	heavy	2+ / y8	538.84	850.49	25	32.5	0.4
KPNA7	LIVDAGLIPR	heavy	2+ / y5	538.84	565.36	22	32.5	0.4
KPNA7	LIVDAGLIPR	heavy	2+ / y6	538.84	636.40	31	32.5	0.4
UHRF1	LNDTIQLLVR	light	2+ / y5	592.85	628.41	31	34	/
UHRF1	LNDTIQLLVR	light	2+ / y8	592.85	957.57	31	34	/
UHRF1	LNDTIQLLVR	light	2+ / y6	592.85	741.50	31	34	/
UHRF1	LNDTIQLLVR	heavy	2+ / y5	597.85	638.41	31	34	6.0
UHRF1	LNDTIQLLVR	heavy	2+ / y8	597.85	967.57	31	34	6.0
UHRF1	LNDTIQLLVR	heavy	2+ / y6	597.85	751.50	31	34	6.0
LAMP2	IPLNDIFR	light	2+ / y5	494.28	664.34	30	34.7	/
LAMP2	IPLNDIFR	light	2+ / y6	494.28	777.43	24	34.7	/
LAMP2	IPLNDIFR	light	2+ / y7	494.28	874.48	21	34.7	/
LAMP2	IPLNDIFR	heavy	2+ / y5	499.28	674.34	30	34.7	6.0
LAMP2	IPLNDIFR	heavy	2+ / y6	499.28	787.43	24	34.7	6.0
LAMP2	IPLNDIFR	heavy	2+ / y7	499.28	884.48	21	34.7	6.0
HSPB1	LFDQAFGLPR	light	2+ / y8	582.31	903.47	28	34.2	/
HSPB1	LFDQAFGLPR	light	2+ / y5	582.31	589.35	28	34.2	/
HSPB1	LFDQAFGLPR	light	2+ / y6	582.31	660.38	31	34.2	/
HSPB1	LFDQAFGLPR	heavy	2+ / y8	587.31	913.47	28	34.2	8.8
HSPB1	LFDQAFGLPR	heavy	2+ / y5	587.31	599.35	28	34.2	8.8
HSPB1	LFDQAFGLPR	heavy	2+ / y6	587.31	670.38	31	34.2	8.8
STMN1	ASGQAFELILSPR	light	2+ / y3	694.88	359.20	30	36	/
STMN1	ASGQAFELILSPR	light	2+ / y8	694.88	974.57	36	36	/
STMN1	ASGQAFELILSPR	light	2+ / y9	694.88	1045.60	36	36	/
STMN1	ASGQAFELILSPR	heavy	2+ / y3	699.88	369.20	30	36	11.2
STMN1	ASGQAFELILSPR	heavy	2+ / y8	699.88	984.57	36	36	11.2
STMN1	ASGQAFELILSPR	heavy	2+ / y9	699.88	1055.60	36	36	11.2
TDRKH	NLDIGLELVR	light	2+ / b3	571.33	343.16	24	36	/
TDRKH	NLDIGLELVR	light	2+ / y6	571.33	686.42	27	36	/
TDRKH	NLDIGLELVR	light	2+ / y7	571.33	799.50	27	36	/
TDRKH	NLDIGLELVR	heavy	2+ / b3	576.33	343.16	24	36	7.4
TDRKH	NLDIGLELVR	heavy	2+ / y6	576.33	696.42	27	36	7.4
TDRKH	NLDIGLELVR	heavy	2+ / y7	576.33	809.50	27	36	7.4
PDCD5	NSILAQVLDQSAR	light	2y10	707.89	1100.61	26	38	/
PDCD5	NSILAQVLDQSAR	light	2y9	707.89	987.52	30	38	/
PDCD5	NSILAQVLDQSAR	light	2y8	707.89	916.48	28	38	/
PDCD5	NSILAQVLDQSAR	heavy	2y10	712.89	1110.61	26	38	2.0

PDCD5	NSILAQVLDQSAR	heavy	2y9	712.89	997.52	30	38	2.0
PDCD5	NSILAQVLDQSAR	heavy	2y8	712.89	926.48	28	38	2.0
ASTL	NGGVVEVPFLLSSK	light	2+ / y10	723.40	1118.65	31	37.7	/
ASTL	NGGVVEVPFLLSSK	light	2+ / b4	723.40	328.16	31	37.7	/
ASTL	NGGVVEVPFLLSSK	light	2+ / b3	723.40	229.09	40	37.7	/
ASTL	NGGVVEVPFLLSSK	heavy	2+ / y10	727.40	1126.65	31	37.7	8.0
ASTL	NGGVVEVPFLLSSK	heavy	2+ / b4	727.40	328.16	31	37.7	8.0
ASTL	NGGVVEVPFLLSSK	heavy	2+ / b3	727.40	229.09	40	37.7	8.0
PDCD5	VSEQGLIEILEK	light	2y8	679.38	914.56	34	38	/
PDCD5	VSEQGLIEILEK	light	2y6	679.38	744.45	34	38	/
PDCD5	VSEQGLIEILEK	light	2y7	679.38	857.53	34	38	/
PDCD5	VSEQGLIEILEK	heavy	2y8	683.38	922.56	34	38	2.0
PDCD5	VSEQGLIEILEK	heavy	2y6	683.38	865.53	34	38	2.0
PDCD5	VSEQGLIEILEK	heavy	2y7	683.38	752.45	34	38	2.0
RBP4	YWGVASFLQK	light	2+ / y8	599.82	849.48	28	39	/
RBP4	YWGVASFLQK	light	2+ / y6	599.82	693.39	28	39	/
RBP4	YWGVASFLQK	light	2+ / y5	599.82	622.36	28	39	/
RBP4	YWGVASFLQK	heavy	2+ / y8	603.82	857.48	28	39	4.0
RBP4	YWGVASFLQK	heavy	2+ / y6	603.82	701.39	28	39	4.0
RBP4	YWGVASFLQK	heavy	2+ / y5	603.82	630.36	28	39	4.0
PRDX3	GLFIIDPNGVIK	light	2+ / y8	643.38	855.49	27	38.5	/
PRDX3	GLFIIDPNGVIK	light	2+ / b3	643.38	318.18	30	38.5	/
PRDX3	GLFIIDPNGVIK	light	2+ / y6	643.38	627.38	39	38.5	/
PRDX3	GLFIIDPNGVIK	heavy	2+ / y8	647.38	863.49	27	38.5	32.3
PRDX3	GLFIIDPNGVIK	heavy	2+ / b3	647.38	318.18	30	38.5	32.3
PRDX3	GLFIIDPNGVIK	heavy	2+ / y6	647.38	635.38	39	38.5	32.3

7.2.2 Relative quantification by SRM

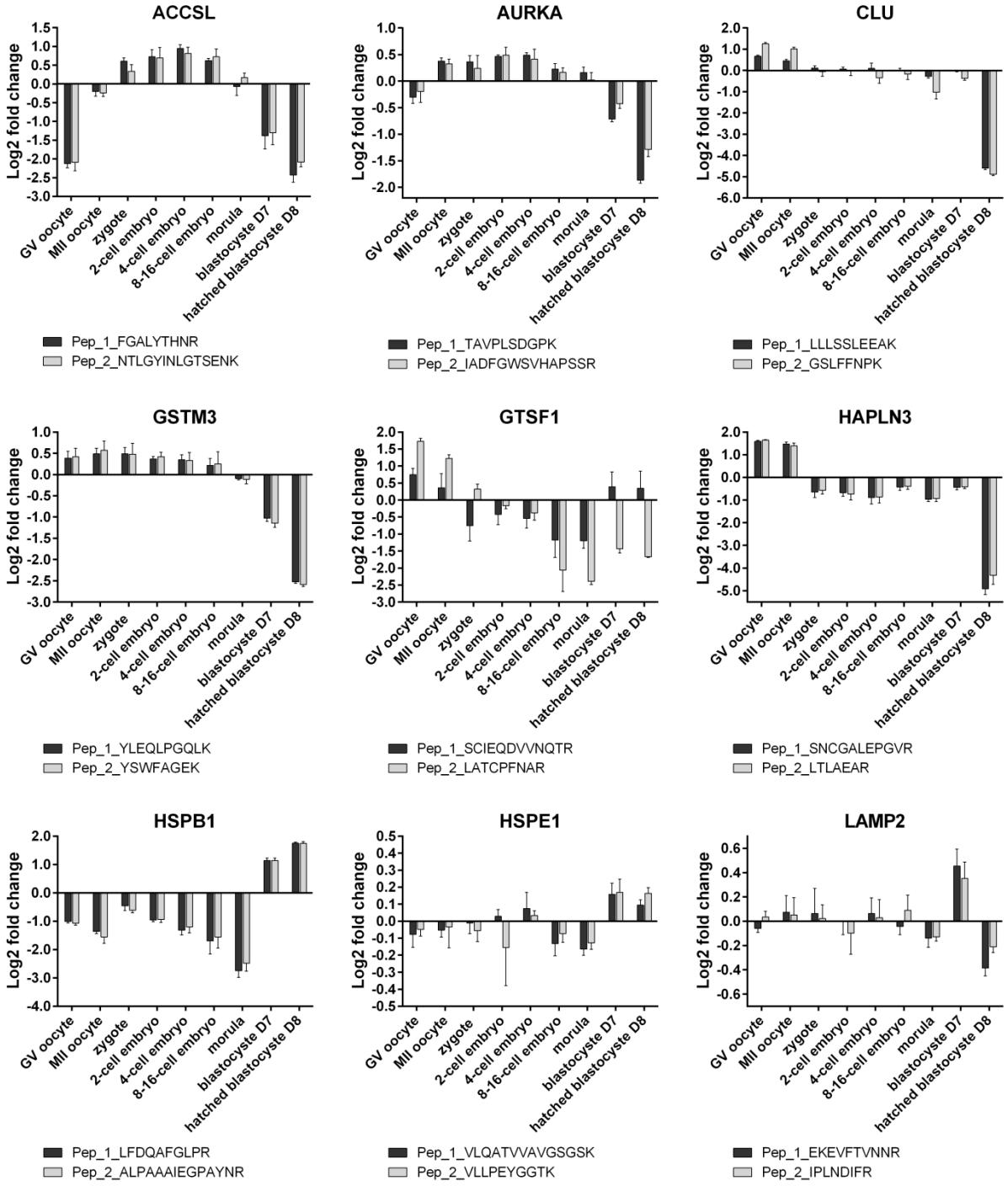

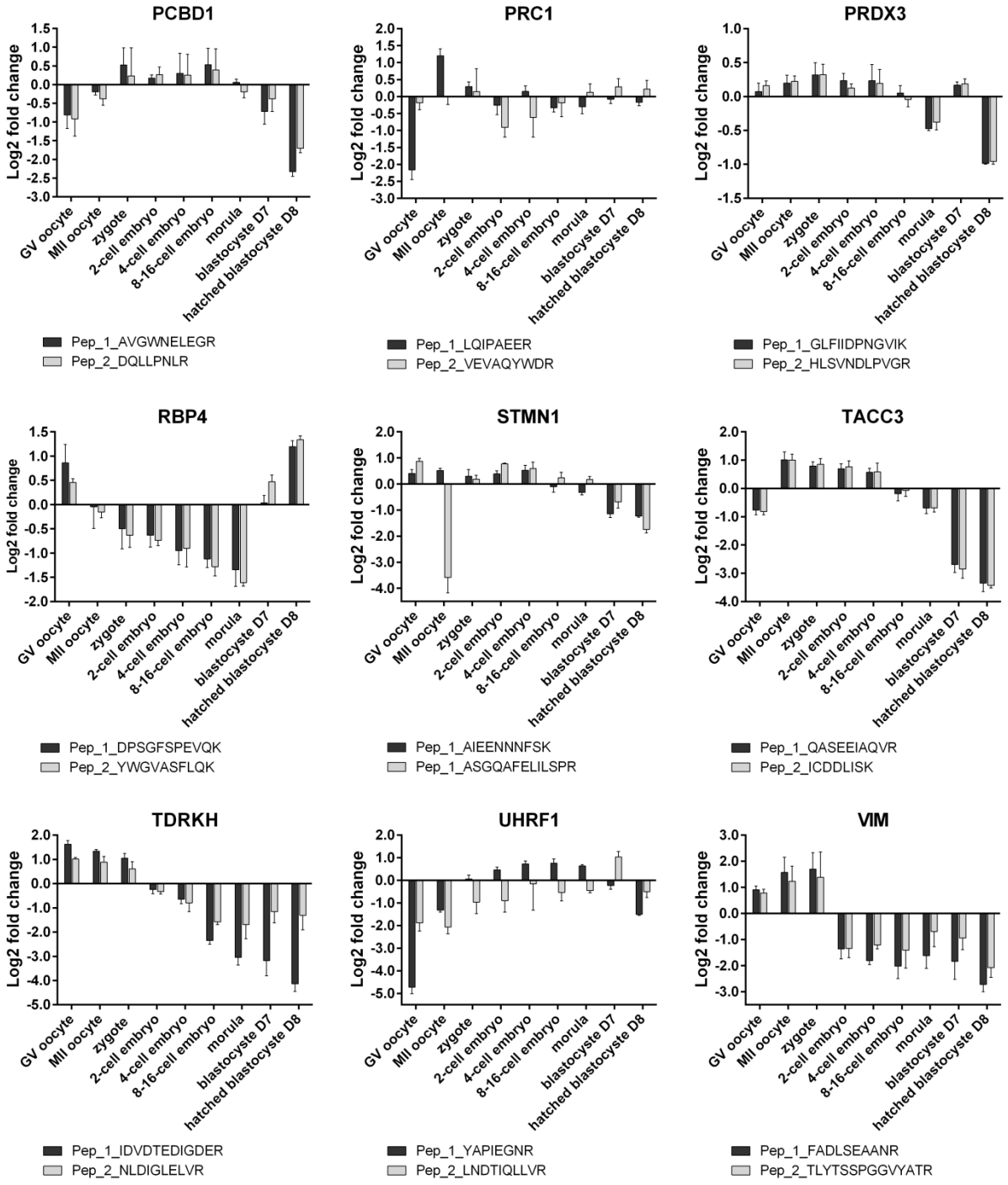
PCBD1
Log2 fold change
GV oocyte
MII oocyte
zygote
2-cell embryo
4-cell embryo
8-16-cell embryo
morula
blastocyste D7
hatched blastocyste D8
Pep_1_AVGWNELEGR
Pep_2_DQLLPNLR
PRC1
Pep_1_LQIPAEER
Pep_2_VEVAQYWDR
PRDX3
Pep_1_GLFIIDPNGVIK
Pep_2_HLSVNDLPVGR
RBP4
Pep_1_DPSGFSPEVQK
Pep_2_YWGVASFLQK
STMN1
Pep_1_AIEENNNFSK
Pep_1_ASGQAFELILSPR
TACC3
Pep_1_QASEEIAQVR
Pep_2_ICDDLISK
TDRKH
Pep_1_IDVDTEDIGDER
Pep_2_NLDIGLELVR
UHRF1
Pep_1_YAPIEGNR
Pep_2_LNDTIQLLVR
VIM
Pep_1_FADLSEAANR
Pep_2_TLYTSSPGGVYATR

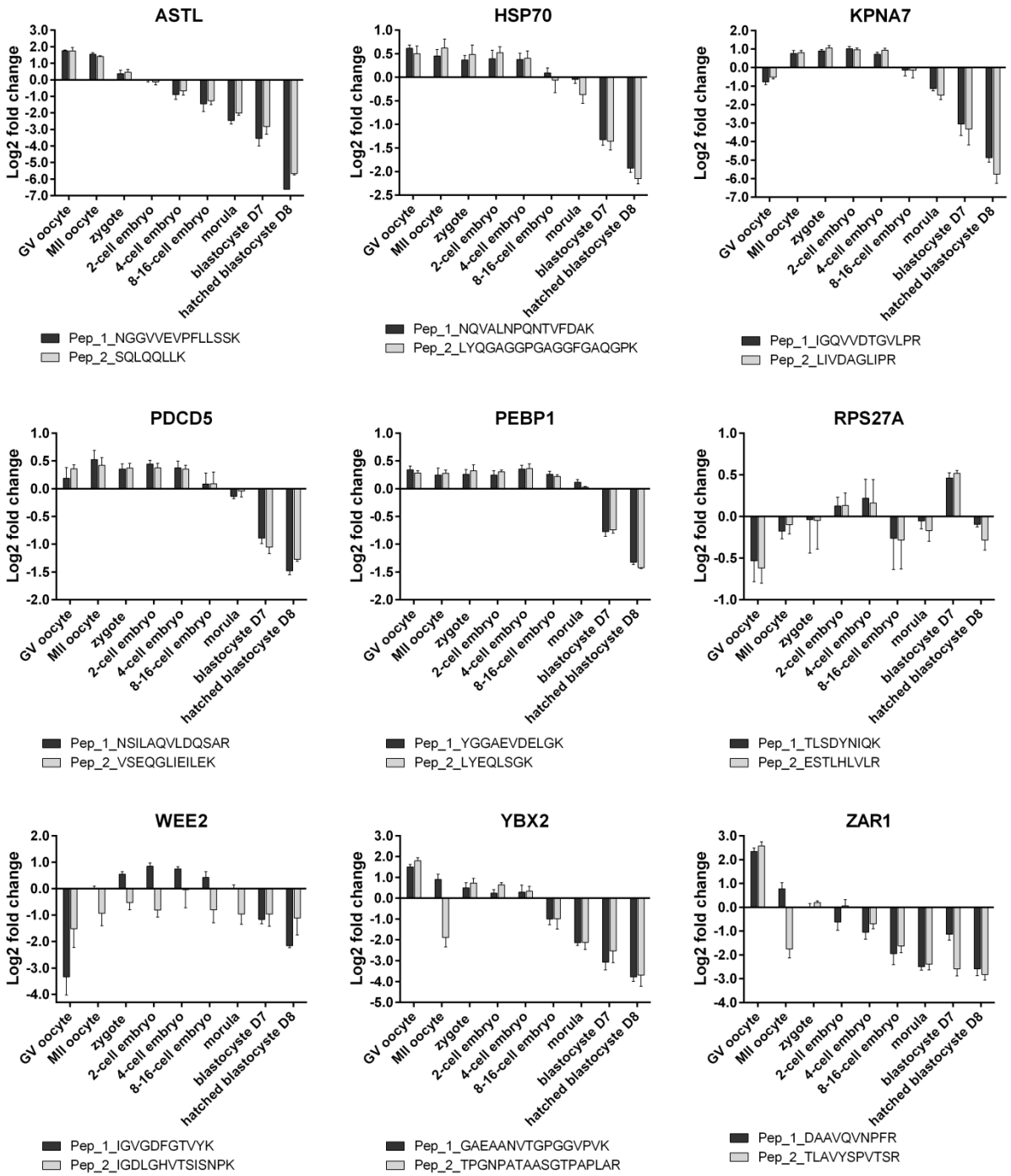

Figure 33. Display of both peptides corresponding to each of the 27 proteins relatively quantified by SRM assays.

7.2.3 Absolute quantification by SRM

Table 11. LOQ and LOD of the 18 SI peptides used for absolute quantification by SRM.

gene name	peptide sequence	charge / fragment ion	LOQ	LOD
ASTL	SQLQQLLK	2+ / y6	100 amol	50 amol
ASTL	NGGVVEVPFLLSSK	2+ / y10	500 amol	250 amol
HSP70	NQVALNPQNTVFDAK	2+ / y9	500 amol	100 amol
HSP70	LYQGAGGPGAGGFGAQGPK	2+ / y14	2.5 fmol	500 amol
KPNA7	IGQVVDTGVLPR	2+ / y8	250 amol	50 amol
KPNA7	LIVDAGLIPR	2+ / y8	50 amol	N/A
PDCD5	NSILAQVLDQSAR	2+ / y10	2.5 fmol	500 amol
PDCD5	VSEQGLIEILEK	2+ / y8	2.5 fmol	500 amol
PEBP1	LYEQLSGK	2+ / y6	50 amol	N/A
PEBP1	YGGAEVDELGK	2+ / y10	50 amol	N/A
RPS27A	TLSDYNIQK	2+ / y7	250 amol	50 amol
RPS27A	ESTLHLVLR	2+ / y5	1 fmol	50 amol
WEE2	IGDLGHVTSISNPK	2+ / y7	1 fmol	500 amol
WEE2	IGVGDFGTVYK	2+ / y8	500 amol	50 amol
YBX2	TPGNPATAASGTPAPLAR	2+ / y11	1 fmol	500 amol
YBX2	GAEAANVTGPGGVPVK	2+ / y3	250 amol	50 amol
ZAR1	TLAVYSPVTSR	2+ / y7	50 amol	N/A
ZAR1	DAAVQVNPFR	2+ / y6	500 amol	50 amol

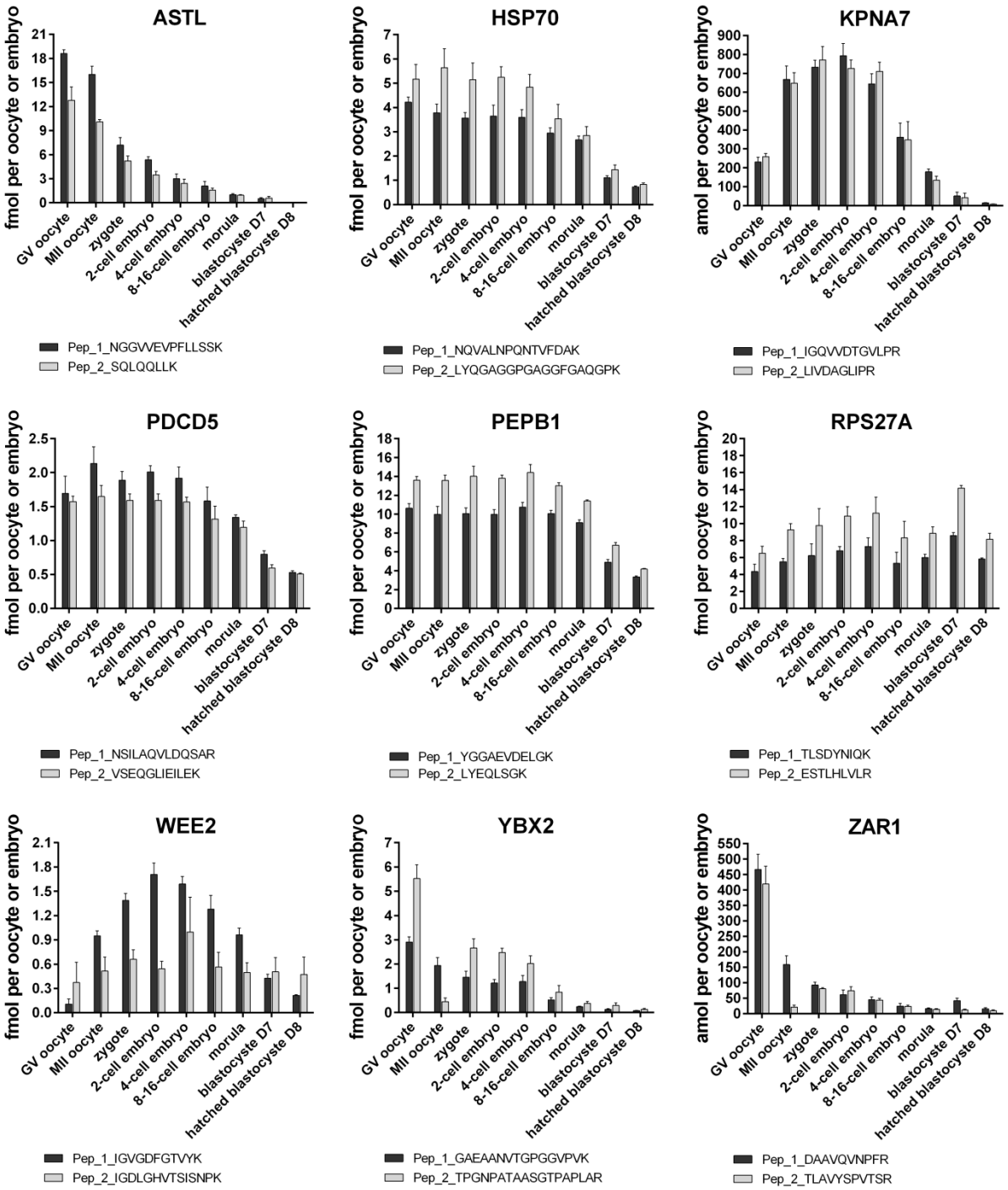

Figure 34. Display of both peptides corresponding to each of the nine proteins absolutely quantified by SRM assays.

7.3 Publications

7.3.1 Papers and Reviews

T. Trapphoff, M. Heiligentag, D. Dankert, H. Demond, D.R. Deutsch, T. Frohlich, G.J. Arnold, R. Grümmer, B. Horsthemke, U. Eichenlaub-Ritter, Postovulatory aging affects dynamics of mRNA, expression and localization of maternal effect proteins, spindle integrity and pericentromeric proteins in mouse oocytes. *Human Reproduction,* (2015, submitted).

D.R. Deutsch, T. Frohlich, K. A. Otte, A. Beck, F.A. Habermann, E. Wolf, G.J. Arnold, Stage Specific Proteome Signatures in Early Bovine Embryo Development. *J Proteome Res*, (2014); published online EpubAug 8 (10.1021/pr500550t).

M. Demant*, D.R. Deutsch*, T. Frohlich, E. Wolf, G.J. Arnold, Proteome Analysis of Early Lineage Specification in Bovine Embryos. *Proteomics*, (2014); published online EpubAug 20 (10.1002/pmic.201400251). *contributed equally

D.R. Deutsch*, T. Frohlich*, G.J. Arnold, Proteomics of Bovine Endometrium, Oocytes and Early Embryos. *Reproduction in Domestic Ruminants VIII* (eds. JL Juengel, A Miyamoto, C Price, LP Reynolds, MF Smith, R Webb), Nottingham University Press, (2014), ISBN13: 9781899043637. *contributed equally

7.3.2 Abstracts and poster presentations

D.R. Deutsch, T. Frohlich, K.A. Otte, A. Beck, F.A. Habermann, E. Wolf, G. J. Arnold, Stage Specific Proteome Signatures in Early Bovine Embryo Development. 41st Annual Conference of the International Embryo Transfer Society (IETS 2015), Versailles, France.

Erica de Monte, Andrea Beck, Daniela Deutsch , Thomas Fröhlich, Georg Arnold, Eckhard Wolf, Felix A. Habermann, Fertilization and the Critical First Steps of Bovine Embryo Development (2014). Forschungsbroschüre der Tiermedizinischen Fakultät.

D.R. Deutsch, T. Fröhlich, K.A. Otte, A. Beck, F.A. Habermann, E. Wolf, G.J. Arnold, Stage Specific Proteome Signatures in Early Bovine Embryo Development (2014). Gene Center Retreat, Wildbad-Kreuth, Germany.

D.R. Deutsch, T. Fröhlich, F.A. Habermann, E. Wolf, G.J. Arnold, Impact *of in vitro* Maturation on the Proteome of Bovine Oocytes (2013). Gene Center Retreat, Wildbad-Kreuth, Germany.

D.R. Deutsch, T. Fröhlich, F.A. Habermann, E. Wolf, G.J. Arnold, Impact of Growth Hormone on the Proteome of Bovine Oocytes during *in vitro* Maturation (2012). 11th Annual World Congress of the Human Proteome Organization (HUPO), Boston, MA in the United States.

D.R. Deutsch, T. Fröhlich, M. Reichenbach, E. Wolf, G.J. Arnold, Multiplexed Absolute Quantification of Proteins during Early Embryogenesis by Selected Reaction Monitoring (2011). 10th Annual World Congress of the Human Proteome Organization (HUPO), Geneva, Switzerland.

D.R. Deutsch, T. Fröhlich, M. Reichenbach, E. Wolf, G.J. Arnold, Multiplexed Absolute Quantification of Proteins during Early Embryogenesis by Selected Reaction Monitoring (2011). Gene Center Retreat, Wildbad-Kreuth, Germany.

A. Cengizeroglu, K. Farkasova, D.R. Deutsch, R. Haase, M. Anton, E. Wagner, M. Ogris, Harnessing Molecular Targets in Human Colon Cancer Cells for Tumor Specific RNAi and pDNA-based Therapies (2010). 7th Annual Meeting of German-Society-for-Gene-Therapy (DG-GT e.V.), Munich, Germany.

7.3.3 Oral presentations

D.R. Deutsch, T. Fröhlich, K.A. Otte, A. Beck, F.A. Habermann, E. Wolf, G.J. Arnold, Comparative Proteomic Analysis of Early Bovine Embryos (2014). Gene Center Seminar, Munich, Germany.

D.R. Deutsch, T. Fröhlich, K.A. Otte, A. Beck, F.A. Habermann, E. Wolf, G.J. Arnold, Qualitative and Quantitative Proteomic Analyses of Early Mammalian Embryos (2014). Annual meeting of the “Zentrum für Translationale Reproduktionsmedizin”, Munich, Germany.

D.R. Deutsch, T. Fröhlich, A. Beck, F.A. Habermann, E. Wolf, G.J. Arnold, Structural, Molecular and Functional Analysis of Early Bovine Embryogenesis: Readouts for Oocyte Potential after *in-vitro* versus *in-vivo* Maturation (2013). 3rd Workshop of the Research Unit 'Germ Cell Potential', Münster, Germany.

7.3.4 Travel grants

Fellowship, Deutsche Gesellschaft für Proteomforschung (DGPF)

D.R. Deutsch, T. Fröhlich, F.A. Habermann, E. Wolf, G.J. Arnold, Impact of Growth Hormone on the Proteome of Bovine Oocytes during *in vitro* Maturation (2012). 11th Annual World Congress of the Human Proteome Organization (HUPO), Boston, MA in the United States.

Fellowship, Deutsche Gesellschaft für Proteomforschung (DGPF)

D.R. Deutsch, T. Fröhlich, M. Reichenbach, E. Wolf, G.J. Arnold, Multiplexed Absolute Quantification of Proteins during Early Embryogenesis by Selected Reaction Monitoring (2011). 10th Annual World Congress of the Human Proteome Organization (HUPO), Geneva, Switzerland.

7.4 Acknowledgements

First of all, I would like to thank Dr. Georg. J. Arnold for giving me the opportunity to work on this fascinating topic, especially for his support, encouragement and scientific guidance enabling this thesis. The scientific debates with Dr. Georg Arnold promoted my own development and have broadened my horizon. I am also deeply grateful for giving me the possibility to attend plenty of congresses and workshops around the world in the last four years, which is of big importance for my professional career.

I would further like to thank Prof. Dr. Eckhard Wolf for being my doctoral advisor from the Gene Center and Department of Veterinary Sciences, for careful reading of publications and this work, and all the helpful scientific input and ideas he provided. I also want to thank Prof. Dr. Ernst Wagner for being my doctoral advisor from the Department of Pharmacy, Center of Drug Research, Pharmaceutical Biology-Biotechnology.

Special thanks to Dr. Thomas Fröhlich, and also Miwako Kösters, for all the kind advice and help they gave me and in particular for the many many hours spend with fixing problems concerning mass spectrometry - without this help, this study would not have been possible.

Many thanks to my oldest colleague Alexander Graf, with whom I once started the journey in Nijmegen, and to the “ZNP Crew”, Florian Flenkenthaler, Kathrin Otte, Julia Knörndel and Lidia Blazques, for the scientific help they provided, especially with bioinformatics, the fun we always had in the lab, on business trips and private occasions, and the general great atmosphere in the lab. It was a pleasure to work with you.

I also want to thank Dr. Myriam Demant for tutoring me, and Stefan Kempf for the great time at the beginning of my PhD.

I thank Dr. Andrea Beck, Dr. Myriam Reichenbach, Dr. Horst-Dieter Reichenbach and Tuna Güngör for helping with IVP, performing of OPU sessions and for providing me with IVP media. I am especially grateful to Andrea for the great collaboration and teaching me the

staining of embryos, and also to Dr. Felix Habermann, for spending all these hours at the microscope.

Many thanks go to the group of Prof. Dr. Eichenlaub-Ritter. I thank Tom Trapphoff for the great collaboration and the witty conversations, and I am especially grateful to have met Martyna Heiligentag. I enjoyed working with her and want to thank her for the great personal support, her friendship, endless conversations and so much more.

Lots of thanks also to my Stammtisch Mädels Sandra, Steffi, Isabella, Jessica and Bettina for all the nice lunches and dinners we had together.

Finally, I want to express my deep gratitude towards Stefan, who stood beside me during all the hard times, and towards my family, for the never-ending support during my whole life.